Distributed Microgrid System Design and Control Algorithms for Oil and Gas fields

A Thesis

Submitted in Partial Fulfilment of the Requirements for the Degree of

DOCTOR OF PHILOSOPHY

By

Deepika Bishnoi

School of Energy Science and Engineering

Indian Institute of Technology Guwahati

Guwahati-781039, Assam, India

July 2022

This thesis is dedicated to my parents, friends, and mentors.

Indian Institute of Technology Guwahati

School of Energy Science and Engineering

Statement

I, hereby declare that the work contained in this thesis titled "**Distributed Microgrid System Design and Control Algorithms for Oil and Gas fields**" is original and has been done by me at the School of Energy Science and Engineering, Indian Institute of Technology Guwahati, Guwahati, India, under the supervision of **Dr. Harsh Chaturvedi**. The work has not been submitted to any other Institute for any degree or diploma. I have followed the guidelines provided by the Institute in preparing the thesis. I have confirmed the norms and guidelines given in the Ethical Code of Conduct of the Institute. Whenever I have used materials (data, theoretical analysis, figures, and text) from other sources, I have given due credit to them by citing them in the text of the thesis and providing their details in the references. Further, I have taken permission from the copyright owners of the sources, whenever necessary.

Guwahati,

July, 2022

Deepika Bishnoi

166151009

Indian Institute of Technology Guwahati

School of Energy Science and Engineering

Certificate

It is certified that the work described in this thesis titled "**Distributed Microgrid System Design and Control Algorithms for Oil and Gas fields**" by Ms. Deepika Bishnoi for the award of degree of Doctor of Philosophy is an authentic record of the results obtained from the research work carried out under my supervision at the School of Energy Science and Engineering, Indian Institute of Technology Guwahati, Guwahati, India, and this work has not been submitted elsewhere for a degree.

Dr. Harsh Chaturvedi

Thesis Supervisor

Assistant Professor

School of Energy Science and Engineering

IIT Guwahati, Guwahati – 781039

Assam, India

"Reflect upon your present blessings, of which every man has plenty;
not on your past misfortunes, of which all men have some."

— Charles Dickens

Acknowledgment

This doctoral thesis would not be completed without several people's help and extended hands. I take this opportunity to express my sincere thankfulness to all of them.

Firstly, I would like to express most profound respect to my thesis supervisor, **Dr. Harsh Chaturvedi,** School of Energy Science and Engineering, for his constant support and positive outlook. He is a wonderful person, always striving for the growth of his students, his lab, and society as a whole. I am thankful to him for accepting the collaboration and providing the interns to widen the research area. I am honored to learn about research, scientific ethics, and life from him. His supportive attitude and guidance have contributed indispensably towards my growth all these years.

I am immensely grateful to **Dr. Gaurav Trivedi** for extending support to achieve my goals. He has always been kind in offering me every possible support, be it academic guidance or financial support in terms of project assistantship, needed for my research career to take a firm shape. I am thankful to **Prof. Senthilmurugan** for selecting me for the Ph.D. program and connecting me with the ABB company. My **internship and research experience in ABB Bangalore** helped me gain the initial insights to drive my research. The inputs from **Mr. Anil Talluri, Mr. G Pradeep, Mr. Vijayan**, and **everyone back in the ABB office** played an incredible role in keeping a check on my research goals. I would also like to thank my doctoral committee members: **Prof. Nemade, Prof. Senthilmurugan,** and **Dr. Deepak Sharma,** for their valuable suggestions and constructive criticism during all assessments of the Ph.D. program. I also thank **Prof. Mohanty, Prof. Moholkar, Prof. Goswami,** Head and former heads, School of Energy Science and Engineering, for their administrative support.

I am immensely grateful to the **employees at ONGC Assam Asset, Nazira, and APDCL**, especially **Mr. Dhiraj Soni, Mrs. Wasifa Choudhary, and Mr. Dhruba Bora,** for their timely help in data collection whenever I needed. I would like to thank the editors of the journals in which I published my research papers for providing timely feedback and a smooth publishing experience.

Furthermore, I would like to thank **other faculty members, research scholars, non-teaching staff of IIT Guwahati** for their support and cooperation in all aspects.

I acknowledge Ministry of Human Resource Development **(MHRD), ABB** and our institute for providing fellowship during my PhD program. I am also grateful for the one time fellowship I got for working in the research and development project by **Titan** and **EICT** (Electronics and Information Communication Technology).

I would like to take this opportunity to thank my friends who were part of my growth during my PhD journey. I wholeheartedly thank *Mr. Om Prakash* from IIT Bombay and *Swanand Pawar* (BTech from IITG) for helping me with the resource allocation and network design optimization. I am grateful to my labmates, *Mr. Prashant Thapliyal, Mr. Brijesh Meena, Mr. Ankit Singh, Ms. Chandrima, Ms. Debika, Ms. Priya, Mr. Chandan Dawo, Mr. Siddhartha, Mr. Jyotishman, Ms. Rachel Sona Iswary, Mr. Vaibhav Ingle, Mr. Jeet Brahma, Mr. Vikas Bhadoria, and Mr. Swastik* for providing a healthy and supportive environment in lab. I am also grateful to Dr. Gaurav Trivedi and Prof Senthilmurugan's lab students: *Dr. Swati, Mr. Praveen, Ms. Meenali, Dr. Viswanth, Ms. Niveditha, and Dr. Muniraja Tippa* for extending all the help whenever I needed. My heartfelt thanks to the entire Youth Empowerment and Skill development (YES+) family, which helped immensely in keeping me mentally and physically strong throughout the course of my Ph.D. The support I got from *Mr. Ghadir Nophal, Mr. Hrishikesh Boro, Ms. Malvika, Ms. Puja Sharma, Mr. Bikas Shah, Mr. Durgesh Kumar, Ms. Ashita Batra, Mr. Himanshu, Ms. Anjali, Ms. Anasua, Ms. Juhi Kumari, Ms. Munmi Bhattacharya, Ms. Sunita Deb, Ms. Radhika, Dr. Ing. Sumit Agarwal, Mr. Nayan, Dr. Arvin, Mr. Rishi, Dr. Ila, Ms. Tako Nama, Dr. Ruchika, Dr. Shruti, Ms. Joyshree, Ms. Jaishree, Ms. Kasturi, Mr. Atanu, Mr. Mohit Mishra and all other friends* made me feel at home even while being away from home. I can't be more thankful to be part of the beautiful campus of IIT Guwahati. The serene environment, birds, ducks, lakes, and trees made my stay pleasant and memorable.

The occasion to express gratefulness to one's family on text does not present itself often, and I genuinely appreciate their eternal care. I am eternally grateful to my parents for supporting me and guiding me to strive for the highest. It is all because of the blessings of my mother – *Dr. Smt. Saroj Bala Shyag Bishnoi* and my father - *Mr. Manoj Bishnoi*, that I have reached wherever I am. Lastly, I am grateful to all my Artofliving friends and mentors outside IIT Guwahati for their blessings and help in need. It is said – '*Guru bin Gati nahi'*; therefore, I am grateful to the *Guru Shakti*/*God almighty* for guiding and protecting me at every moment of my life.

Sincerely,

Deepika Bishnoi

June 2022

Abstract

Gas flaring is an issue of severe environmental and economical concern worldwide. Globally approximately 100 BCM (Billion Cubic Metres) of natural gas is flared yearly, leading to 400 million tons of CO_2 (Carbon Dioxide) emissions and wastage of nearly 20 million dollars annually. India ranks 19th in the latest global list of gas flaring and oil production. India annually burns 850 MMSCM (Million Metric Standard Cubic Metre) of natural gas. Out of India's total onshore natural gas production, 33.63% occurs in Assam, and 6.29% of this is wasted in flares. The burning of expensive natural gas is an economic as well as environmental loss to the flora-fauna and posses risk of health abnormalities for human settlements around oil and gas fields, petroleum refineries, and petrochemical plants. There are several policies in place at national as well as global level to curb carbon emissions and introduce more and nore renewables in the total electricity generation mix. Apart from the problems caused by gas flaring, another problem is the unreliability of electricity infrastructure, especially in remote locations like that of gas flaring sites. There is a significant disparity in the number of hours a household in the city and a settlement around a gas flaring site gets electricity. Flare natural gas can be used for power generation via microturbine at remote flare locations, and can be an efficient power generator in a microgrid, solving the problems of gas flaring and shortage of electricity effectively. According to World Bank, these flared gas can produce more electricity than the entire African continent is consuming today.

Energy management in a microgrid can be achieved by strategic allocation of power generators, which will bring benefits like enhancement of power quality and reliability of supply, reduction of network losses, etc. Several such microgrid systems, when operated in conjunction, can reduce the chances of failure in the overall system. However, effective implementation of these systems relies on the accuracy of sizing / designing / operation and management / dispatch algorithms. For energy and cost efficient power distribution in microgrid systems, novel algorithms are being researched. The site for installation of such systems should be selected carefully as the success of any hybrid renewable energy system depends on the social, ecological, physical, and technical conditions of that locality. There have been several case studies reported in literature on Hybrid Renewable Energy System (HRES) site selection. Nonetheless,

there is a lack of study on HRES including gas microturbines to be installed in gas flare sites to reduce flaring. Similarly there is lack if studies on gas microturbine integrated microgrid power and energy management system design and dispatch. Furthermore, plethora of optimization and machine learning algorithms can be employed for the above mentioned purposes. The present study explores the implementation of existing algorithms, and develops new ones to overcome the shortcomings of the existing ones.

The presented thesis gives algorithmic answers to the following questions - 1) selection of appropriate location for installation of the HES (Hybrid Energy Systems) in oil and gas fields, 2) selection of the right set of components for the HES design, 3) development of dispatch strategy for an oil and gas well based HES, 4) power and energy optimisation in multi-microgrid systems.

This thesis proposes a complete solution for converting the power-consuming and emission causing oil and gas fields to power generating - reduced emission system. The proposed solution can be a role model for carbon transition and achieving the Intended Nationally Determined Contributions (INDC) set by India to meet the Sustainable Development Goals (SDG).

First, it addresses the issue of choosing the best gas flare site for hybrid renewable energy systems. Additionally, each location's choice of the appropriate gas turbine technology is examined using mixed integer linear programming. The decision-making process considers the power demand, the coordinates of the gas flaring locations and the demand sites, in addition to the fuel availability in each place. Due to the lack of trustworthy data in oil and gas areas, the previous algorithms were insufficient for site selection of HRES deployment, therefore a combination of two multi-criteria decision making algorithms was considered.

Once the best locations have been determined, it is also necessary to design hybrid energy systems to meet the needs, which is addressed for two specific case studies. Modeling of solar photovoltaic energy, hydrokinetic river turbines, and gas microturbines are all included in these case studies, along with modelling of anticipated demand. After considering these factors, effective dispatch techniques are offered.

Knowing how to forecast the amount of electricity that will be produced at any given time using renewable sources is another important consideration for a successful integration of various energy sources. It is particularly well known that the susceptibility

of both solar and wind energy to shifting weather conditions is one of its issues. As a result, it is challenging to predict in advance how much energy will be obtained from any of these sources at any given time, which complicates integrated energy systems. The difficulty of forecasting solar energy generation is the focus of the thesis that is being presented. The models employed enable a somewhat good projection of the contribution that this technology will make, allowing for an adequate balancing of it with other sources (particularly gas flaring) to achieve the goals of the project.

Finally, the issue of various Microgrid coordination is addressed. This means that any microgrid may eventually have surplus or deficits in generation to satisfy its needs, which may be made up for by those of other microgrids close by.

In future, it would be interesting to study different optimization frameworks to establish the energy transaction (purchase / sales of energy) between different Microgrids. The concepts of global resource optimization, or in each independent microgrid maximising its benefits, or an intermediate situation dealing with different type of fairness (e.g., that the microgrid that benefits the least should benefit the most). All of this would certainly be an interesting topic for future study.

91

Abbreviations

BCM	Billion cubic meters
GGS	Group Gathering Station
GCP	Gas Compression Plant
MMSCM	Million Metric Standard Cubic Metres
INDC	Intended Nationally Determined Contribution
GDP	Gross Domestic Products
ONGC	Oil and Natural Gas Corporation
APDCL	Assam Power Distribution Company
HES	Hybrid Energy Systems
UN	United Nations
GW	Giga Watt
MT	Micro Turbine
COP21	Conference of Parties
UNFCCC	United Nations Framework Convention on Climate Change
TWh	Tera Watt Hour
DER	Distributed energy resource
BESS	Battery Energy Storage System
PCC	Point of Common Coupling
HRES	Hybrid Renewable Energy Systems
DS	Dispatch Strategies
LF	Load Following
CC	Cycle Charging
WBDG	Whole Building Design Guide
SDG	Sustainable Development Goals
TOPSIS	Technique for Order of Preference by Similarity to Ideal Solution
Ci	Closeness to ideal solution indexing
LCOE	Levelized Cost of Energy
NPC	Net Present Cost
ROI	Return on investments
MCDM	Multi-Criteria Decision Making
AHP	Analytical Hierarchy Process
WASPAS	Weighted Aggregated Sum Product Assessment
PROMTHEE	Preference Raning Organization Method for Enrichment Evaluation
ARAS	Additive ratio assessment method
GIS	Geographical Information System
PV-EV	Photo Voltaic Electric Vehicle
GHI	Global Horizontal Irradiance
MLFFNN	Multi-Layer Feed-Forward Neural Network

SVR	Support Vector Regression
FIS	Fuzzy Inference System
ANFIS	Adaptive Neuro Fuzzy Inference System
GMDH	Group Method of Data Handling
LP	Linear Programming
MILP	Mixed Integer Linear Programming
NLP	Non-linear Programming
OF	Objective Functions
GHG	Green House Gas
RER	Renewable Energy Resources
ESS	Energy Storage System
RTH	Rolling Time Horizon
P2P	Point to Point
LV	Low Voltage
RBF ANN	Radial Basis Function Artificial Neural Network
HOMER	Hybrid Optimizer for Multiple Energy Resources
SWT	Small Wind Turbines
PVG-BESS	Photo Voltaic Genrator Battery Energy Storage System
FC	Fuel Cell
DG	Diesel Generator
COE	Cost of Energy
SVM	Support Vector Machine
ANN	Artificial Neural Network
PCS	Power Conditioning System
RDS GGS1	Rudrasagar Gas Gathering Station
SCMD	Standard Cubic Metre per Day
RMSE	Root Mean Square Error
LR	Linear Regression
MLR	Multiple Linear Regression
PSO	Particle Swarm Optimization
GA	Genetic Algorithm
XgBoost	Extreme Gradient Boosting
AdaBoost	Adaptive Boosting
ANN	Artificial Neural Network
SCADA	Supervisory Control and Data Acquisition
GMT	Gas Microturbine
IEC	International Electrotechnical Commission
NOCT	nominal operating cell temperature
HKRT	Hydrokinetic River Turbines
ROI	return on investment
TEM	Transactive Energy Management
SPV	Solar Photovoltaic
WT	Wind Turbine

LEM	Local Energy Market

92

Contents

List of Figures

List of Tables


भारतीय प्रौद्योगिकी संस्थान, गुवाहाटी • Indian Institute of Technology, Guwahati •

Chapter 1

Introduction

In the oil industry, gas flaring has long been a cause of worry. The natural gas obtained as a by-product in Oil and Gas fields is burnt due to a number of variables, such as market and economic constraints, a lack of efficient regulation, and a lack of political will. As a result of the flaring technique, a number of pollutants, including methane, carbon dioxide, and black carbon (soot), are released into the atmosphere. In 2020, world oil demand dropped by 7% due to COVID-19 pandemic but flaring reduced only by 5%. Figure 1-1 shows the satellite map of gas flaring across the globe for the year 2022. In order to prevent a rise in the average world temperature above 2 degrees Celsius, the Paris Climate Accord mandates that CO_2 emissions be zero by 2060 [1]. As a result, thirty-four governments and oil & gas corporations have pledged to the 'zero routine flaring by 2030' initiative of world bank launched in 2015, and this Ph.D. thesis is a contribution to the energy revolution.

In 2021, petroleum exploration and production installations worldwide flared 144 billion cubic meters (BCM) of gas. According to estimates from the World Bank, gas flaring

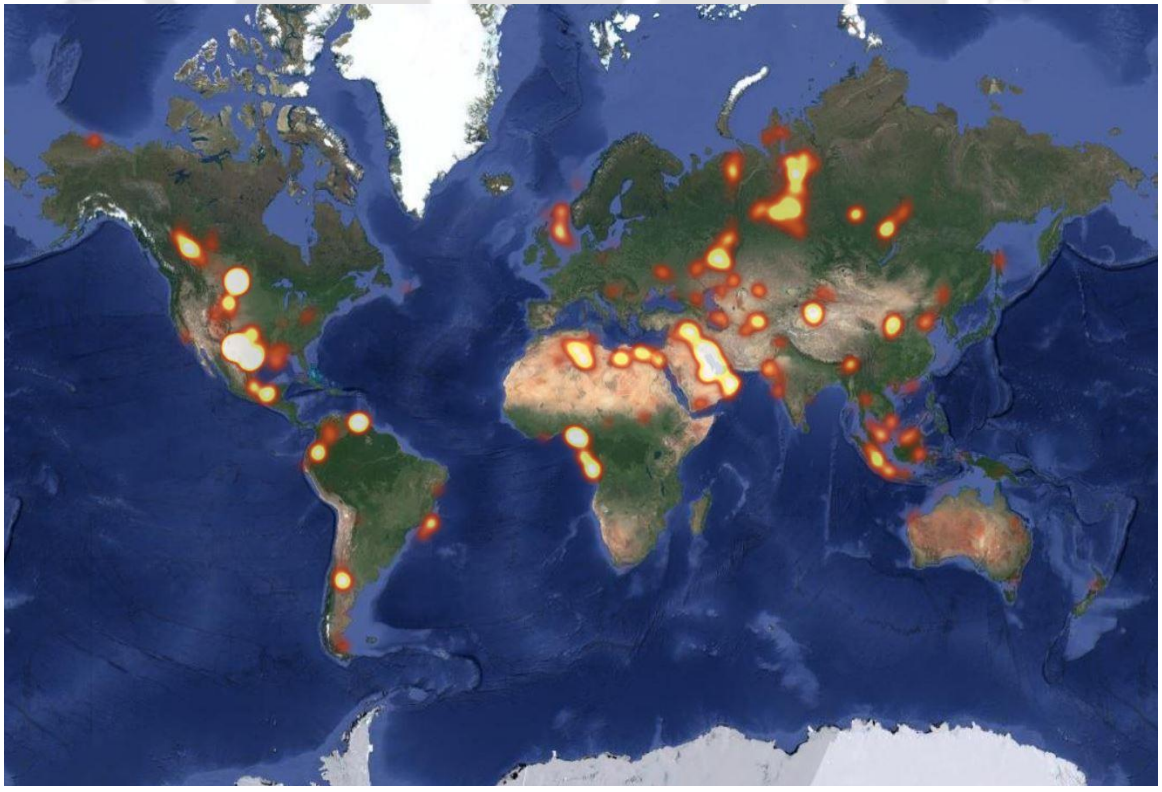

Figure 1-1 Gas Flare Map (2022) (Source: skytruth.org)

contributed to around 400 million tonnes of carbon dioxide (CO_2) equivalent worldwide emissions last year. Figure 1-2 projects the volume of natural gas flared worldwide from the year 2012 to 2021. For the past ten years, seven of the top ten emitting nations—Venezuela, Russia, Iran, Iraq, Algeria, the United States, and Nigeria—have maintained this ranking. China, Mexico, and Libya are the bottom three, and they all have shown notable rises in flaring recently. The United States is the only country that has successfully reduced its flaring by 50% in the last three years. India ranks 19th in the global gas flaring scenario.

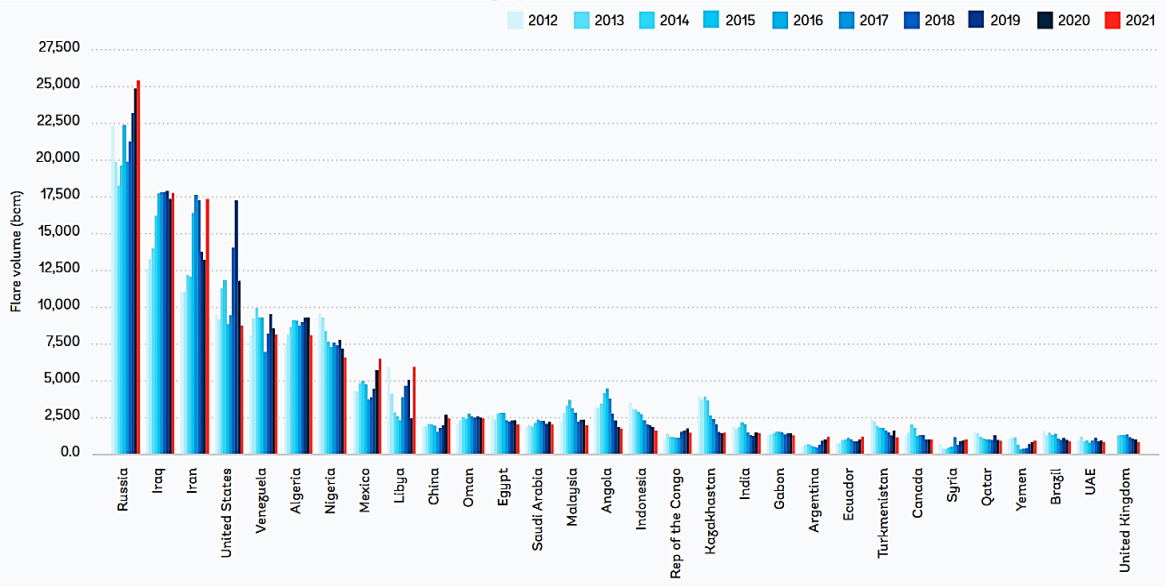

Figure 1-2 World Gas Flaring Data from 2012 to 2021 (Source: World Bank Flare Gas Report 2022)

Flaring of natural gas is malpractice which causes detrimental loss to the health of human settlements around the gas flare site and deteriorates the air quality causing loss to flora and fauna in nearby areas. The oxides generated from flaring are acid anhydrides which cause acid rain by combining with the air's inherent humidity. People and animals living close to gas flaring sites frequently experience severe health issues such as cardiovascular illnesses[2].

The content in this chapter has been published in the following papers:

- Deepika Bishnoi, Om Prakash, and Harsh Chaturvedi, 'Utilizing Flared Gas for Distributed Generation : An Optimization Based Approach', AIP 2019. https://doi.org/10.1063/1.5096498.
- Deepika Bishnoi and Harsh Chaturvedi, 'A Review on Emerging Trends in Smart Grid Energy Management Systems', IJRER, vol. 11, no. 3, September 2021. https://doi.org/10.20508/ijrer.v11i3.11832.g8228.

2.1 Gas Production-Transportation-Distribution Architecture

Natural gas production is a spurious and uncontrolled process. A portion of the produced gas is sold off to customers as per their demands, and the remaining is flared off. Flaring occurs due to many reasons, such as the lack of political will to invest in the gas transportation, storage, and sales grid network. Flaring off the gas instead of spending money to develop a new gas storage and transportation network is more cost-effective because gas prices are very low. As a result, the gas flaring out at the oil and gas production sites is enormous. Natural gas is frequently flared not just at oil and gas producing facilities but also in the natural gas sector, oil refineries, and petrochemical industries. On a global scale, 3.5% of the total natural gas production is wasted in flares [3].

Additionally, natural gas releases methane, a powerful greenhouse gas, into the environment when it is not flared and discharged into the air. Over the next ten years, the Indian government wants to reduce the emission of methane from the gas and oil sector by 40 to 50 percent. But, flaring the surplus gas is a problem too. It releases an unimaginably massive amount of carbon dioxide into the atmosphere and contributes to atmospheric pollution leading to global warming.

In any oil and gas production corporation, transporting gas from the gas production site to the utilities requires many infrastructure assets and processing steps. Gas produced at the gas wells is transported to GGS (Group Gathering Station), where all the contaminants are removed, and oil, water, and gas are segregated. It is then transported to GCP (Gas Compression Plant), where the gas is pressurized and compressed for long-distance transportation to consumers. In the process, gas is vented and flared at three locations, namely: gas well sites, GGS, and GCP [4][5]. Figure 1-3 is a depiction of the gas storage, transportation, and distribution architecture with well-defined flaring spots.

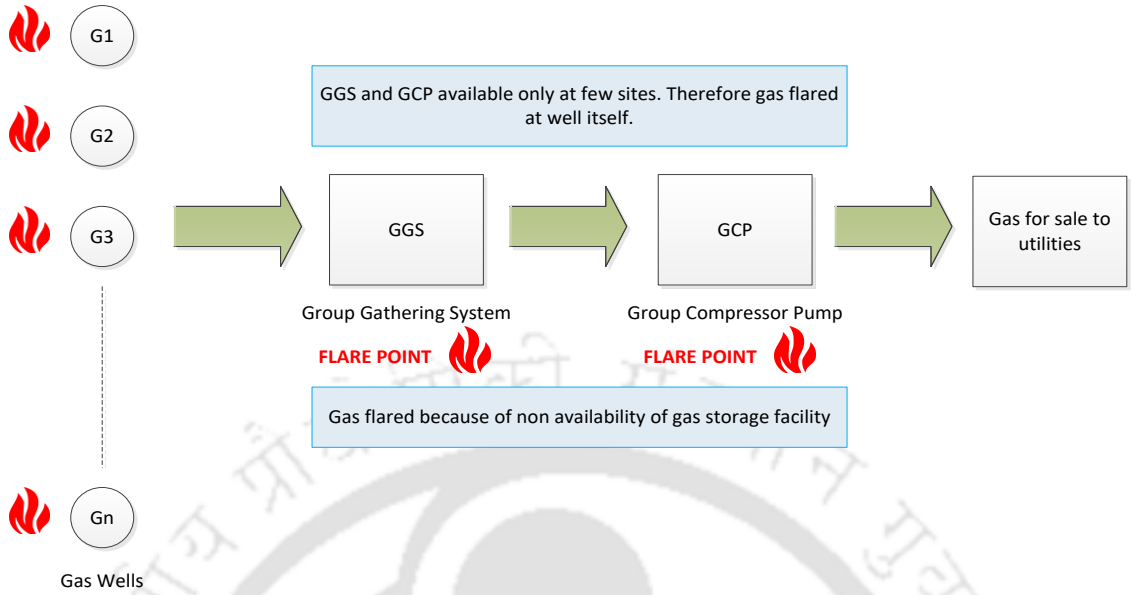

Figure 1-3. Gas Generation, Gathering, and Distribution Architecture

At any of these sites, the gas flares can be broadly categorized into two categories: Technical flares and additional flares. This categorization is largely based on the quantity of gas being flared over a period of time. Technical flare is crucial for maintaining oil and gas production. This means that it never changes over the day, month, or year. In contrast, the amount of added flare varies significantly hourly, daily, and monthly.

The imbalance between supply and demand is what causes fluctuating extra flare. All of the produced gas must be flared because it cannot be sold or stored. Due to the following factors, GGS and GCP are significant places for gas flaring[6]:

- The amount of gas produced might not be adequate to warrant building pipes to serve distant processing facilities.
- For a well to be successfully drilled and flow rates to be established, it is occasionally required to produce natural gas for a brief period of time. It is necessary to flare off such a modest amount of created gas.
- Natural gas can be released as a result of incidents that happen during pipeline installation, production, processing, or drilling.

2.2 Gas Flaring in the Indian Context

33.63 percent (2958.25 MMSCM) of the entire onshore natural gas output (8795.63 MMSCM) is produced in Assam alone [12], and 6.29 percent of it is wasted due to flaring.

The Indian Government has set a target to reduce carbon emissions as a percentage of GDP by (33–35%) from 2005 levels by 2030, according to INDC (Intended Nationally Determined Contribution). Additionally, by 2030, India promises to generate 50% of its electricity from sources other than fossil fuels [7].

Figure 1-4 presents the monthly average technical and additional flares data at three oil and gas producing fields: Lakwa, Geleky and Rudrasagar. These thirteen gas flare locations have been considered for the analysis in this Ph.D. thesis. The energy which could have been generated if the additional flare was utilized to generate electricity is calculated and presented in the figure (Lakwa – 536 MWh, Rudrasagar – 160 MWh, Geleky – 10 MWh). Also, the daily carbon dioxide emission due to the current flaring status is calculated and presented (Lakwa – 118 Megatons, Rudrasagar – 16 Megatons, Geleky – 46 Megatons).

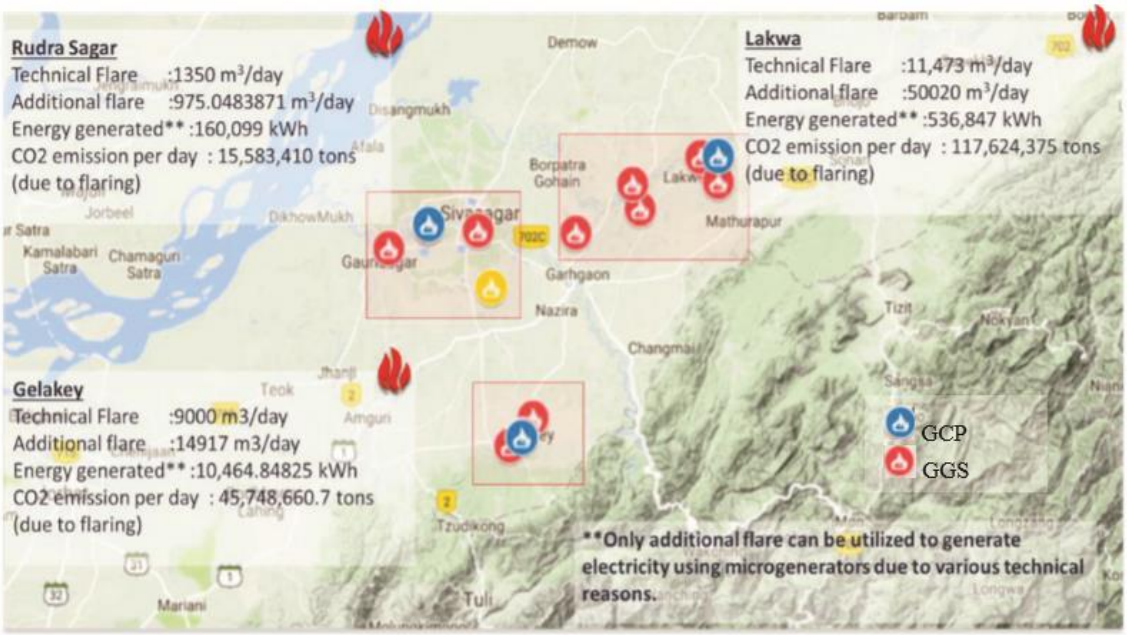

Figure 1-4. Gas flaring sites in Nazira area (ONGC, Assam asset). Source - Google Maps

2.3 Electricity scenario in India and the World

The growing population, rising GDP, and industrialization all over the world are responsible for a rise in energy consumption. China is the most populous country with the highest energy consumption. India ranks second in terms of population but is far behind China and the United States in terms of energy consumption. However, India is projected to cross China in terms of population by 2023, and then the per capita energy consumption will also shoot up. Figure 1-5 and Figure 1-6 show the trends of energy consumption and population growth in the most populous countries of the world. After the Paris agreement,

there is pressure worldwide to increase energy efficiency and switch to sustainable sources of power generation.

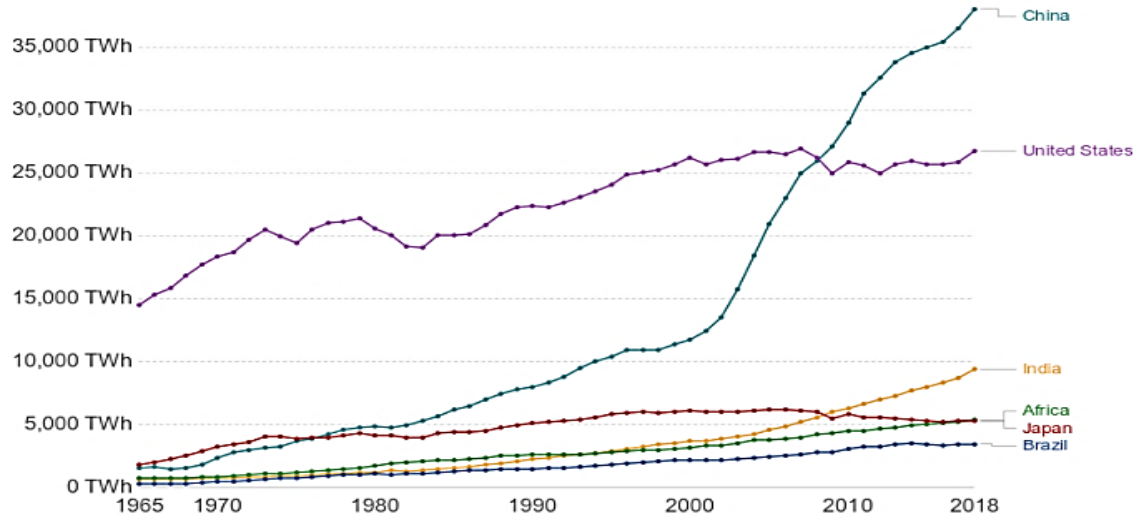

Figure 1-5 Trend of energy consumption by most populous countries of the world (Source – World Energy & Climate Statistics – Yearbook 2022, Enerdata)

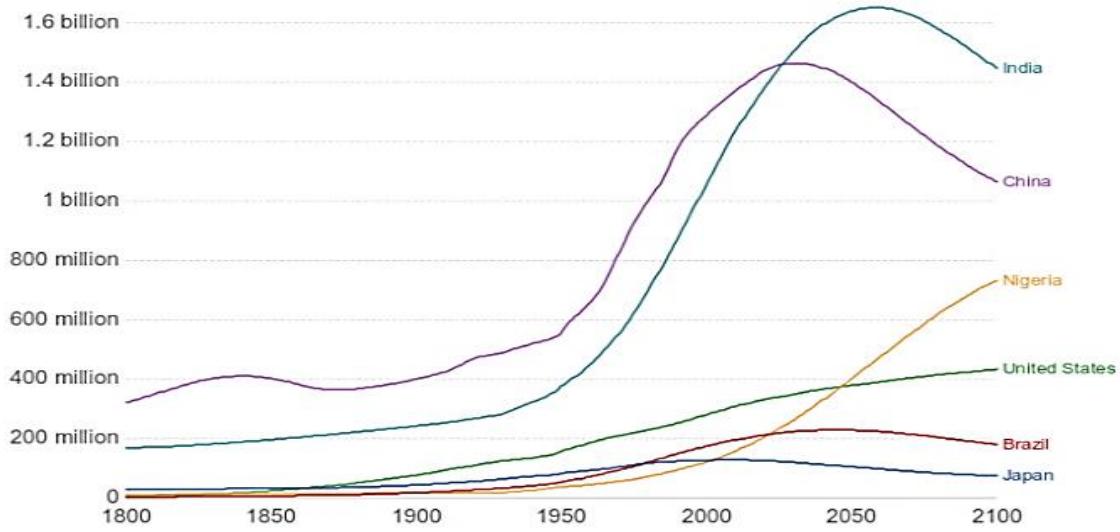

Figure 1-6 Trend of population growth of most populous countries across the globe (Source – World Energy & Climate Statistics – Yearbook 2022, Enerdata)

India contributes 18% of the global population while using only 6% of the primary energy. By 2023, India will have the largest population in the world, which will result in a 156 percent increase in primary energy consumption [14,15]. India currently has a severe electricity crisis, which is only going to get worse over the coming decades. Even though data show that by February 2019, all Indian families would have access to electricity, the status of the power supply in electrified villages is appalling, with low supply dependability

and 27 percent of the village's energy needs unmet. The major difficulty for India currently is providing better quality energy, not just access to it. The amount of hours a home receives power varies significantly across the nation. In India, 20% of families have access to less than 8 hours of electricity each day, and just 47% have access to more than 12 hours. The majority of gas flare locations are in rural areas without power and with unstable supplies.

The national average for per-person energy use is 1149 kWh, however, Assam's use is incredibly low at 339 kWh. Assam's situation is typical of many other Indian states, including all of the northeastern states, which have inadequate rural electrification. Naturally, the need for electrification in the rural areas of Assam and several other states resulted in a number of policy measures, which were then funded on a national and international level. These rural electrification initiatives have been running for many years.

As per our discussions with governmental agencies, extensive site visits, and villagers, the power tariff of Assam is higher than most of the states in India. This is because of the following reasons:

- The cost of distribution is high due to the extensive network for difficult terrain in Assam.
- Assam is one power deficit region. Assam Power Distribution Company (APDCL) faces an increase of nearly 10% every year in importing power to meet consumer demands. It imports 1500 to 1800 MW from other utilities to fulfill its energy demands.

The problems are both: a lack of sufficient power generation capacity and a lack of transmission and distribution infrastructure. It is observed from existing literature [8]–[14] that 15-20 % of the power generated in India is lost in transmission and distribution networks, and around 10-20% of power loss is accounted to theft across utilities in India, which is also known as power pilferage. In total, approximately 40 % of power is lost in transmission. So such a situation requires implementing a microgrid, which is a decentralized generation using several available Distributed Energy Resources (DERs), including the waste flare gas. Due to reliance on dynamic weather conditions, it is seen that integrating renewable energy sources like solar and wind adds intermittencies and stochasticity into the system. However, research [16,17] has shown that combining several energy sources can successfully address the issues of randomness, variability, and

unpredictability of solar or wind energy [15]. In comparison to single energy source systems, hybrid (many source-based) energy systems have a lower net present cost, higher energy efficiency, and a more consistent supply of electricity [26][27].

2.4 Policy Initiatives to push renewables all around the world

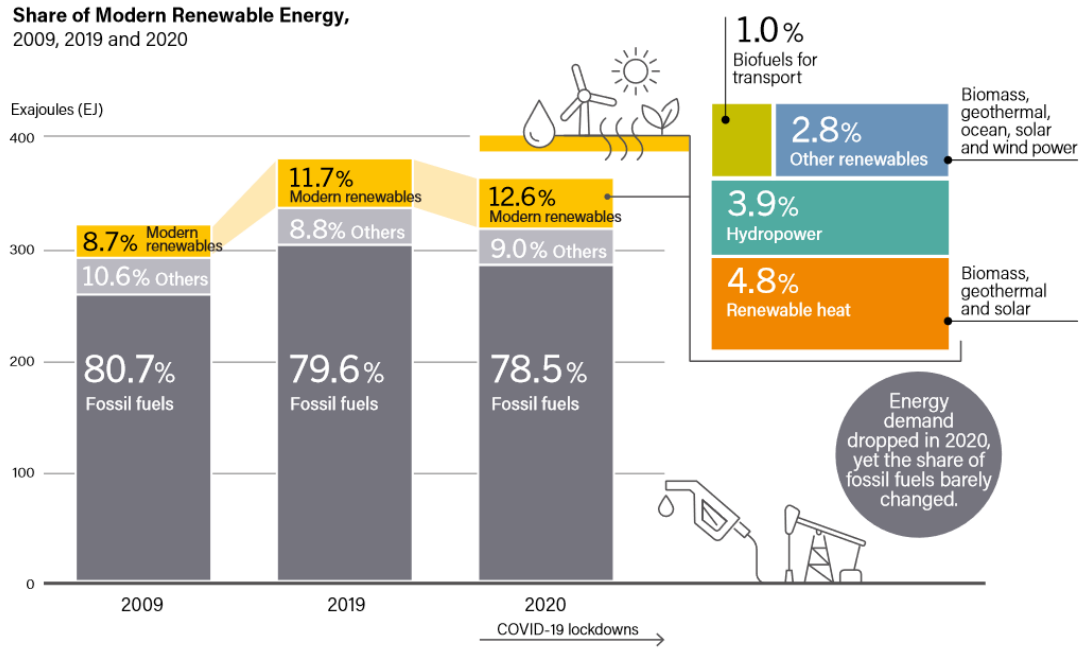

Figure 1-7 Share of renewables and fossil fuels in total energy production at global (Renewables 2022, Global Status Report)

Fossil fuel sources (coal/oil) power 78.6 % of electricity worldwide and 85% in India [16] (refer to Figure 1-7). Our continued dependence on fossil fuels for energy generation will lead to an emission of 750 billion tons of carbon on finishing all the currently known reserves [17]. To keep the average global temperature rise below 2˚C (as has been agreed in the UN-Paris agreement) [18], we have to leave 75-80% of fossils untouched [19]. Since energy generation and energy demands are increasing exponentially year after year, the percentage of renewables in the total electricity production has to be raised by at least to 50% by 2030 worldwide [20]. As per a report, the renewable power capacity additions increased by 17 percent in 2021 to a new high of more than 314 GW of installed capacity. The total installed capacity of renewable energy increased by 11% to about 3,146 GW, but this is still far short of the deployment required to keep the world on pace to achieve 'net zero emissions' by 2050 (see Figure 1-8).

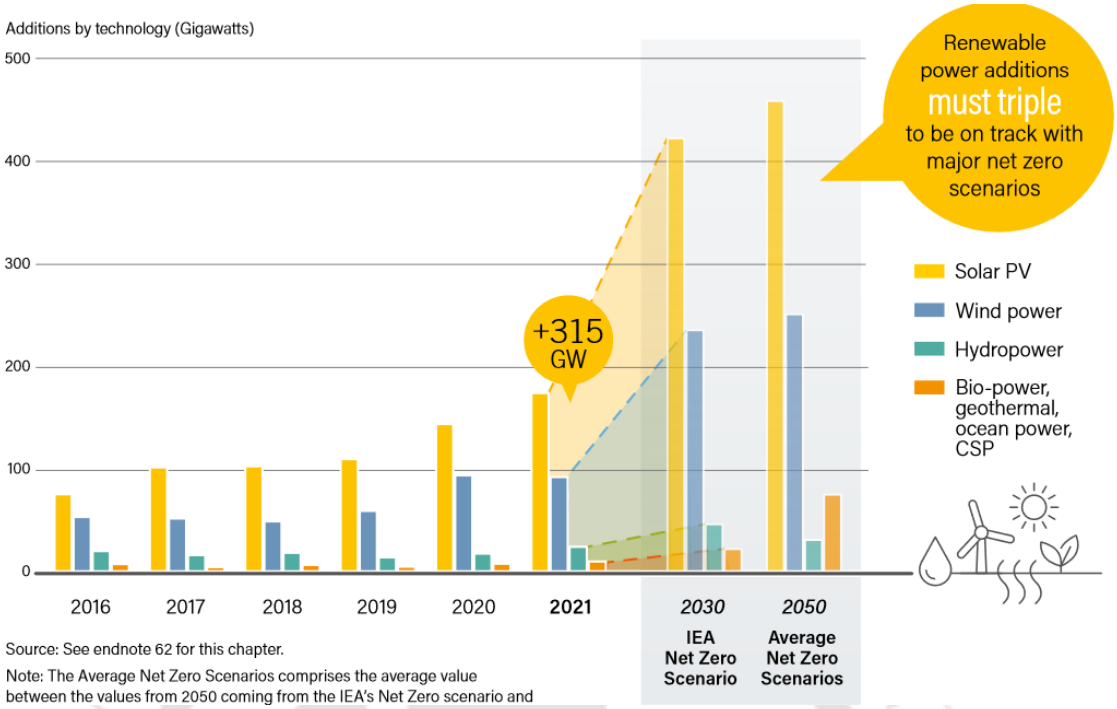

Figure 1-8 Trend showing growth in renewable energy installations from 2016 to 2021 and projected targets by 2030 and 2050 (Source - Renewables 2022, Global Status Report)

To achieve the world targets of net zero emissions, all countries all over the globe have set up policies to push renewables and have invested heavily in Hybrid Energy Systems (HES) / Smartgrids/ Microgrids/ Distributed Generation. A list of country-wise carbon dioxide emission and renewable generation status and targets are tabulated in Table 1-1.

The extent and rate of smart grid deployment vary depending on the various needs, regulatory contexts, legacy systems, and energy resources of various countries [21]. Countries like the USA, UK, and Japan with high per capita CO_2 emissions are looking forward to reducing carbon emissions by investing more in electricity production through renewables. Therefore, the current policies in economically developed countries focus on data protection, consumer privacy, cybersecurity, net metering, time-based tariffs, etc. [21]. Whereas, for developing economies with a high population density, keeping pace with the globally proposed renewable integration targets becomes difficult.

Table 1-1. CO_2 emissions, reduction targets, and share of renewables in total electricity production for a few countries [22]

Countries	**USA**	**UK**	**Japan**	**South Korea**	**China**	**India**	**Saudi Arabia**	**Turkey**
Per capita CO_2 emissions (MT)	16.56	5.62	9.13	12.89	7.05	1.96	18.48	5.21
% Renewable Generation	17.29	36.86	18.82	5.47	26.68	19.04	0.5	43.60
CO_2 emission reduction targets	26-28 % below 2005 by 2025	50% below 1990 levels by 2023-27	26% below 2013 levels by 2030	37% by 2030	60-65% in carbon intensity by 2030.	11 million tonnes in less than a year	130 million tonnes by 2030	No record found

As depicted in Figure 1-9, the emerging economies with high population density like India, Saudi Arabia, and China are trying to cut carbon emissions by providing subsidies, financial incentives, investing in research and development, etc., to meet the global renewable energy targets. For example, with the second-highest population and fossil fuel reserves sufficient to meet the energy demands for the next 150 years, India ranks third with a renewable energy investment worth Rs 1.75 lakh crore in the year 2021-22. India encourages its citizens to give up cooking gas, kerosene, and diesel subsidies and support river rejuvenation projects, waste management, and tree plantation. As per the new Nationally Determined Contribution announcement (November 2nd, 2021), the Indian government targets to bring down carbon emissions by 1 billion Giga tons and increase the share of renewables by 50% by 2030 [23]. India also targets to have net zero carbon emissions by 2070. After the 21st Conference of Parties (COP21) of the UNFCCC [24], there is tremendous pressure on developing countries like India, with a high population density of 382 people per sq. Km.[25] and even higher energy demands (9410 TWh in 2018) [26] to limit their carbon emissions. To maintain its GDP growth targets, China states that its CO_2 emissions will be at it's peak in 2030, but it promises to reduce the carbon intensity by 60-65%. Being a petroleum-dependent economy, Saudi Arabia is investing more in research and development to find ways to mitigate or utilize flare gas from oil and gas fields. According to World Bank, these flared gas can produce more electricity than the entire African continent is consuming today [27].

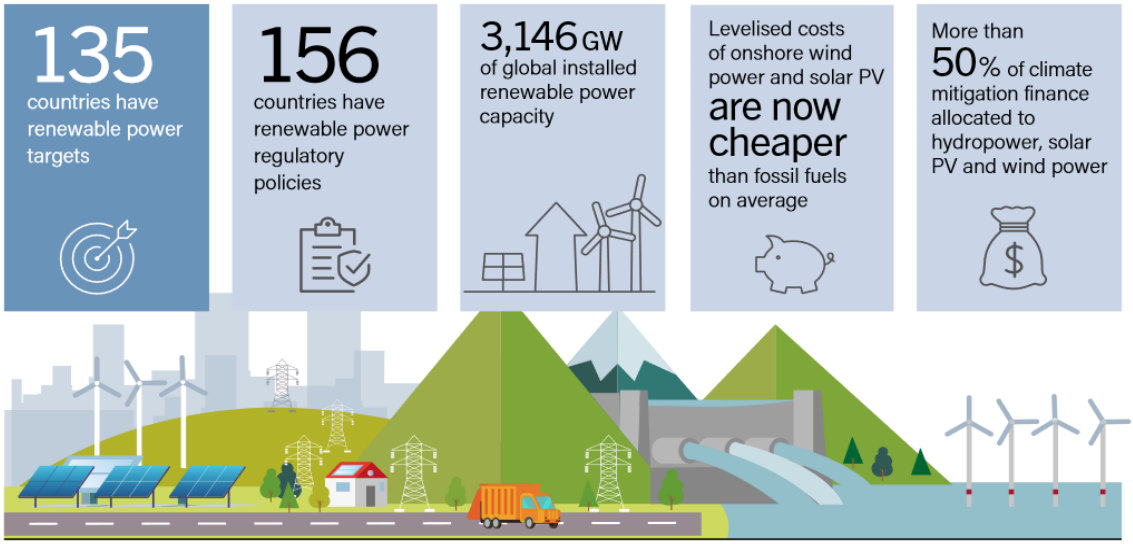

Figure 1-9 Renewable integration targets, status, and incentives worldwide (Source - Renewables 2022, Global Status Report)

2.5 Decentralized Hybrid Renewable Energy Generation: A Possible Solution

While developed economies are pushing for more renewable integration and independence from fossil fuels, the developing economies are trying to mitigate the ever-escalating gap between electrical power generation and consumption due to rapid industrialization and urbanization. In many developing countries, there may be no power access at all. People may not have any other option than getting electricity through renewable-powered decentralized off-grid generation. In other areas with grid power availability, the power can be so unreliable that a decentralized Hybrid Renewable Energy System (HRES) proves to be a safer and more reliable option. Although the situation and goals are different, HRES is the techno-economically apt solution in all the scenarios. Most oil and gas fields are remotely located with unreliable grid connectivity and surplus natural gas availability which is always wasted as flares. Therefore distributed microgrid systems utilizing the waste flare gas to generate power as a microgrid system are best solution for solving the electricity problem as well as problem of gas flaring.

Centralized power generation in big scale facilities using fossil fuels or nuclear technologies is no longer a vision that climate change scientists, policymakers, and growing majorities of voters support. By allowing consumers to select and install various energy sources in tiny increments, distributed energy generation (DEG) makes it easier to utilise these resources. The power that is needed to satisfy end-user demand is provided by these

units.Technology including gas turbines, fuel cells, diesel and gas reciprocating engines, solar panels, and wind turbines are used to generate distributed electricity at or close to the place of use.

The conversion of centralised energy production facilities to a DEG system has numerous benefits. The key environmental advantage of distributed systems is the decrease of carbon dioxide emissions from fossil fuels and the replacement of those emissions with renewable sources like wind and solar energy. As DEGs allow governments and utility division decision-makers to avoid substantial capital investments in new fossil fuel-based power plants and create transmission and distribution infrastructure, long-term cost benefits can be attained. Due to the proximity of DEG facilities to commercial, industrial, and residential consumers, there are fewer energy losses that could result from inefficient power lines. Additionally, the close proximity of production and consumption allows for easy access to tiny heat sources and sinks as well as the opportunity to utilise waste heat for cooling and heating, which is hardly practical in centralised power generation. Furthermore, DEG's location flexibility has a significant favourable impact on energy costs. The distributed system offers a variety of alternatives for different fuels and energy resource types using various technologies. As a result, there is no need to utilize one type of fuel only, which can lower fuel prices for consumers.

In addition to the economic advantages, DEGs have advantageous technical effects on system performance, such as enhancing voltage profile and power quality. By supplying enough power in relation to demand and limiting unused power flow inside the transmission network, they can lower the power losses in the distribution networks.

Compared to traditional power generation systems, combined heat and power (CHP) units are more cost-effective. A combined heat and power system allows DEGs to capture energy that would otherwise be lost and wasted. They use waste heat for heating, cooling, or creating extra electricity to increase their efficiency, which is not possible when using centralised power generation.

The decentralized HRES can be categorized into the following:

1. **Pico-power System**: When appliances that are directly linked to a power source produces between 0.001 and 0.01 kW of electricity, such systems are referred to as Pico-

power systems. The classic example is the pico-solar lantern, which offers both light and power for charging cell phones.

2. **Solar Home Systems**: A combination of solar photovoltaic panels and batteries that generate 0.01 to 1 kW power for a single building are described as solar home systems. In developing nations, such systems are typically fully DC (in generation and consumption), with a capacity under 200 W.
3. **Microgrids**: They have a generating capacity between 1 kW - 1 megawatt. They operate on low or medium voltage levels and are typically not geographically spread out. The idea of a Microgrid is generation at the point of consumption with only localized power transmission capability. They may operate in either grid-connected or islanded mode.
4. **Virtual Power Plants**: They are cloud-based virtual power plants that integrate the capabilities of various distributed energy resources (DER) capabilities to increase power generation and trade or sell power on the market for electricity. When multiple distributed generation or microgrid systems are situated nearby, they may operate collaboratively to share each others' resources optimally as a VPP. *Figure 1-10* gives a general idea of a VPP.

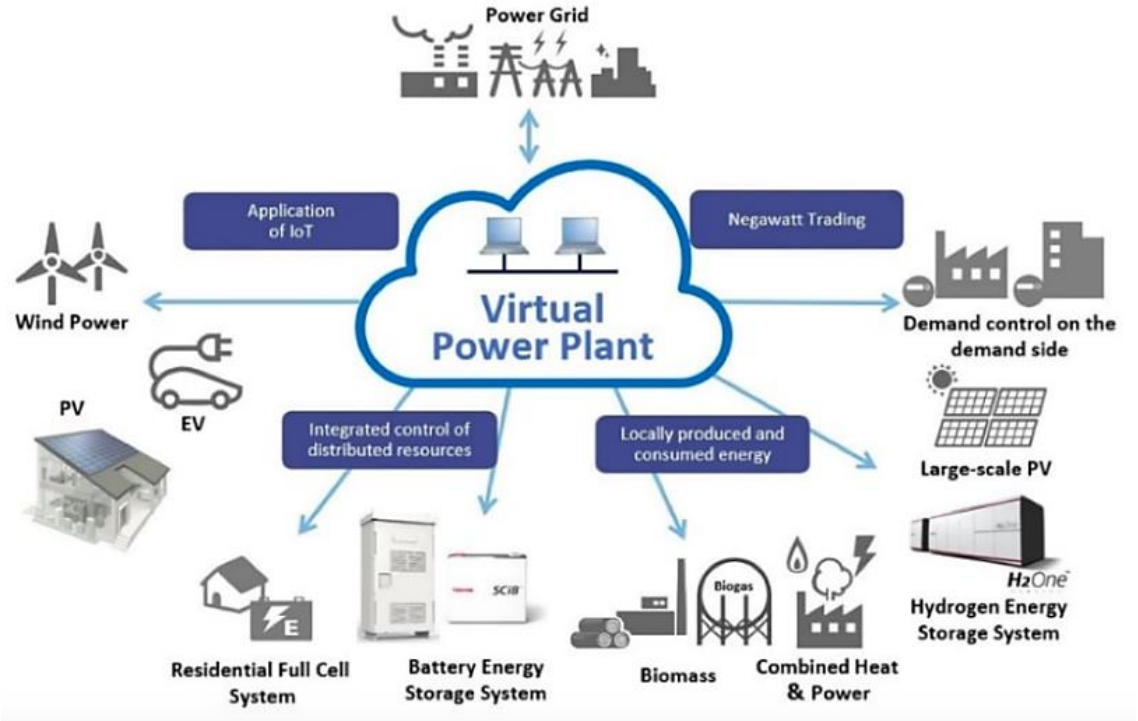

Figure 1-10 Schematic of a Virtual Power Plant (Source: Global Infrastructure hub)

VPP and microgrids have some resemblance. The difference is that a microgrid has a defined network boundary that can detach from the broader grid to form a power island.

VPPs have far greater geographic reach and can grow or contract in reaction to the existing market conditions.

VPPs generally use Decentralized Control (DC) for their operation. The distinction between Decentralized and Centralized Control (CC) and advantages of DC over CC are presented in Table 1-2.

Table 1-2 Centralized Control Vs. Decentralized Control

Attributes	Centralized Control	Decentralized Control
Necessary communication infrastructure	Data traffic from all the multi-agent systems will be too heavy to handle for one single controller.	Selective data can be screened from neighboring nodes for further processing at each decision-making node.
Number of controllers	Only one controller will be required.	Multiple controllers are required.
Type/ capability of controller	More high-performance controllers are required to handle the heavy data traffic.	A little inferior in performance controller will be sufficient to do the job since they have to deal with lesser data traffic.
The overall cost of control framework	The cost of setting up the control framework may be less, but the cost due to failure will be quite high.	The initial cost of setting up of control framework may be high due to more number of controllers involved. But decentralized control framework will prove to be cheaper in the long run, taking into account the socio-economic cost due to failure.
Robustness	If the central controller fails, the entire system fails. Hence, the chances of failure more.	If anyone of the controllers fails, there will be other controllers available to keep the system operational. Hence, the chances of failure are less.
Self-healing capability	Since there's only one main controller, if it goes down due to communication or device failure, the central control strategy will be expensive considering the cost of repair, maintenance, and penalty due to the non-availability of power.	A decentralized control framework will be blessed with self-healing capability because if any controller faces a device or communication failure, others in the network will serve its purpose.
Decision making	Entire decision-making is in the hands of one central controller. The central controller is the boss. Rest all follow its commands.	All controllers have equal decision-making capability. None of the controllers is boss or dominant when it comes to decision-making.

Attributes	Centralized Control	Decentralized Control
Specificity of the control algorithm	With a centralized architecture, the control algorithms are predominantly fixed and allow little room for modifications.	With de-centralized architecture, the algorithm can be flexible and need-based depending on the number and type of controllers making the overall operations of the Microgrids efficient.
Means of interaction between controllers	There is no interaction between the controllers as the central controller takes all the processing and decisions.	A communication ring needs to be created for interconnecting the controllers and enabling peer-to-peer communication.
Response time and execution time	Inter-controller communication over lower bandwidth may lead to greater response time. The processing and execution may take more time as s single controller doing all the job consume more RAM space.	Here only the required data is exchanged between the controllers, reducing the latency and improving the response times. Also, as only specific logic is implemented, the execution time is reduced.

2.6 Microgrids

Till 2016, microgrid solutions have provided electricity to nearly 90 million people worldwide [20]. Literature defines microgrids in numerous ways. The most popular one is- "Electricity distribution systems, up to 1MW in capacity, comprising of different loads and distributed energy resources like distributed generators, storage devices, or controllable loads which generate a controlled output. These distribution systems operate in a coordinated manner even when isolated (island condition), commonly known as microgrid" [28].

In recent years, Microgrid has become popular due to their ability to integrate different power generation resources. Renewable penetration is basically encouraged because of its capability to reduce carbon emissions. Wind, solar, hydropower, geothermal, biomass, and natural gas are the six major forms of renewable energy sources, which can act as distributed energy resources (DER) and can be captured by organizing these resources into Microgrid.

Following are the generation source and loads in a microgrid:

- Renewable generating sources like solar photovoltaic panels, wind turbines, hydro turbines, microturbines for natural gas, etc.
- Diesel generators

- Battery Energy Storage System (BESS)
- Loads connected to feeders

A microgrid can provide quality, reliability, and stability because it uses advanced technology like – controllers, power conditioning equipment, battery storage, etc.

Figure 1-11

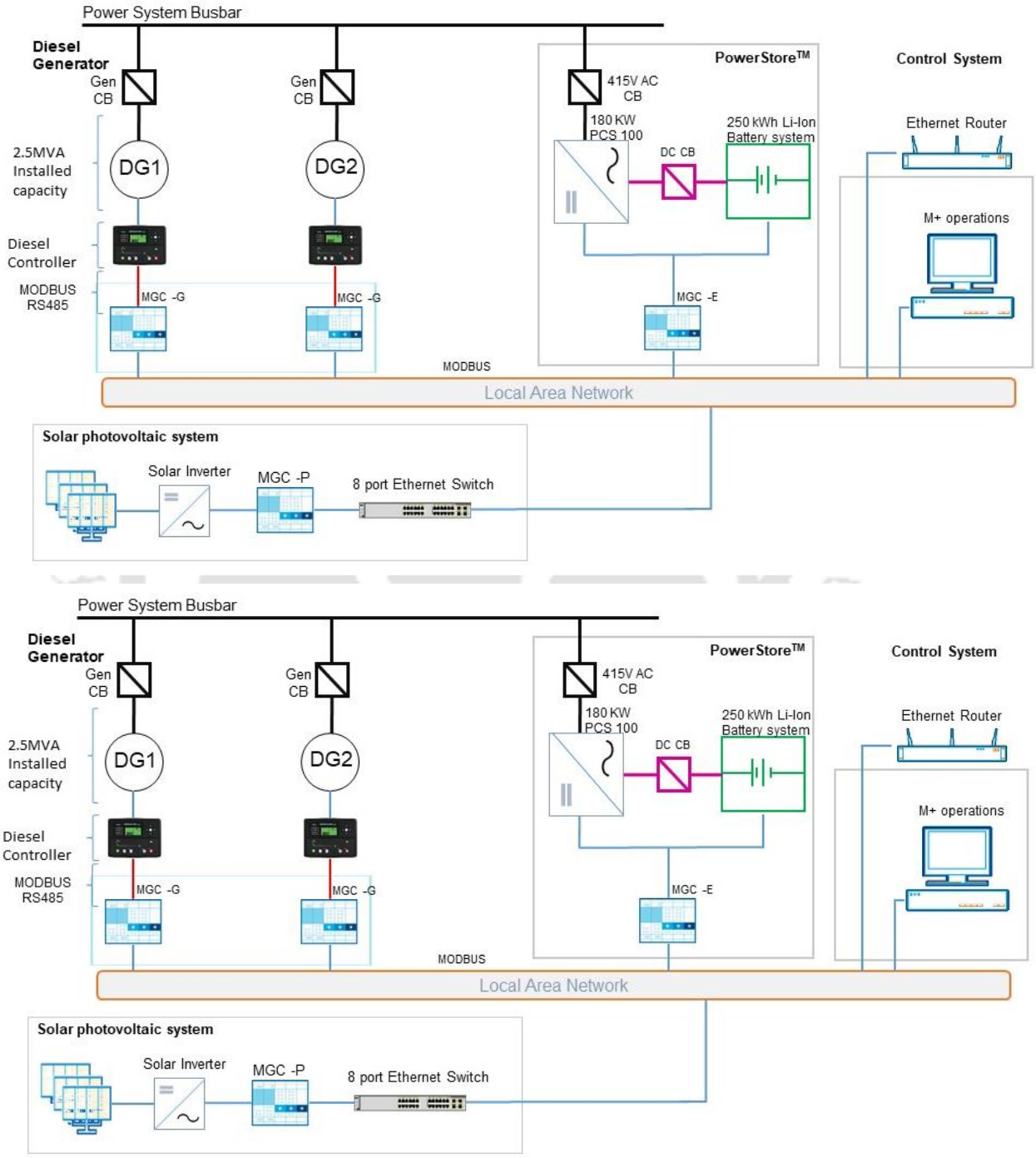

Figure 1-11 Schematic of a Typical Microgrid

shows the schematic of a microgrid having two diesel generators as a backup system, one Power Store, one solar photovoltaic system, and the microgrid control system. A controller is required for each generating source, load feeders, and point of common coupling between Microgrid and grid. A hierarchy of three layers—primary, secondary, and tertiary—represents current best practices in microgrid control. Primary control manages transients that threaten the system's stability, secondary control is in charge of restoring the voltage and frequency of the microgrid, and tertiary control, acting over longer time horizons, is in charge of maximizing the microgrid's economic performance [29].

Power conditioning equipment and battery storage systems are required for active and reactive power support, maintaining power factor at the point of common coupling (PCC), and providing hot spinning reserve per the system requirement.

Further, Microgrid provides the possibility of power availability in remote areas where the connectivity of conventional transmission and distribution networks is not feasible by scheduling and distributing the demand amongst renewables, diesel generators, and battery storage. This scheduling and distributing demand amongst various DERs can be performed using an efficient '*dispatch strategy*'.

- ***Microgrid Dispatch Strategies***

Different dispatch techniques for hybrid renewable energy systems (HRES) with numerous storage and auxiliary/backup components can be designed based on these components' consumption and charging sequence. The Dispatch Strategies (DS) govern the sequence of operation of various components in a microgrid and can be seen as the brain of the microgrid system. An efficient dispatch strategy is responsible for reducing operational costs and maximum utilization of available resources. Load Following (LF) and Cycle Charging (CC) are two dispatch methods used by many researchers.

Load Following Dispatch: In the load following approach, the generator generates only enough power to meet the load demands. Renewable energy sources are reserved for lower priority tasks like recharging the storage bank or supplying the deferrable load.

Cycle Charging Dispatch: In the cycle charging dispatch strategy, the generator operates at full capacity, and any excess electricity charges the battery bank.

The dispatch strategies can also be customized to suit the unique requirements of a microgrid project. The dispatch strategies are discussed in detail in chapter 5 with flow charts, wherein a novel dispatch algorithm for oil and gas fields is developed.

2.7 Gas Microturbine

Gas microturbines are thought of as a possible remedy to lessen gas flaring at oil and gas operations. Historically, the majority of gas turbines used in power generation were massive, producing more than 1 MW of electricity. However, microturbines are also designed for use in distributed generation or microgrid systems for continuous or backup power and peak shaving applications in Microgrids. These micro turbines vary from 20 kW to 300 kW in rating. Instead of the axial components that are prevalent in bigger gas turbines, a typical microturbine will use a radial compressor and turbine. The single-stage compressor and turbine are attached to the same shaft and separated by a combustion chamber. On the same shaft, a high-speed generator will be installed. Figure 1-12 shows the operational schematic of a gas microturbine. The fuel enters the combustion chamber, and hot combustion gases spin the turbine, which is connected to the shaft of an electrical generator. The exhaust transfers heat to the incoming air. Air passes through compressor and is warmed by the exhaust gases before entering the combustion chamber. The microturbines have a high rotational speed ranging from 40,000 to 1,20,000 revolutions per minute. The generator's frequency is 1000 Hz. Microturbines are equipped with power electronic frequency conversion equipment to match the grid frequency. These tiny turbines have the option of operating independently or in sync with the grid. Microturbines typically have recuperators fitted to boost their efficiency to 25-30%.

These turbines are more durable without recuperators but only offer lower efficiency of up to 15%. A recuperator's job is to reuse exhaust gas to warm up compressed gas before it reaches the combustion chamber.

The biggest advantage of using a gas microturbine is that it can use any kind of fuel (gas/ oil) with any calorific value, and the emission output is almost negligible. NOx is the only gas found in emissions from a gas microturbine. With special attachments, the emission output can further be reduced. Gas Microturbines are widely used in the United States to reduce carbon emissions and produce electricity wherever possible. *Table **1-3*** shows a

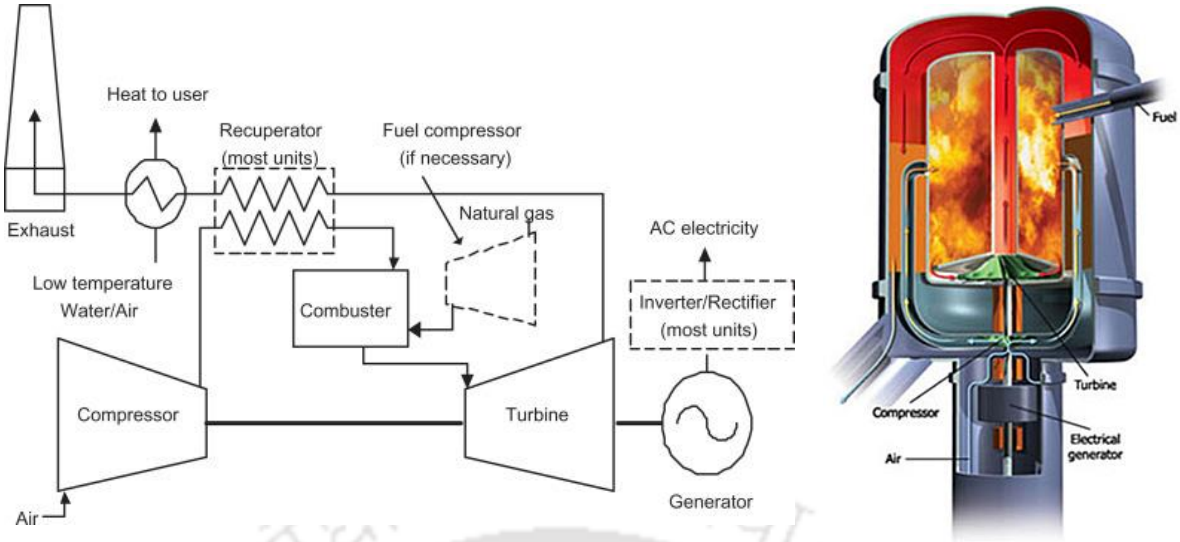

Figure 1-12 Operational schematics of a gas Microturbine (Source: WBDG)

comparison of various ready-to-install gas microturbine technologies available on the market.

It was shown using several case studies [30] that natural gas, which is flared, could be a potential source of generating electricity. Davis [31] suggested that flare natural gas can be used for power generation via microturbine at a remote location, where the cost of the required infrastructure is uneconomical. Thus it can be an efficient power generator in a microgrid and will be able to solve the problems of gas flaring and unreliable electricity effectively. Backed up by policy initiatives and financial incentives worldwide to reduce carbon emissions and push renewable integration, microgrids incorporating gas microturbines seem to be an effective solution. Various algorithms for selecting site for installing such systems, power dispatch strategy, distribution network design, and power and energy management in such systems are explored in this Ph.D. research.

Table 1-3 Comparison of various gas microturbine technologies available in market

Technology	Power Output Range	Fuel used	The concept behind the design	Efficiency	Cost
ElectraTherm's Power+ Generator (Employed in North Dakota Oil wells)	Up to 110 KWh	Waste heat (77-122 degree centigrade) from Gas Flares, Oil & Gas, Geothermal, Biomass / Biogas, Boilers	Organic Rankine Cycle	15%	$ 0.03 US/kWh (minimum for Power+ GeneratorTM Heat to Power Generator). Further pricing available on seeking quotation.

		& Process Heat, Waste Water Treatment				(source: gulfcoastgreenenergy.com)	
GE's Jenbacher Gas Engines	0.3 to 9.5 MW	natural gas, biogas, coal seam gases and associated petroleum gas.	Brayton Cycle	Up to 40%. electrical efficiency. More efficiency with CHP and CCHP applications.		Available on seeking quotation (source: clarke-energy.com)	
Capstones Microturbine	25-500 KW	Any combustible gas	Brayton Cycle	Un-recuperated	15%	Capital Cost	$700-$1,100 /kW
				Recuperated	20-30%	O&M Cost	$0.005-0.016/kW
				With Heat Recovery	Up to 85%	Maintenance Interval	5,00-8,00 hrs

2.8 Summary

The first section of the introduction chapter presents the current global and Indian scenario of gas flaring, along with various disadvantages of natural gas flaring. This section has also discussed the natural gas production, transportation, and distribution architecture. The second section highlights the growing energy demands with a rise in the global population. The problems with current electricity infrastructure at the global and Indian level has been covered. The introduction highlights the pressing need for an increase in renewable penetration and carbon emission reduction. Various policies and financial incentives adopted by multiple governments worldwide have been presented in this chapter. Finally, microgrids incorporating gas microturbines for utilizing waste flare gas to generate power in oil and gas fields has been identified as a potential problem to solve the pressing issue of gas flaring and unreliable electricity.

Chapter 2
State of The Art

2.1 Foreword

Gas flaring is an issue of severe environmental and economic concern. Employing a gas microturbine-based microgrid system has been identified as a potential solution to reduce flaring and generate electricity. This solution aligns with the United Nation's Sustainable Development Goals (SDGs) of reducing carbon emissions and increasing renewable penetration in electricity production. Several researchers have explored the designing of various combinations of microgrid management systems. Distributed generation and microgrid concepts were introduced about ten years ago, and researchers worldwide continue to examine them. However, a microgrid generation system has been used to cater to the requirements of oil and gas fields. The first step in installing a microgrid system is to select the correct location. Out of the hundreds of gas flare sites in an oil and gas field, choosing the appropriate one is crucial to enhance the efficiency of the system. Designing a Distributed Energy Resource (DER) scheduling and dispatch strategy suiting the requirements of oil and gas fields is also crucial to maximize the utilization of waste flare gas to generate power. Prediction of DER generation is essential to designing the appropriate dispatch. When multiple gas-well-based Microgrids are situated close to each other, power and energy management in the multi-microgrid system will be crucial for maximum utilization of available resources and increasing overall system efficiency. Therefore, this chapter reviews various multi-criteria decision-making (MCDM) algorithms for site selection. A systematic review of hybrid energy systems and various software available for their design, simulation, and optimization has been covered. A study has been presented on various machine learning and optimization techniques used for renewable energy prediction and power management in microgrid and multi-microgrid systems.

The content in this chapter has been published in the following papers:

- Deepika Bishnoi and Harsh Chaturvedi, 'Optimised Site Selection of Hybrid Renewable Installations for Flare Gas Reduction using Multi-Criteria Decision Making', Energy Conversion and Management X, 2022. https://doi.org/10.1016/j.ecmx.2022.100181.
- Deepika Bishnoi and Harsh Chaturvedi, 'Optimal Design of Microgrid Power Management System for Economic and Environmental Sustainability of Onshore Oil and Gas Fields', Energies 2022. https://doi.org/10.3390/en15062063.

2.2 Site Selection for gas well-based Microgrid Installation

While designing a microgrid, selecting the right location to get maximum yield from the microgrid project is crucial. The selection should consider multiple conflicting objectives because of multifaceted social, ecological, economic, and technological aspects. Since Multi-Criteria Decision Making (MCDM) methods take into account several competing objectives and decision-makers' preferences, they are growing in popularity in the site-selection decision-making of renewable energy power plants. For the complex site selection problem, MCDM approaches to aid in dealing with many, often contradictory criteria in an organized manner, allowing different preferences to be addressed. MCDM methods have the advantage of using several criteria or attributes to produce an integrated decision-making outcome compared to single-criteria approaches.

The MCDM problem for choosing a renewable energy site typically involves several alternatives that are assessed using a multitude of distinct criteria. This procedure consists of six major steps: alternative formulation, criteria selection, data normalization, criteria weighting, alternative evaluation, and outcome validation. These six steps don't need to appear in the abovementioned order in a real-world scenario. The six steps might even overlap in some cases. The problem and the study area must be defined in the first step, the formulation of alternatives. The problem here is the ranking of installation locations of one or perhaps more renewable energy sources, and the study area is chosen by the researcher based on actual circumstances. The selection of criteria is the next step. This stage involves gathering and defining the exclusion and evaluation criteria, which profoundly affect determining whether a particular site is suitable for the installation of Hybrid Renewable Energy Systems (HRES). The third stage involves gathering and normalizing data related to the criteria. The starting data originates from actual numerical figures, decision judgments, or both. They are then subjected to a normalizing procedure in order to make them suitable for quantitative calculations. The fourth stage involves calculating the weight factors for the evaluation criteria. The criteria used to create practical solutions do not always have equal weights; therefore, it is vital to specify each one's influence using the proper weight coefficients. The normalized weights of the criterion are determined using weighting techniques. In the fifth stage, when exclusion criteria are specified, problematic areas are eliminated from further analysis based on the exclusion criteria. Then, using MCDM techniques and the inputs on the alternatives and criteria, a regional suitability evaluation or ranking of the locations is carried out. The

sixth stage validates and evaluates the outcomes. The most advantageous site for the development of HRES will be identified if the validation confirms that the results are legitimate.

In this regard, Kumar et al. [32] considered social, economic, technical, and environmental traits to select suitable energy alternatives for designing the microgrid. Nazari et al. [33] chose solar radiation, average temperature, grid accessibility, distance from the demand site, land availability, social acceptability, the effect of progress on the surrounding environment, security, and risk, as the deciding factors for site selection for solar power plant installation in Iran. In another Iran-based site selection study, Azizkhani et al. [34] considered solar radiation index, economic, technical, and geographical factors for solar power plant installation. In a similar Indian context, Sindhu et al. [35] evaluated the feasibility of solar power plant installation in the Haryana district based on social, technical, economic, environmental, and political aspects. Yunna et al. [36] attributed site selection for solar-wind hybrid power stations to accessibility to the grid connection, solar and wind resource availability, cost-benefit ratio, and social and ecological impact on surroundings. In a similar solar-wind farm site selection study by Jun et al. [37], wind power density, frequency, direction, turbulence intensity, solar radiation, local power demand, construction cost, operation and maintenance cost, traffic, transmission line length, pollution, and social factors were considered for the analysis.

Several MCDM methods such as AHP (Analytical Hierarchy Process), TOPSIS (Technique for Order of Preference by Similarity to Ideal Solution), WASPAS (Weighted Aggregated Sum Product Assessment), and PROMTHEE (Preference Ranking Organization Method for Enrichment Evaluation) were discussed and compared to solve issues in the energy sector by Butkiene et al. [38]. Table 2-1 Comparison of popular MCDM algorithms compares some of the most used MCDM algorithms on the basis of input data they can work on. In an oil and gas field, obtaining exact data is impractical. For most of the existing methods (MAUT, WS, AHP, PROMTHEE, and TOPSIS as shown in Table 2-1 Comparison of popular MCDM algorithms), evaluating alternatives against criteria that have a wide range of units (some even unitless) is unmanageable. However, the desired attributes of two or more algorithms can be clubbed up to reproduce a novel algorithm to work on a specific case.

Table 2-1 Comparison of popular MCDM algorithms

Method	Type of Data					
	Compensatory Data	Partial Compensatory Data	Non-Compensatory Data	Quantitative Data	Qualitative Data	Mixed Data
MAUT (Multi-Attribute Value Theory)	✓	—	—	—	—	✓
WS (Weighted Summation)	✓	—	—	✓	—	—
AHP (Analytical Hierarchy Process)	✓	—	—	—	—	✓
PROMETHEE (Preference Ranking)	—	✓	—	—	—	✓
TOPSIS (Technique for Order of Preference by Similarity to Ideal Solution)	—	—	✓	✓	—	—

Out of the available methods, TOPSIS (Technique for Order of Preference by Similarity to Ideal Solution) is one of the most commonly used methods by researchers in renewable energy technologies due to its rational and comprehensible logic [38]. Ramezanzade et al. [39] selected the best HRES design based on social, technical, and economic criteria using TOPSIS. Perera et al. [40] established a Pareto front between levelized energy cost, unmet load fraction, wasted renewable energy, and fuel consumption using fuzzy-TOPSIS multi-criteria decision-making while designing an HRES for Hambanthota in Sri Lanka. AHP is a good tool when a mixture of qualitative and quantitative criteria has to be evaluated as it evens out inconsistent judgments due to the difference in criteria measurement and estimation units. Sliogeriene et al. [41] used AHP and ARAS (additive ratio assessment method) to choose Lithuania's power production mix. Veysel Coban [42] explored hesitant fuzzy linguistic expressions with technical, economic, and political sub-criteria-based AHP models to evaluate solar energy plant projects. Taylan et al. [43] used fuzzy AHP for weight determination and Fuzzy Vikor with TOPSIS for the selection of energy system alternatives when there were conflicting opinions amongst decision-makers. Zhou et al. [44], Tahri et al. [45], and Merrouni et al. [46] used GIS (Geographical Information System) *and* Multi-Criteria

Decision Making (MCDM) to evaluate locations for installation of PV-EV charging stations [44] and solar farms [45], [46] in Beijing [44] and Morocco [45], [46]. A summary of literature available on-site selection using MCDM methods is provided in Table 2-2.

Table 2-2 Literature on Site Selection for Hybrid Renewable Energy System Installation

Ref	Location	Type of Installation	Assessment Criteria	MCDM method used
Nazari et al. [33] (2018)	Iran	Solar farms	Solar Radiation, Average Temperature, Geographical Location, Status of Substructures, Grid Accessibility, Distance from where demand power, Distance from the settlement, Land Availability, Social acceptability, effect of progress on the surrounding region, security, and risk	TOPSIS
Azizkhani et al. [34] (2017)	Iran	Solar farms	Global Horizontal Irradiance (GHI), Economics, Technical, Geographical factors, Land Use	AHP, GIS
Sindhu et al. [35] (2017)	Haryana, India	Solar farms	Social, Technical, Economic, Environmental, Political	AHP-fuzzy TOPSIS
Yunna et al. [36] (2014)	China	Solar-Wind	Grid accessibility, Wind resource (speed, power density, utilization time), Solar resource (sunshine hours, radiation), Economy (payback period, ROI, profit on capital), Social risk (public security, policy support), Environment (energy saving benefit, emission reduction, noise and light pollution, ecological damage, water and soil loss, impact on local residential life)	AHP
Jun et al. [37] (2014)	China	Solar-Wind	Wind energy resource assessment (power density, frequency, direction, turbulence intensity), Solar assessment (radiation, stability), Economic factors (Power demand, construction cost,	ELECTRE-II

			O&M cost), Traffic Conditions, Environmental factors, Social factors	
Zhou et al. [44] (2020)	Beijing	PV integrated EV charging stations	Traffic flow, road distribution, natural resource, economic, technical, social	GIS, TODIM
Tahri et al. [45] (2015)	Morocco	Solar farm	Location, Geography, Land Use, Climate	GIS, AHP
Merrouni et al. [46] (2018)	Morocco	Solar farm	Climate, Orography, Distance from residential areas, distance from road-rail network, Distance from electricity grid, Distance from water ways – dams- ground water.	GIS, AHP
Mokarram et al. [47] (2020)	Iran	Solar farm	Solar radiation, temperature, distance to load–road – residential area, elevation, slope, land use, cloudy days, relative humidity, dusty days	Fuzzy AHP–ANP
Wu et al. [48] (2018)	China	Large commercial rooftop photovoltaic system	Sustainability, resource (annual radiation, temperature, rooftop available area), economy (investment cost, annual capital income, payback period, operation and maintenance cost, local government subsidies), risk factor (extreme weather damage, policy risk), environmental factor (light pollution, emission reduction, energy saving benefit), social factor (local economy, public support)	Fuzzy ANP–VIKOR
Taufik et al. [49] (2021)	Morocco	Offshore wind farm	Technical (Wind speed, water depth, distance from airport, distance from submarine sediment thickness, shipping route, exclusive economic zone), Socio-economic (distance from power grid – shoreline – ports, tourism density, blue flag beaches), Environmental (protected areas, migratory bird routes)	Fuzzy AHP

The literature indicates that the decision-making process is complex due to the need to consider a wide range of criteria for appropriate site selection from the given alternatives [50]. Primitive MCDM methods are not sufficient to evaluate oil & gas field locations as collecting exact data is a tedious process. Also, evaluating alternatives against criteria that have a wide range of units (some even unitless) is unmanageable for most existing methods. A hybrid approach involving a combination of two or more MCDM methods could potentially be helpful in solving such complex decision-making problems. However, such attempts have not yet been carried out especially in problems involving oil & gas fields. The main objective of this study is to develop a hybrid MCDM method for selecting the optimal location for HRES installation to reduce gas flaring at oil and gas fields.

2.3 Machine Learning Techniques for Renewable Energy Prediction

After selecting the appropriate site for renewable energy installation, the next step is the prediction of renewable energy available locally in the selected area, which can further be utilized for power generation in the microgrid system. The DERs like solar and wind are highly fluctuating in nature, and therefore introduce intermittencies in the power generation. However, researchers have proven that a combination of multiple energy sources clubbed up for distributed generation can reduce intermittencies in the power output. Several DERs (controllable and uncontrollable) working together offer a smoother and more reliable power production.

The DERs can be classified as controllable / dispatchable and non-controllable / non-dispatchable.

1. **Dispatchable DER**: As the name suggests, the power output of dispatchable DERs can be controlled by droop control techniques like voltage and frequency control. Examples of dispatchable DERs are coal-fired power plants, energy storage, hydroelectric power plant, ocean thermal energy conversion, biomass, geothermal, etc. The dispatchable units can be used to serve as a spinning reserve to compensate for power shortages or frequency drops within a given time span.
2. **Non-Dispatchable DER**: The non-dispatchable energy sources are the ones that cannot be controlled in accordance with the fluctuating demands. Solar and Wind are

two prominent non-dispatchable DERs amongst others like tidal power and wave power.

Since the non-dispatchable DERs cannot be controlled, it is essential to predict them using machine learning techniques so that the dispatchable DERs can be controlled accordingly to maintain an equilibrium in the microgrid system. The machine learning techniques used in data-intensive energy management problems can be categorized into supervised, unsupervised, and reinforcement learning. Basic machine learning steps are data collection and pre-processing, feature selection and extraction, model selection, and model verification. Machine learning algorithms (MLA) often use computational methods to learn any information directly from any form of data (labeled or unlabeled). The algorithm tends to adaptively progress in its performance as the samples for models become more available and learning increases gradually. Figure 2-1 shows a classification of the MLA. In supervised learning, MLAs take labeled data to train a model. It mostly uses regression and classification techniques for developing models. In unsupervised learning, the MLA tries to draw inferences from unlabeled data. Clustering is the most commonly used unsupervised learning technique, it deals with finding a structure in a collection of unlabeled data. Semi-Supervised learning is an approach that combines a very small amount of labeled data with a huge amount of unlabeled data during training for prediction. Reinforcement learning is referred to as goal-oriented algorithms, which learn how to achieve a complex objective or by what method to maximize along a specific dimension over a number of steps, emphasizing how to act based on the environment to maximize the expected benefits.

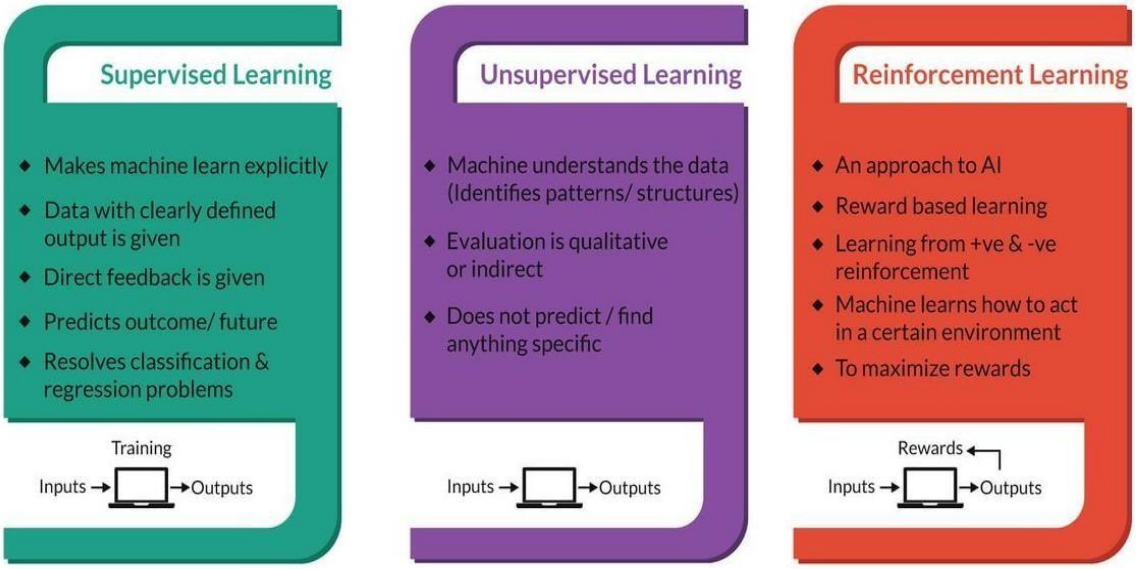

Figure 2-1 Types of Machine learning at a glance [5]

The weather data information is a fundamental input for microgrid scheduling, meteorological conditions mainly determine the amount of renewable energy production and, the load inside the microgrids. Weather forecasts are therefore necessary to establish the optimal plans for operational objectives and priorities for each microgrid. J. Lai et al. [51] have reviewed the literature on machine learning for renewable energy predictions. Ronay et al. [52] predicted solar energy and used the predicted value in the mathematical models developed for solar, microhydro, load, and energy storage systems in a microgrid. They used it for optimal resource management and maintaining the supply-demand balance in a microgrid.

Barbosa et al. [53] used ANN and ARIMA (Autoregressive Integrated Moving Average) models for day ahead wind power generation prediction. The wind power prediction models may be broadly classified into the following three categories: the physical model, the statistical and computational model, and the hybrid model for prediction [54].

In [55], Liu et al. estimated the day ahead of photovoltaic power generation by considering parameters like temperature, wind speed, and humidity. However, these predictions were not adequately accurate under extreme weather conditions leading to errors in prediction by the model. It was found that aerosol index (AI) has a strong linear positive correlation with solar radiation attenuation and has an immense impact on the power generated by photovoltaic panels. This paper proposed a novel photovoltaic power

forecasting model, considering AI data as the input parameters. Further, based on seasonal weather classification, the back-propagation artificial neural network (BP-ANN) approach was used for forecasting the following 24-h photovoltaic power output. Their model has improved prediction accuracy compared to conventional methods using artificial neural networks.

In[56], Gonzalez et al. used the Multiple Linear Regression (MLR) model to determine hourly solar photovoltaic production by using the Performance Ratio (PR) factor of the power plant. The data was gathered from several photovoltaic plants that were studied within the different regions at Chile: Antofagasta and San Pedro de Atacama. In this study, it has been determined that their model could be extrapolated to different climatological emplacements, where the RMSE (root mean square error) values were quite lower than 16% in all cases. Therefore, the model has a novel improvement in prediction with respect to any other literature models, where their performance ratio was variable and decisive to define the accuracy of the model.

In the last two decades, many researchers have explored cloudiness based [57][58], sunshine based [59], and temperature based [60] empirical models for accurate solar radiation prediction. [61] and [62] provide a comprehensive review and comparison of the various empirical models available in the literature. [63] evaluated six different models for global solar radiation estimation in Nigeria. [64] compared four artificial intelligence-based models to predict solar irradiation in China. Similarly, wind speed prediction [65] compared multi-layer feed-forward neural network (MLFFNN), support vector regression (SVR), fuzzy inference system (FIS), adaptive neuro-fuzzy inference system (ANFIS), and group method of data handling (GMDH). They concluded that the GMDH method and ANFIS combined with PSO and GA predict wind speed with higher accuracy. *Table 2-3* compares some of the popular MLAs' advantages and disadvantages.

Table 2-3 Comparison of advantages and disadvantages of developed ML methods

Methods	Advantages	Disadvantages
ANN	• It can learn and process data parallelly. • It has a non-linear and adaptive structure. • Generalization does not depend on system parameters explicitly. • It provides a faster response as compared to other conventional methods.	• Historical data is needed for the learning and training of the model. • Artificial neural networks require processors with parallel processing power.

Reinforcement learning	• Conducts a learning process with no prior knowledge about the data. • It can be combined with an artificial neural network for deep RL to solve continuous state-space control problems as well.	• The long-time convergence in a real-world problem. • Prone to susceptibility error.
LSTM	• Fine parameter tuning works well for a wide range of parameters like learning rate. • It is able to generalize well relevant to inputs • LSTM brides the time lag error in backpropagation	• Need strong insights into neural networks for implementation • High complexity
Gradient boost algorithm	• It is easy and fast to implement the algorithm. • Boosting is a resilient method that curbs over-fitting easily.	• Sensitive to outliers • Gradient boost algorithms are harder to tune
AdaBoost Algorithm	• Less prone to over-fitting • The model tends to have a great generalization power.	• Sensitive to noisy data and outliers in the data. • Uses progressively boosted learning techniques, hence requires high-quality data.
K-means Clustering	• Unsupervised clustering makes sure that similar data are under one group at a time. • Very effective in high dimensional spaces with better prediction accuracy	• It is not suitable for large data sets. • Minor prediction error leads to the system instability

Usually, there are four types of forecasting, as shown in Table 2-4 [66]. Very short-term forecasting is necessary for monitoring the system. A short-term forecast is required for unit commitment and demand-supply balance. Electricity producers and grid operators use the medium-term forecast to determine the operation and maintenance schedule of their facilities cost-effectively. The long-term forecast is helpful in site selection, determining the capacity of power plant components during installation network operations etc. To improve system stability and reduce financial losses during maintenance, the system control engineers require accurate very short-term wind and solar power forecasting.

Table 2-4 Time-horizon-based categorization of the type of forecast and their application.

Type of Forecast	Prediction Time Step	Application
Very Short Term	Few seconds to minutes ahead	Real-time monitoring
Short Term	48 to 72 hours ahead	Unit Commitment, Demand-Supply balance
Medium Term	One week ahead	Maintenance scheduling
Long Term	Months or Years ahead	Installation and Operation

Aslam et al. [67] employed deep learning-based methods for very short-term solar energy forecasting for improved microgrid energy management. They considered weather conditions like temperature, irradiation, humidity, etc., to forecast solar energy generation based on historical data.

Maintaining a power and energy balance in the microgrid system using an efficient dispatch strategy requires accurate short-term prediction of non-dispatchable DERs like solar and wind. The discussed literature has majorly explored empirical and machine learning models for short term and very-short term forecasts. The statistical models are based on historical data, whereas the neural network-based methods recognize patterns in data using training data sets. Surprisingly, the existing literature contradicts itself in proving the reliability of a particular model for short-term renewable predictions. In [68], the stability of XgBoost and Adaboost in case of short term forecasting is demonstrated. Whereas, Ogliari et al. [69] surveyed several empirical models including Xgboost and Adaboost, and reported that they are not suitable for short-term forecasts due to huge computational load. Meenal et al. [70] compared the performance of empirical models with support vector machine (SVM) and artificial neural network (ANN) and reported that SVM significantly outperforms empirical models and ANN. Yang et al. [71] claimed that statistical time-series forecast also known as regression methods are best suited for very short term forecast.

Some studies have quoted benefits of using ensemble learning methods over linear regression methods as they provide stability especially in short term forecasting which the regression methods fail to provide. However, studies applying ensemble methods on wind data are still a rarity. Therefore Chapter 4 investigates the fresh domain of solar as well as wind power generation prediction using ensemble learning methods and

reinforces the advantages of ensemble methods over regression methods for dynamic wind and solar energy prediction. For the purpose of forecasting solar and wind energy, the provided research compares and analyses the performance of MLR, AdaBoost, gradient boost, and XgBoost algorithms. Such an extensive comparison is quite improbable in the concurrent literary works.

2.4 HRES Design and Optimization

Numerous studies have been conducted on modeling, simulation, unit size optimization, and techno-economic assessment of hybrid energy systems (HES). The primary objective identified from those studies was maximizing the renewable fraction while minimizing the overall cost of the system design. For the design optimization of the hybrid renewable energy system (HRES), several metaheuristic optimization techniques and software are used. In [72], Mo et al. used branch and bound method and radial basis function artificial neural network (RBF ANN) algorithm to maximize renewable fraction at low cost while designing HRES using Modelica language. The capital and cost of energy have been minimized in [73] using cuckoo search and compared with genetic algorithm and Particle Swarm Optimization (PSO). In [74] and [75], Fodhil and Yahiaoui et al. compared results for PSO and Hybrid Optimizer for Multiple Energy Resources (HOMER) and found that the system designed by HOMER provides sufficient sizing margin while designing the system components, which leads to lesser load loss. Ayodele et al. [76] compares the microgrid design using HOMER and analytical method and concludes that the HOMER designs are techno-economically more suitable as the analytical method produces exaggerated component sizes. Meta-heuristic computational approaches do not produce reasonable results when the hybrid system complexity is higher. Moreover, PSO and HOMER give similar results with hardly 1% variability. Therefore, HOMER is more popular in the research community to reduce the computation time, improve the accuracy of results, for a thorough techno-commercial analysis of the production mix, and effective comparison of all possible system designs.

Sen et al. [77] were among the first few to use HOMER to design an off-grid HRES comprising small-scale hydropower, solar photovoltaic systems, wind turbines, and bio-diesel generators for remote villages in Chhattisgarh, India. It is to be noted that 79.34% of studies in the existing literature are purely based on 'off-grid / islanded' solutions [15]. In a similar grid independent study [78], Wondwossen et al. designed a wind turbine generator, diesel generator, and solar panel-based hybrid renewable energy system for a

remote rural community in Ethiopia. In another grid independent study, Murthy et al. [79] designed a stand-alone poly-generation microgrid catering to the electrical, thermal, and hydrogen needs of a typical 50-household remote Indian village.–Shahzad et al. [80] designed a grid-independent PV/biomass for a remote agricultural farm in Punjab, Pakistan.-Similarly, Rezk and Dousoky [81] presented a feasibility study of a stand-alone photovoltaic, battery, fuel-cell, wind-based HRES for a remote agricultural area in Egypt. In [82], Gonzalez et al. used small wind turbines (SWT) for off-grid electrification of 2000kWh load in two different rural Venezuelan communities. In a similar rural context in West Africa, Ayodele et al. [76] designed an optimal hybrid configuration comprising WT, SPV, gasoline generators, and BESS for a microfinance bank. In a similar Malaysian study, wind turbine and PV-based off-grid HRES were designed by Shezan et al. [83]. Multiple researchers have explored off-grid HRES for remote rural as well as islands. In a feasibility study for Lakshadweep islands, Singh et al. [84] found that SPV, WT, and BESS are the best combination to lower the emission, cost of energy, and dummy load of the existing diesel-operated electricity production system in the region. In a similar study, Fazelpour et al. [85] declared that a wind-diesel hybrid system with BESS is ideal for supplying power to a hotel in Kish islands, Iran. Bhakta and Mukherjee [86] studied the feasibility of SPV-BESS powered system for a single household load in Andaman and Nicobar Island. Similarly, Tsai et al. [87], and M B Khan et al. [88] also proposed HRES over diesel generators for the Batan Island, Philippines, and resort island in the South China sea, respectively. Later on, Tsai et al. analyzed the impact of increasing renewable fraction on system cost for a SPV/DG/BESS system in a Chinese island [89]. Some microgrid system design studies have been conducted for academic institutions/university buildings. In [90], Kumar et al. used HOMER to design a microgrid system for an educational institution that utilizes the biogas from the institute's food waste to generate electricity. Similarly, Sarkar et al. [91] designed and implemented a microgrid comprising solar PV, wind, biomass, and vanadium redox flow battery storage for the Indian Institute of Engineering Science and Technology (IIEST) Shibpur. Bhattacharjee et al. [92] analyzed the contribution of PV and wind in a PV-wind-based HRES for an educational building in Tripura, India. Meanwhile, Saiprasad et al. [93] performed optimal sizing and HRES feasibility study for Victoria University at the St Albans campus in Melbourne. Ghenai et al. [94] analyzed the performance of an off-grid PV-FC-DG-based HRES using HOMER software for a university building. A few studies for urban residential buildings can also be highlighted. Liu et al. [95] performed a techno-economic feasibility analysis

of hybrid renewable energy power systems for high-rise buildings in urban locations. Similarly, Al-Ammar et al. [96] designed a stand-alone HRES for a residential area and compared nine different SPV/Wind/diesel/battery combinations using HOMER software to determine the most economical and environmentally safe configuration. In a similar context, Lv et al. [33] used HOMER to perform a techno-economic feasibility analysis of a 100% renewable energy-based residential household in China. Tiwary et al. [97] devised a biomass-based community-scale hybrid energy management system for waste and energy management in the UK and Bulgaria urban areas. Rad et al. [98] designed a hybrid SPV/wind/biogas/fuel-cell-based system for stand-alone and on-grid applications. In all these studies [76]–[83], there was no mention of the strategy used to schedule the dispatch of various HRES components. Table 2-5 presents a brief comparison of some recent research papers that focused on HRES design.

Table 2-5 Comparison of HRES designs from literature

Ref	HRES Mix	Load Type	Grid Connection	Dispatch Strategy	Performance Measure
[78]	Wind, Solar, Diesel	Rural community	Off-grid	No mention	Cost
[80]	Solar, Biomass	Agricultural	Off-grid	No mention	
[81]	Wind, SPV, Battery storage, Fuel cell	Remote Agricultural Area	Grid	No mention	
[82]	Wind	Desert and mountain	Off-grid	No Mention	LCOE
[83]	Wind, Diesel, Battery, SPV	Daily load	Off-grid	CC	NPC, COE
[84]	SPV, Battery	Islands	Grid	No Mention	NPC, COE
[85]	Wind, Diesel, Battery	Hotel	Grid	No Mention	COE
[86]	SPV, Battery	Island	Off-grid		COE, NPC, RF
[87]	SPV, Diesel, Wind, Battery	Island	Off-grid	No mention	COE
[88]	Diesel, SPV, Wind, Hydro, Battery	Island	Grid	LF, CC	COE, NPC, RF
[89]	Diesel, SPV, Battery	Island	Off-grid	LF,CC	COE, NPC, RF
[90]	SPV, Battery	IIT Guwahati campus	Grid / Off-Grid	LF, CC	COE, NPC
[91]	SPV, Wind, Biomass, Vanadium redox flow battery (VRFB)	IIEST	Off-Grid	No mention	COE
[93]	SPV, Wind	Campus	Off-Grid	No Mention	NPC, COE, RF
[94]	SPV, Fuel cell	Commercial Building	Off-Grid	LF, CC	COE
[95]	SPV, Wind	High-rise building	Grid	No Mention	LCOE
[97]	SPV, Wind	Residential Area	Off grid	CD	COE, NOC
[98]	Wind, SPV, Biogas	City	Grid	No Mention	LCOE

LF: Load following, CC: Cycle charging, CD: Combined dispatch, SPV: Solar Photovoltaic, NPC: Net present Cost, COE: Cost of energy, RF: Renewable fraction

Several studies have declared renewable-based systems to be more economical and environmentally friendly than only-diesel or only-grid systems. In a grid-connected HRES study by Rad et al. [98], it was observed that the system cost of a stand-alone system was higher than the cost of a system with the same components and a grid connection. Therefore, renewable fraction and cost decrease by introducing grid connection in the same set of system components. Maximizing renewable penetration in grid-connected systems, at the least possible cost is challenging, as most of the system's energy requirements will be met by the grid if a connection is available. However, it is crucial to improve the renewable percentage in the production mix to curb environmental pollution.

From the above discussion, it is observed that most of the hybrid system design studies were non-grid-connected and for remote rural locations. Furthermore, several studies can be found for cattle farms [99], [100], agricultural lands [80], [81], hilly regions [83], government organisations[101], microfinance institutions[76], office buildings[72], or islands[84]–[89]. Nevertheless, there is a lack of hybrid energy system design specifically for the oil and gas field area, supplementing the existing grid connection. Most of the concurrent studies are either designed using the default LF and CC dispatch strategies, or there is no mention of the dispatch or design method at all. There is a lack of studies focused on the design and development of dispatch methods customized for gas microturbine, solar, and river turbine-based grid-connected systems. Accordingly, the present study has focused on a grid-connected design, optimization, and modeling of HRES for oil and gas field areas utilizing the waste gas flares to produce power, thus minimising environmental pollution from oil and gas production sites at the least possible cost. A novel dispatch strategy specifically designed to suit the requirements of oil and gas fields has been proposed in Chapter 6.

2.5 Optimization Techniques for Power and Energy Management in Microgrid Networks

Several literary works have considered LP (Linear Programming) [102], MILP (Mixed Integer Linear Programming) [103], [104], and NLP (Non-linear Programming) [105], [106] for Microgrid Energy Management System (EMS). In all cases [102], [105], [106], ultimately, the problem was converted to MILP by linearising the non-linear

constraints in the case of NLP and introducing a binary constraint in the case of LP. This is done due to the lesser computation time of MILP and that switching operations can be performed only by introducing binary constraints. In this genre, the target of the objective functions (OF) is to minimize the energy transaction cost [107], outages and interruption cost [108], cost due to losses [8][109], GHG emission cost [110][111], operational and maintenance cost, levelized cost of RERs [112], and maximizing the demand response incentives [113]. Commonly used constraints were – Network constraints, power and energy balancing constraints, output limits of RERs, physical limits of ESS and generator sets, and in some cases, reactive power support. Most of the studies have used the CPLEX TOMLAB solver for optimization in MATLAB [114], whereas some have also used GAMS for this purpose [115].

When coupled with prediction algorithms, the optimization problem formulation (LP, MILP, MIQCP…) is called Rolling Time Horizon (RTH) strategies. The prediction algorithms are used for predicting intermittent and stochastic behaviours such as solar intensity, wind speed, etc. At each time sample, the prediction algorithm obtains estimations by optimization algorithm in order to compute the optimal solution.

Although many case studies have proven RTH strategies to be robust and effective, they suffer from dependence on prediction accuracy. On the contrary, rule-based systems such as fuzzy sets / "IF-ELSE" rules allow a higher level of interpretability and ease of implementation. Therefore, RTH EMS, which is basically a cascade of optimization and prediction algorithms, can be substituted by simpler and lighter decision-making systems such as fuzzy logic, "IF-ELSE" rules, and neural networks, especially when they produce similar or even better outcomes.

A hierarchical system architecture is presented in [116] to recognize and classify the prominent functionalities and techniques associated with P2P energy trading. This trading platform was developed and simulated, employing game theory. Experimental analysis in an LV grid-connected microgrid shows that P2P energy trading can strengthen the local balance of power generation and power consumption. In [117], Zhang and Chow have solved the fundamental centralized economic dispatch issue in a distributed way by considering every power generating unit's incremental cost as the consensus variable. Artificial intelligence, neural networks, and fuzzy logic will play critical roles in

microgrid energy management. More and more researchers [118]–[122] are using these soft computing techniques for microgrid control.

2.6 Gas Microturbine based Power Generation and Distribution

The ongoing transition in the power production sector toward more dispersed and renewable generation enhances the need for dependable and effective small-scale dispatchable supply units. Due to the non-dispatchable nature of intermittent renewable energy sources like solar and wind, increased use of these resources introduces a bigger volatility in the amount of electricity input to the grid. They deliver erratic, location-specific power levels that fluctuate and are unknown. Because of this, it's necessary to use hybrid technologies and supplemental systems to ensure smooth electrical output and meet demands. In order to satisfy energy demands, micro gas turbines can guarantee smooth outputs while providing quick and dependable power correction for renewable oscillations.

A scenario for decentralised power generation that incorporates MGTs with wind turbines, solar panels, biomass plants, fuel cells, and energy storage would offer a safe, dependable, cost-effective, efficient, and environmentally friendly energy production system that is located close to the points of consumption and delivers heat and electricity without suffering significant transportation and conversion losses. MGTs are noted for their dependable operations, well-known technology, quick startup, and low maintenance requirements. With a maintenance interval of 400–8000 operating hours, which is longer than most internal combustion engines, tiny gas turbines can reach an economic lifetime of up to 80,000 operating hours. They have been widely utilised in various engineering sectors and have previously been demonstrated to be dependable, operate satisfactorily, and are appropriate for integration with other systems or as a subsystem in a larger energy system. Compared to other DEG technologies, they feature lower startup costs and the potential for low-cost mass manufacturing. Other financial benefits of using MGT systems include the potential to use waste fuels (such agricultural residues or organic wastes) and energy recovery. When using an economizer, MGTs can achieve an overall efficiency (electricity + heat) of up to 90% and emit less pollutants than large-scale gas turbines.

2.7 Multi-Microgrid Optimization and DER Control Strategies

The introduction of microgrids with various renewable energy sources in recent years has brought up some basic difficulties in managing, coordinating, and controlling power exchange between microgrids and the power grid. Out of the various critical like – privacy, inter-operability and security issues, packet corruption, packet loss, jittering, disconnection, and other communication-related problems, one of the significant setbacks in incorporating microgrid technology is the massive amount of capital investment involved [123]. BESS and PCS (Power Conditioning System) are the costliest and most essential elements in a microgrid power management system. To reduce the requirement of BESS and other microgrid control assets, it is necessary to integrate multiple microgrids into a single collaborative microgrid network, wherein all controllers will communicate with each other for optimal utilization of resources within the collaborative microgrid network. Collaborative/nested microgrid is undoubtedly the future of the microgrid power management system. Such an interconnected microgrid power management system will reap the following benefits [124], [125]:

- Reduced peak loads for interlinked grids.
- Lesser outages and for a lower duration
- Fewer emissions and decreased installation costs than isolated microgrids as a smaller number of generators will have to be installed.
- Reduction in BESS requirement
- Robust and resilient collaborative power grid in contingency conditions.

Considering the reduction in battery storage requirement [126], increased resilience, reduction in emissions and overall cost [127], research and development are focused on multi-microgrids / collaborative microgrids / nested microgrids to overcome the setbacks in widespread microgrid installation. A review of various nested microgrid projects around the world is provided in Table 2-6.

Table 2-6 Nested Microgrid Projects Around the World

Projects	Year / Status	No. of Microgrids involved	Peak Demand	Special Features
Bronzeville-Illinois Institute of Technology	Started in 2017 Currently in the simulation phase	2	10 MW 12 MW	Tie line between two Microgrids for load sharing. Both can operate independently or as grid-connected.
Onley Town Center	2014-2017 – Single MG 2017 onwards – nested MG	6	7 MW Aggregate	A primary aim is to reduce SAIDI to less than 2 minutes, emissions by 20%, and increase efficiency by 20% as it accommodates 33,000 residents with several critical loads such as schools, police stations, hospitals, etc. Prioritization of loads is done using optimization techniques
Alstom Microgrid System for Philadelphia Navy Yard	2014 -2022	4	27 MW Aggregate	Previously the region had a connection to 15 MW and 19 MW substations. But, as the navy yard houses 145 companies and 11,500 employees, the purpose of this project is to have four separate Microgrids, connected to 4 different substations and connected to each other for resilience. Composed of- 1 MW solar, 600 KW fuel cell, 300 KW storage, and 3 KW combined heat and power plant.

				Demand Response balancing algorithm was employed within nested Microgrid network.
Oncor	2015 till present	4	1.25 MW aggregate	Centralized Control. -- Four Microgrids controlled by a single controller. Consists of 9 different sources grouped under four different Microgrids.
San Deigo Navy Cluster	2013 till present	3	42 MW 26 MW 15 MW	Each Microgrid can operate autonomously or individually connected to the primary grid. When collaborated to operate as a single nested Microgrid, they have a new hierarchy of a centralized Microgrid controller.
Yamagata Site Microgrid	2016 till present	3	15 KW of DG each and 100 KW of storage. (50,25,25)	Centralized control for the energy exchange. Targeted to reduce power store requirement by 40%

In [128], Aghdam et al. used Chance Constrained Programming (CCP) for day-ahead scheduling for the multi-microgrid system taking the degradation cost of the energy storage system into account. Their main aim was to avoid the misuse of batteries. Xie et al. [129] developed an optimization model to automate the dispatch between the distribution network and Microgrids connected to the distribution grid, which they called as analytical target cascading (ATC) theory. They modelled a tie-line flow between the distribution network and Microgrids as a pseudo generator/load so that the Microgrids or distribution networks can autonomously utilize their distinct resources to optimize their operation and economic benefits. They also considered chance-constrained programming to model the uncertainties. Zadsar et al. [130] developed a two-stage optimization model for the distribution network when multiple Microgrids are connected in the network. In the first stage the day-ahead scheduling and outage management scheme for a single

microgrid is proposed, and in the second stage, a contingency plan is proposed, which can dynamically create multi-microgrid clusters. The second stage also enables the islanding of microturbines, energy storage, and load shedding. The main objective in the second stage is to minimize load shedding. In [131], Cheong et al. analyzed and tested various types of clustering algorithms to examine their suitability for microgrid formation.

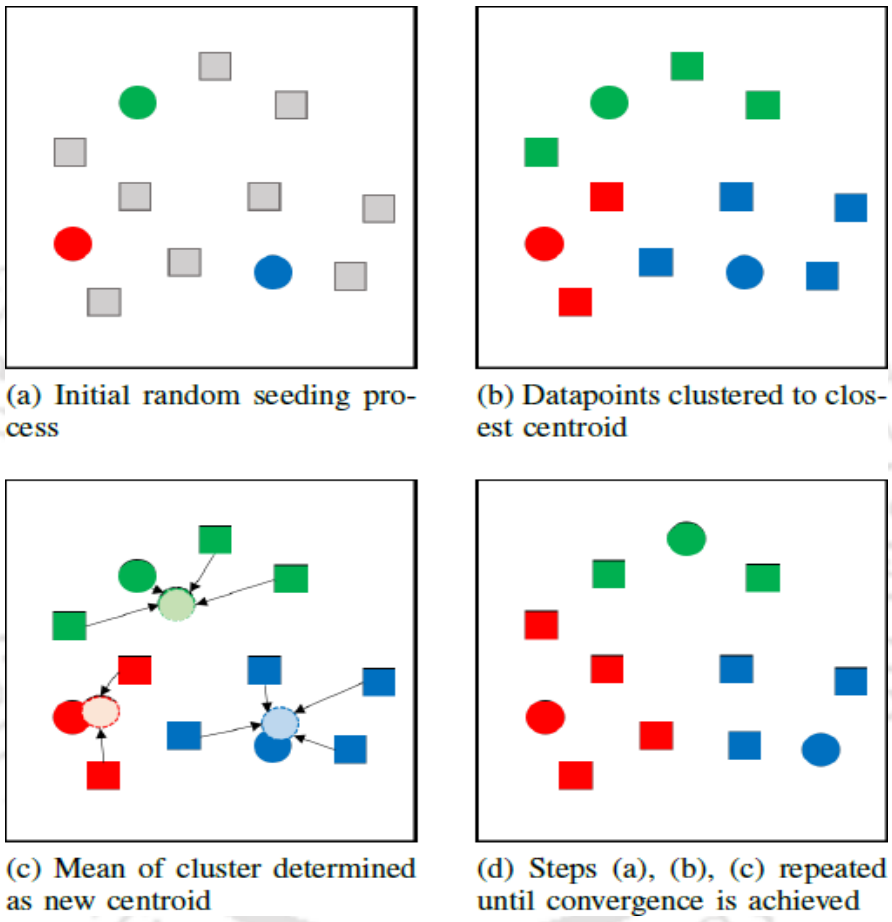

Figure 2-2 K-means Clustering Approach

The k-means clustering was found to be arguably the most popular partitioning clustering algorithm that follows the procedure Figure 2-2. Its computational efficiency and simplicity make k-means an appealing method for prediction. The results had suggested that the Hierarchial clustering type of unsupervised algorithms was most appropriate for sporadically populated and remote locations. The main advantage of this algorithm is their compliance to different datasets to be isolated in large clusters.

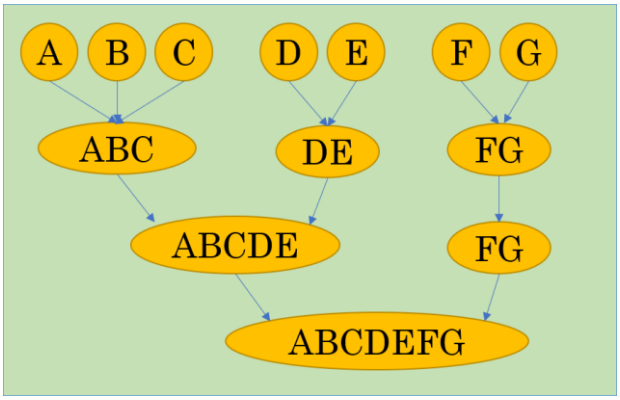

Figure 2-3 Agglomerative Hierarchical Clustering

The agglomerative clustering as shown in Figure 2-3 is a bottom-up process that begins with all points in the data as clusters and merges them on the basis of highly similar pair of clusters successively until a single similar group of clusters is achieved. The major contributions of the paper are the planning methodology schemes to form an uncoupled multi-microgrid network where every algorithm is assessed through a numerical simulation. The pitfalls and benefits of each clustering algorithm in relative regard to microgrid formation were also discussed for economic benefactions.

2.8 Literature Closure

The following conclusions can be made from the above discussion:

- Site selection plays a crucial role in increasing the efficiency and profitability of an Hybrid Renewable Energy System (HRES). Several researchers have explored multi-criteria decision making (MCDM) process for choosing the most appropriate location for HRES installation. Since gathering data pertaining to oil and gas fields is a laborious process, primitive MCDM approaches are inefficient in comparing alternatives to criteria that have a large range of units (some even unit-less). Such complicated decision-making challenges may benefit from a hybrid strategy that combines two or more MCDM techniques.
- Several researchers have explored HRES design and energy management optimization. In this context, Load Following (LF) and Cycle Charging (CC) are two most common dispatch strategies used by researchers (refer to studies in Table 2-5). However, there isn't a hybrid energy system design that is especially for the location of the oil and gas fields specific to augment the current grid link. Studies on the design and development of dispatch strategies specific to oil and gas field based HRES systems are lacking.

- Prediction of non-dispatchable DERs is essential to development of a robust and efficient dispatch strategy for power and energy management in an HRES system. Various studies on short-term and very short-term forecasting of solar and wind power generation using ensemble learning and linear regression techniques have been discussed. Studies have cited the advantages of ensemble learning techniques over linear regression techniques because they offer stability, particularly in short-term forecasting, which the regression techniques do not.
- Several researchers have explored mathematical, meta-heuristic optimization, and machine learning-based approaches for microgrid and multi-microgrid power and energy management. Some researchers have used a rule-based approach for the same. However, it is observed that the rule-based approach gives less accurate results, and meta-heuristic optimization approaches are computationally heavy. Convex optimization approaches seem to be an ideal approach in terms of computational complexity.

Considering the above-mentioned points from the literature review, this thesis seeks to advance knowledge in the field by developing novel algorithms for microgrid and multi-microgrid power and energy management for oil and gas fields.

2.9 Objectives of the Research

1. Selection of optimal gas flare location for the Hybrid Renewable Energy System (HRES) installation.

One of the most important considerations when building hybrid renewable energy systems at oil and gas fields is choosing the proper site since it assures high efficiency and productivity throughout the life-cycle of the system. Therefore, developing an algorithm for site selection to install the HRES system is an essential objective. Various site selection multi-criteria decision-making algorithms have been explored in the literature. The gaps in the existing algorithms have been presented in Chapter 2. A novel decision-making algorithm satisfying the requirement of a gas flaring location has been developed under this objective.

2. Developing an algorithm for the optimal design of a gas microturbine-based power generation and distribution network.

The presented thesis has adopted a bottom-up approach in utilizing flared gas for distributed generation. It starts with a gas microturbine-based distributed generation system, expands it to include other locally available renewable energy resources, forms a microgrid, and further interconnection of many microgrids creates multi-microgrid systems. The second objective serves the purpose of employing 30kW to 300kW gas microturbines at the gas flaring locations to generate power and feed the local power demands of the region. This objective attempts to

i) Identify the rating and type of generator used to convert gas flares to electricity,
ii) Design an optimal distribution network to minimize power loss,
iii) Minimise power intake from utilities, and make the oil and gas well power system self-sustainable.

3. Renewable energy prediction using Machine Learning

To make the oil and gas well power system more environmentally and economically efficient, alternative sources of renewable energy, such as solar, wind, and hydro energy, were clubbed with gas flare wastes to produce power. Accurate prediction of the available renewable energy resource plays a significant role in the further scheduling and optimization of a microgrid system. Therefore, various boosting (XgBoost, AdaBoost) and regression (Multiple linear regression) algorithms were used to predict the renewable sources in the area.

4. Dispatch strategy for oil and gas well-based Microgrid power management system

Load Following (LF) and Cycle Charging (CC) dispatch strategies are used by default for scheduling various Distributed Energy Resources (DERs) in a microgrid system. These dispatch strategies are inefficient for oil and gas field power systems where the gas flare wastes are utilized to generate power. Therefore, a novel dispatch strategy is developed to schedule the microgrid power generation in oil and gas fields.

5. Multi-Microgrid power and energy management

As there are multiple gas flare locations, there is a possibility of numerous gas well-based microgrid systems located in the vicinity of each other. Therefore, developing an

algorithm for power and energy management between multiple microgrid systems becomes an essential requirement.

This thesis proposes a complete solution for converting the power-consuming and emission-causing oil and gas fields to a power-generating - reduced emission system. The proposed solution can be a role model for carbon transition and achieving the Intended Nationally Determined Contributions (INDC) set by India to meet the Sustainable Development Goals (SDG).

2.10 Thesis Structure

For efficient power and energy management in microgrid and multi-microgrid systems which utilize flared gas to produce power, detailed research was proposed, which is further divided into the following objectives:

Chapter 1) ***Introduction***

This chapter provides an overview of the Microgrid and Smartgrid technology and explains the concurrent gas flaring and energy deficit scenario as the motivation behind this research work. This chapter also presents the objective and scope of this thesis.

Chapter 2) ***State of the art***

A systematic review of hybrid energy systems and various software available for their design, simulation, and optimization has been covered. This section also compares various hybrid energy system design case studies based on parameters like renewable penetration and dispatch strategy followed (like – Load following, cycle charging, etc.).

- Various multi-criteria decision-making algorithms and their advantages, disadvantages, and suitability for specific cases are reviewed, and gaps in the existing algorithms for oil and gas field suitability have been presented.
- A review of various machine learning and optimization techniques for renewable energy prediction and energy management in microgrid and multi-microgrid systems has been covered.

Based on the conclusions of the literature survey, the objectives of the current thesis are framed.

Chapter 3) ***Micro-Turbine based Power Generation and Distribution network***

In this chapter, a Mixed Integer Linear Programming problem is formulated to determine the optimal design of a microturbine-based power generation and distribution system that utilizes the waste flare gas in oil and gas fields to generate power. The following steps were involved in solving the resource allocation and network design problem:

i) Identifying objective functions for resource allocation and network design problems.
ii) Deciding various terms in the objective function so that it produces optimum results.
iii) Identifying the correct equality and inequality constraints that will bound the solution as per requirement.
iv) Applying robust optimization as a tool to the above problem to find the optimum rating of microturbine to be installed at the flare gas site and minimum power loss network configuration connecting the demand and generation sites.

Chapter 4) ***Renewable Energy Prediction using Machine Learning***

Renewable energy forecasting has become an important part of microgrid power management system design. Out of all the available renewable energy sources, it is most challenging to estimate wind and solar energy. It is not possible to predict the exact wind speed and solar radiation due to the constantly changing weather conditions. Therefore advanced prediction tools are necessary to reduce error margins and increase the accuracy of solar and wind power prediction. Literature has majorly explored empirical and machine learning models for short-term and very-short term forecasts. The statistical/ empirical models are based on historical data, whereas the neural network-based methods recognize patterns in data using training data sets. Surprisingly, the existing literature contradicts itself in proving the reliability of a particular model for short-term renewable predictions. Therefore, in this chapter, the performance of four different machine learning models - XG-Boost, AdaBoost, and Multiple Linear regression has been studied for prediction of solar and wind power generation.

Chapter 5) ***Site Selection for Hybrid Renewable Energy System Installation for Assam Asset***

This chapter creates a brand-new multi-criteria algorithm for choosing installation sites for hybrid renewable energy systems. One of the most important considerations when building hybrid renewable energy systems at oil and gas fields is choosing the proper site since it assures high productivity and efficiency throughout the system life cycle. This chapter explains how to choose appropriate locations for building three different hybrid renewable energy systems for oil and gas fields using a combinational multi-criteria decision-making technique. To establish the selection criteria weights, three approaches—equal distribution, intuitive distribution, and AHP—have been suggested. After weights have been established, the rankings of suitable gas flare locations have been determined using the modified "technique for order of preference by similarity to ideal solution" (TOPSIS). Three different hybrid renewable energy system configurations have been tested for installation at three separate sites using the suggested combinational algorithm. With a change of 1.32 percent in Ci (Closeness to optimal solution indexing), the results choose the same sites for all three scenarios. The accuracy of the modified TOPSIS method for assigning the rank of locations is demonstrated by the concordance of results for all the cases utilizing various criteria weights. In order to reduce gas flaring and produce electricity from waste gas flares and other available renewable energy sources, the oil and gas flaring areas are graded according to ecological, technological, and sociological criteria.

Chapter 6) ***Dispatch Strategy for Microgrid Power Management System in Nazira (Assam)***

A dispatch strategy is a logical set of instructions that control how energy is transferred between different HRES components and how they operate. It identifies which equipment must be in use at that precise moment after taking into account the component's current power/energy condition. HOMER Pro software uses cycle-charging (CC) and load-following (LF) strategies by default. Both strategies prioritize using generators that rely on renewable resources to supply the load. However, in the present scenario, gas-microturbines are regarded as being equal to generators powered by renewable resources because the natural gas-based generator utilizes flare gas wastes to produce energy. The dispatch strategy has been altered as a result to accommodate the needs of oil and gas fields.

Following are the key steps followed in microgrid system design presented in this chapter:

i) Developing the power and energy management algorithm on MATLAB specifically suited to oil and gas field microgrid systems.
ii) Modeling the Microgrid configuration on HOMER software
iii) Integrating the HOMER model with MATLAB dispatch strategy
iv) Simulating the modeled configuration to validate the developed dispatch strategy.
v) Running optimization algorithms on the viable Microgrid system options to calculate LCOE (Levelized Cost of Energy), NPC (Net Present Cost), ROI (Return on investments), and net cash flow and determine the most suitable system configuration.

Chapter 7) ***Algorithm for Power and Energy management in a Multi-Microgrid system***

An individual isolated microgrid does not utilize all its resources optimally. When there are multiple microgrid sites in the vicinity of each other, it is an intelligent decision for the microgrids to have collective power and an energy-sharing platform so that the nested microgrid system is economically optimal. One of the significant blockheads in the growth of microgrids in India is the high capital cost. Forming such a collaborative network will reduce the battery storage requirement and the capital cost to a great extent. To achieve this collaborative microgrid network, a power and energy-sharing algorithm have to be developed.

This chapter focuses on reallocating or shifting resources and partitioning the system into different configurations based on the spinning reserve availability to establish a Microgrid system that is cost-saving and more techno-commercially beneficial.

Chapter 8) ***Conclusion and Future Work***

Important conclusions drawn from the numerical and experimental research work have been presented in this chapter. The chapter also covers the scope for future work and recommendations.

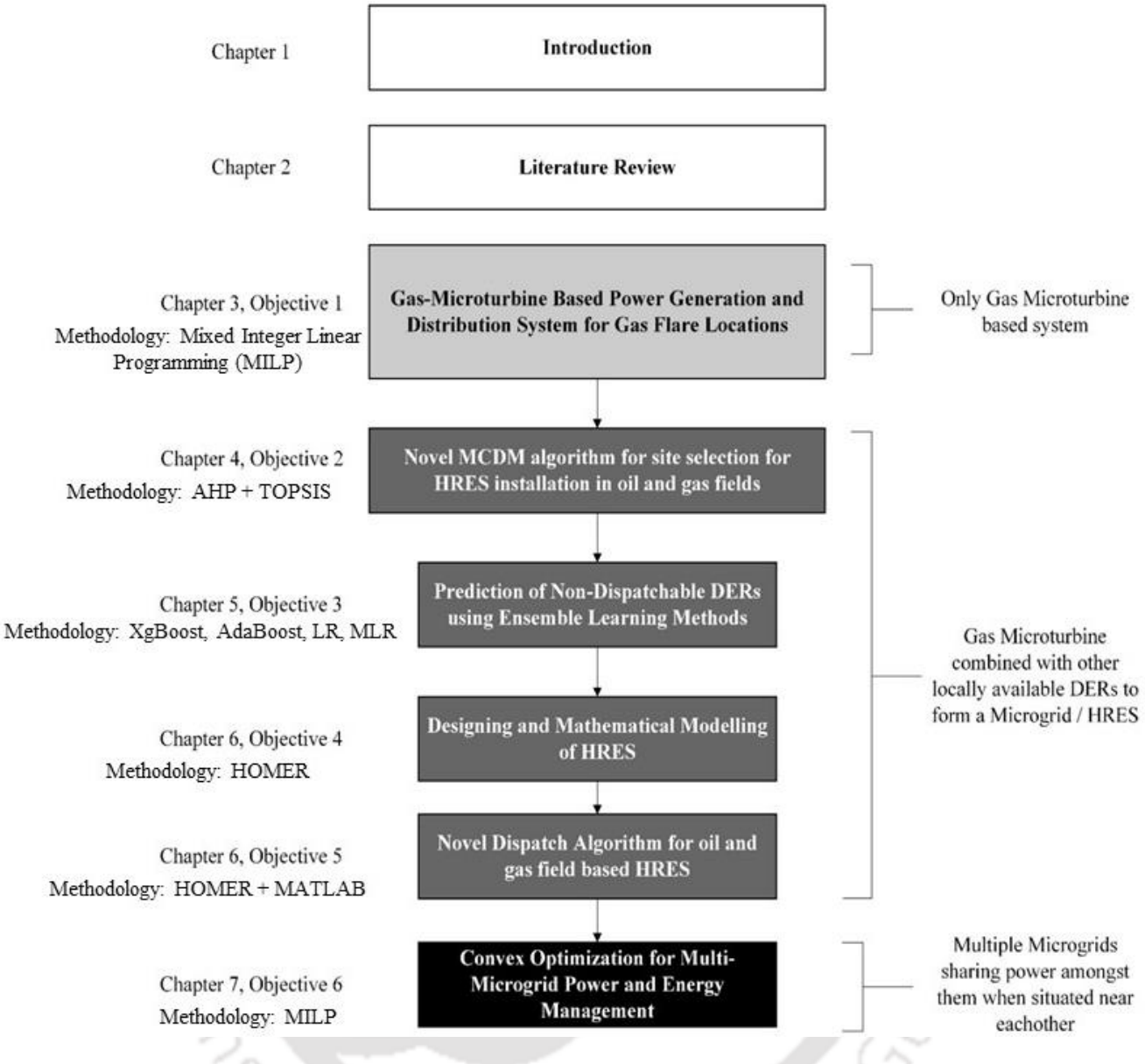

Figure 2-4 Thesis Organisation

2.11 Summary

This chapter presents a detailed literature survey, covering the following aspects:

i) Explored the possibilities of employing MCDM for site selection for HRES installation
ii) Emphasized the importance of renewable energy prediction in designing an optimal energy dispatch algorithm for microgrid power management.
iii) Literature on machine learning techniques for renewable energy prediction covered.
iv) Studies on modeling simulation and optimization of HRES covered.

v) Explored literature on power and energy optimization in HRES and emphasized the usability of each optimization technique.

vi) Studies on power generation and distribution using gas microturbines explored.

vii) Finally the importance and techniques available for multi-microgrid optimization covered.

viii) To sum up, the research objectives and thesis structure has been detailed.

Chapter 3

Gas Microturbine Placement and Design of Power Distribution Network

3.1 Foreword

In any oil and gas production site, there are hundreds of gas flaring locations situated haphazardly all over the region. Several researchers have already established the credibility of gas microturbines in using gas flares for power generation. However, research on the correct placement and selection of gas turbine technology to harness the waste natural gas potential for localized power generation and distribution is still lacking. Therefore, this chapter proposes an algorithm to determine an optimal gas-microturbine-based power generation and distribution system supplementing the existing grid connection, which could utilize the waste flare gas for power generation in oil and gas fields. In this chapter, Mixed Integer Linear Programming (MILP) has been used to determine the rating of gas microturbine to be installed and the lowest power loss network configuration. It is a resource allocation and network design problem wherein, upon feeding in the coordinates of gas flaring sites, coordinates of demand sites, amount of fuel availability, and power demand, it gives the most optimal network design and selects the most techno-economically viable generator configuration for each flare site while minimizing the power intake from the grid.

The content in this chapter has been published in the following paper:

- Deepika Bishnoi, Om Prakash, and Harsh Chaturvedi, 'Utilizing Flared Gas for Distributed Generation : An Optimization Based Approach', AIP 2019. https://doi.org/10.1063/1.5096498.

Figure 3-1 shows the satellite image of an oil and gas producing zone in India, having 34 flare locations spread across an area of 675 Km^2. Medium to reasonably dense settlements comprising tea gardens, hospitals, schools, colleges, churches, and temples are located around the oil and gas well sites. These settlements often face power shortages and electricity failure. Various gas turbines can utilize waste flare gas for power generation. This work aims to suggest economically viable options for developing necessary infrastructure that will enable the use of natural gas from wells to produce power. The benefit of this distributed generation is that it will provide power to the nearby areas and will help to save a lot of power extraction from the grid.

Figure 3-1 Khagorijan oil and gas field, OIL, Assam, 34 flare locations; Area: 675 km2; yellow stars – Flare Locations

In recent years, a lot of research has been performed to minimize the power loss in the domain of network design and reconfiguration of the distributed system. Merlin and Back[132] were the first to propose power loss reduction in the distribution system reconfiguration. Civanlar et al. [133] have also proposed a heuristic method to reduce power line loss by using a simplified formula to calculate loss reduction as a result of power transfer between two nodes. Khattam et al. [134] have formulated a mixed integer non-linear problem for resource allocation and distribution systems and used GAMS software tool to solve it.

Table 3-1 Specifications of three different kinds of Microturbines [143][144]

Equipment	Size (kW)	Cost ($/kW)	Electrical efficiency (%)	Operating and maintenance cost ($/kWh)
Reciprocating Turbine	300-5000	1000	35	0.025
Microturbine	30-300	825	28	0.014
Gas Turbine	300-10000	910	31	0.024

Table 3-1 presents the cost and capacity specifications of the three types of gas turbines available in the market. In this problem, we are considering three different technologies having different cost and capacity constraints (Table 3-1) to convert gas flares into electricity. Once the technology to produce power is decided, a distribution network will be needed to efficiently transfer power to meet the demands. Therefore, a model is developed, which will decide the availability and capacity of technology at each well, and simultaneously, it will provide the best network to transfer the power to meet the electricity demands of locals. It is typically a resource allocation and network design problem.

3.2 Mathematical Model

The mathematical formulation addresses the development of an optimal dynamic configuration for optimal resource allocation and network optimization. Given the geographical location of wells and demand sites, available fuel capacity, required power at different demand sites, economic data and properties of distribution wire and technology constraints, this formulation will determine an optimal selection of technology at different well sites and their capacity required, an optimal network for distribution of electricity to local users, electricity requirement from the central grid at demand site (if any) and power sold to the central grid at well site (if any).

The sets involved with the problem can be summarized as:

$Wellsites = \{i: 1 \leq i \leq total\ well\ sites\ | i\ \in Z\}$ set of total well sites.

$Demandsites = \{i: 1 \leq i\ \leq total\ demand\ sites\ | i \in Z\}$ set of total demand sites.

$totalsites = \{i: 1 \leq i \leq total\ sites\ | i \in Z\}$ set of total sites which include both well and demand sites.

$Tech = \{t: 1 \leq t \leq total\ technology\ | t \in Z\}$ set of total type of technology.

The super configuration for resource allocation and distribution network is illustrated in *Figure 3-2*.

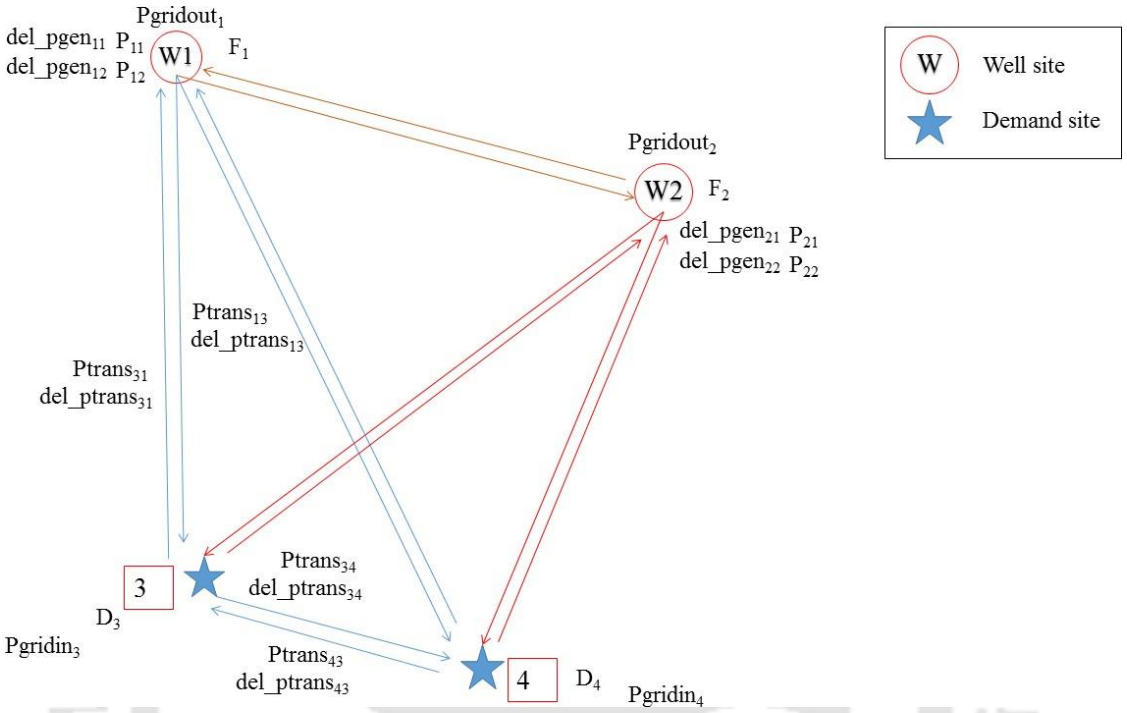

Figure 3-2 Representation of networks, Well, and power demand sites

The representation in *Figure 3-2* conceptually explains the basis of resource allocation and distribution network design. Well, sites are numbered before the demand sites. For representation, two different technologies are considered at each well site. Since it's a design problem, the network lines are not fixed. As the direction of flow of electricity from one site to another is unknown prior to the solution, initially, all sites are bi-directionally connected to each other in the representation. The distance between all wells and demand sites will be calculated using their coordinates.

The parameter of the problem includes the location of wells and demand sites, available fuel capacity, required power at different demand sites, economic data, and specification of distribution wire and technology. The parameters are defined below:

F_i: Capacity of fuel at i^{th} well site in standard cubic meter per day ($i \in Well\_Sites$)

D_i: Power requirement at i^{th} demand site in kW ($i \in Demand\_Sites$)

l_{ij}: Distance from i^{th} to j^{th} site in km ($i, j \in Total\_Sites$)

η_t: Efficiency of t^{th} technology ($t \in Tech$)

Ω: Resistance of wire in Ω / km

pf: Power factor

C_f: Multiplying factor associated with fuel as in equation 11

C_g: Selling value of electricity in $/kWh

C_p: Usual Cost of electricity in $/kWh

C_{td}: Cost of distribution line in $/km

Ct_t: Cost of generating technology in $/kW

P_t^{max}: Maximum power generation by t^{th} technology in kW ($t \in Tech$)

P_t^{min}: Minimum power generation by t^{th} technology in kW ($t \in Tech$)

$Ptrans_{ij}^{max}$: Maximum power transfer in i^{th} to j^{th} line in kW ($i, j \in Total\_Sites$)

$Ptrans_{ij}^{min}$: Minimum power transfer in i^{th} to j^{th} line in kW ($i, j \in Total\_Sites$)

$volt$: Voltage maintained in transmission line in volt

wt_{loss}: Factor associated with thermal loss

wt_o: Factor associated with power sold to grid

C_{ann}^{cap}: Annual capital cost of technology in $

C_{ann}^{grid}: Total annual cost of power exchanged with the grid in $

C_{ann}^{loss}: Annual cost occurred due to thermal loss in the distribution of power in $

$C_{ann}^{o\&m}$: Annual operating and maintenance cost of technology in $

$C_{ann}^{t\&d}$: Annual power distribution cost in $

C_{ann}^{tot} : Objective function in $

$C_t^{o\&m}$: Operating and maintenance cost of technology in $/kWh

Following are the decision variables of the resource allocation and network design problem:

δ_{ij}: Availability of path from i^{th} to j^{th} site, a binary variable ($i, j \in Total\_Sites$)

$Ptrans_{ij}$: Power transfer in i^{th} to j^{th} line in kW ($i, j \in Total\_Sites$)

δ_{it}: Availability of t^{th} generating technology at i^{th} well site ($i \in Well\_Sites, t \in Tech$)

P_{it}: Power generation by t^{th} technology at i^{th} site ($i \in Well\_Sites, t \in Tech$)

$Pgridin_i$: Power taken from grid at i^{th} demand site in kW ($i \in Demand\_Sites$)

$Pgridout_i$: Power sold to grid at i^{th} well site in kW ($i \in Well\_Sites$)

Cost models are used qualitatively to determine the optimal solution. It aims to minimize the equipment cost of power technology, payments toward purchasing power from the grid and payments toward loss compensation services. Following five types of costs are involved in the presented objective function:

a) The annualized capital cost associated with equipment, C_{ann}^{cap}.

b) The fixed cost of transmission, $C_{ann}^{t\&d}$.

c) The cost associated with power loss in transmissions, C_{ann}^{loss}.

d) The cost incurred due to power exchange from the grid, C_{ann}^{grid}.

e) The cost of power technology which consists of both fixed cost and variable operating and maintenance cost, $C_{ann}^{o\&m}$.

The fixed cost of transmission is generally the cost associated with laying the wire. Cost of power loss is basically introduced to minimize the power loss in transmissions. Cost of grid power is introduced to minimize the grid exchange unless there is a deficiency of power. Cost of equipment will decide the best economic technology.

The mathematical formulation is described in Eq. (1) – (15). The objective function C_{ann}^{tot} in Eq. (1) aims to minimize the equipment cost of power technology, payments toward purchasing power from the grid and payments toward loss compensation services., subject to various constraints. These constraints are described in Eq. (7) – (13). An assumption is taken to simplify the problem which is described in Eq. (14) – (15).

$$C_{ann}^{tot} = C_{ann}^{cap} + C_{ann}^{o\&m} + C_{ann}^{loss} + C_{ann}^{t\&d} + C_{ann}^{grid} \quad (1)$$

$$C_{ann}^{cap} = (\sum_{i,t} Ct_t * P_{it}) * CRF \qquad \forall\ i \in Wellsites,\ t \in Tech \quad (2)$$

$$C_{ann}^{o\&m} = \sum_{i,t} 8760 * P_{it} * C_t^{o\&m} \qquad \forall\ i \in Wellsites,\ t \in Tech \quad (3)$$

$$C_{ann}^{loss} = \sum_{i,j} 9.3793 * C_p * l_{ij} * Ptrans_{ij}^2 \qquad \forall\ i,j \in totalsites \quad (4)$$

$$C_{ann}^{t\&d} = \sum_{ij} C_{td} * l_{ij} * \delta_{ij} \qquad \forall\ i,j \in totalsites \quad (5)$$

$$C_{ann}^{grid} = \sum_{i} C_p * Pgridin_i + C_g * Pgridout_i.wt_o) * 8760 \qquad \forall\ i \in totalsites \quad (6)$$

Here, wt_o is tuning parameter for $Pgridout_i$. Here wto is 0.9. $Pgridout_i$ is relatively given less weightage than $Pgridin_i$. It means priority to minimize $Pgridin_i$ is more than $Pgridout_i$. The system will ensure that a demand site will take power only when there is insufficient power generation. Here cost associated with $Pgridout_i$ is also added, which is basically a profit, and here the system tries to minimize it. Because the objective is not to maximize profit but to satisfy power demand as much as it can via distribution generation. 9.3793 is the thermal power loss coefficient, and 8760 is a factor used to annualize the costs. The decision variables P_{it} and $Ptrans_{ij}$ are dependent on binary variables δ_{it} and δ_{ij}. Only when these binary variables are one the decision variables will be active. To avoid non-linearity, a special inequality is considered (equations 8, 10, 12), which makes the problem a mixed integer quadratic one with quadratic constraints.

Following are the constraints involved in the presented mathematical formulation:

- *Total power conservation:* Summation of all incoming and outgoing power, taking power losses into consideration and power produced by generator should be equal to demand.

$$\sum_t P_{it} + \left(\sum_j Ptrans_{ji} - \sum_j 0.0010707 * l_{ji} * Ptrans_{ji}^2 \right) - \sum_j Ptrans_{ij} + Pgridin_i - Pgridout_i = D_i \quad \forall\ i,j \in total\ sites,\ t \in Tech \tag{7}$$

- *Thermal capacity constraint:* Electricity transferring through a wire must not cross the maximum thermal capacity of the wire.

$$Ptrans_{ij}^{min} * \delta_{ij} \leq Ptrans_{ij} \leq Ptrans_{ij}^{max} * \delta_{ij} \quad \forall\ i,j \in total\ sites \tag{8}$$

- δ_{ij} is a binary variable which determines the presence of electricity flow in line i to j. If δ_{ij} is zero implies there is no electricity flow in line i to j. And the constraint assures that electricity flowing through a line i to j is unidirectional at a time.

$$\delta_{ij} \in \{0,1\} \quad \forall\ i,j \in total\ sites \tag{9}$$

$$\delta_{ij} + \delta_{ji} \leq 1 \quad \forall\ i,j \in total\ sites \tag{10}$$

- Power produced by generators at a site should be less than the power generating fuel capacity of the well

$$\sum_t \frac{P_{it}}{\eta_t} = F_i * C_f \quad \forall\ i \in Well, t \in Tech \tag{11}$$

- Power produced by a technology at a well site should satisfy the capacity constraint of that technology. δ_{it} is a binary variable which assures the availability of technology 't' at a site 'i'.

$$P_t^{min} * \delta_{it} \leq P_{it} \leq P_t^{max} * \delta_{it} \quad \forall\ i \in Wellsites, t \in Tech \tag{12}$$

$$\delta_{it} \in \{0,1\} \quad \forall\ i \in Wellsites, t \in Tech \tag{13}$$

The model is formulated as a mixed integer quadratic problem with quadratic constraint. The complexity of MIQP with QC is very high. In this work, the model is simplified by linearizing the power loss term as follows:

$$C_{ann}^{loss} = \sum_{i,j} 938.196 * C_p * l_{ij} * Ptrans_{ij} \quad \forall\ i,j \in totalsites \tag{14}$$

$$PowerLoss = \sum_{j} 0.1071 * l_{ji} * \ Ptrans_{ji} \qquad \forall\, i,j \in totalsites \qquad (15)$$

Now, this assumption will give a higher weightage to power loss. Therefore, the model will always prioritize minimizing the power loss. But this assumption will also give a slightly bigger capacity for the generator because the power loss is increased here. Now, the problem becomes a standard mixed integer linear problem which is solved by CPLEX package of Tomlab in MATLAB environment.

3.3 DISCUSSIONS

Various cases are considered to check the robustness of the optimization problem. Variation of decision variables are checked with respect to parameters like, the quantity of fuel, location of well site, thermal capacity constraint of distribution line.

3.3.2 Analysis of a system with variable quantity of fuel

In case 1, one well and two demand sites are considered as shown in *Figure 3-3*. Distance between well site-1 and demand site-2 and demand site-3 is 1 km and 1.3483 km respectively. Distance between demand site-2 and demand site-3 is 0.559 km. Hybrid technologies namely, microturbine, reciprocating turbine and gas turbine, are considered at each well for analysis. Power demand at site-2 and site-3 is 40 kW and 60 kW respectively.

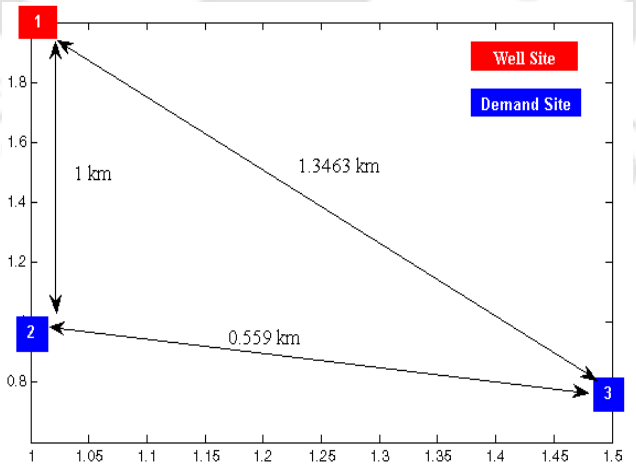

Figure 3-3 Graphical representation of gas flare site (well site) and demand site in case 1

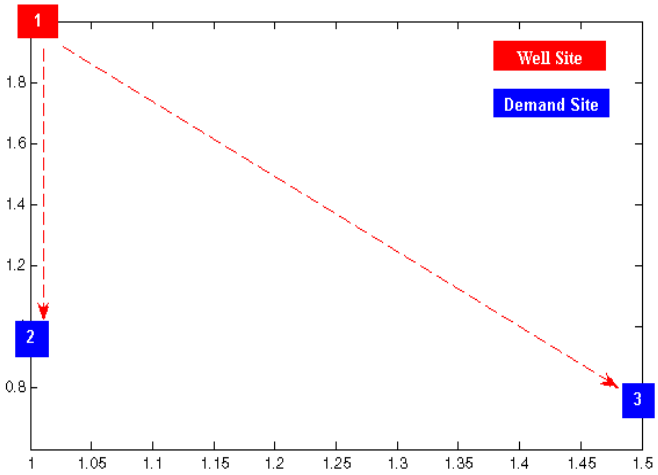

Figure 3-4 Network selected in case 1 as a result of the optimization formulation

Variation of generation capacity of different technologies, power transmission, power loss incurred, and power exchange with different quantities of fuel is shown in Table 3-2. For every scenario, the same distribution network is produced as shown in *Figure 3-4*. It can be noticed from Table 3-2 that when fuel is low i.e., 500, 700 SCMD, demand site-2 is first satisfied, and the rest power is sent to demand site-3 because power loss incurred to satisfy site-3 would have been relatively significant. Therefore site-3 takes extra power from the grid to satisfy its demand. It is observed that power loss varies from 10% to 14%. There is no change in power transfer and power loss when fuel is changing from 1000 to 1500 SCMD; because fuel is present in excess, and after the demand is satisfied, the remaining power is sold to the grid. It can be noticed that microturbine is selected in every scenario because reciprocating turbines and gas turbines are available with more than 300 kW and demand is less than it. Here different available technologies can be introduced and their capacity constraint can be integrated into the system to provide the best-optimized result.

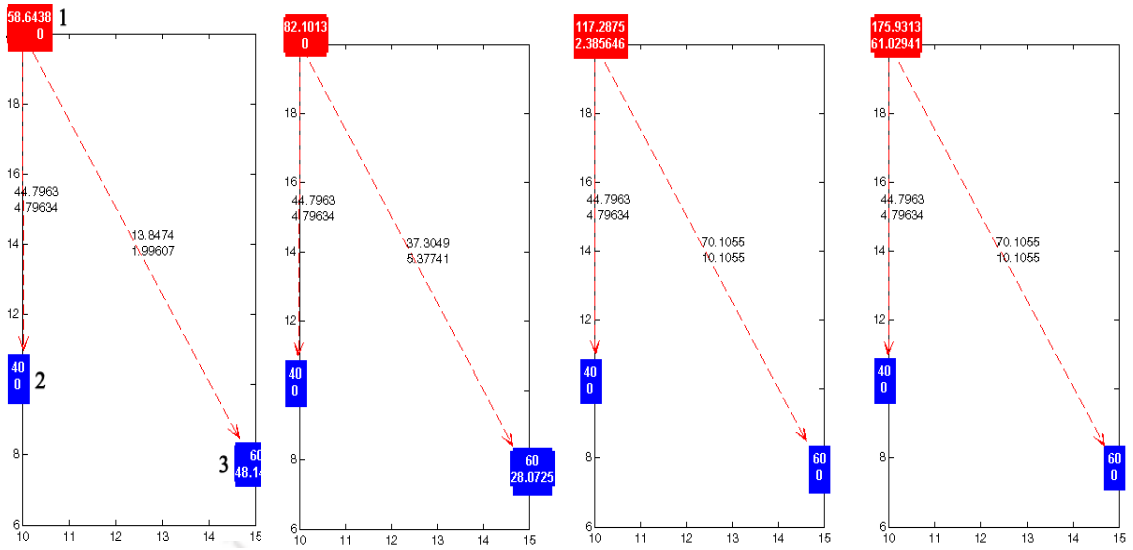

(a) Fuel at well 1= 500 SCMD

(b) Fuel at well 1 = 700 SCMD

(c) Fuel at well 1= 1000 SCMD

(d) Fuel at well 1 = 1500 SCMD

Figure 3-5 Optimized network design with respect to capacity of well

Table 3-2 Variation of generation capacity, power transfer and loss with respect to available fuel

Scenario	***Fuel (SCMD)***	***Generation Capacity (kW)***	***Power transfer (kW)***	***Power loss (kW)***	***Pgrid_In (kW)***	***Pgrid_Out (kW)***
(a)	500	MT – 58.64	1 → 2 - 44.8	1 → 2 - 4.8	3 → 48.15	
			1 → 3 - 13.8	1 → 3 - 1.99		
(b)	700	MT – 82.1	1 → 2 - 44.8	1 → 2 - 4.8	3 → 28.07	
			1 → 3 - 37.3	1 → 3 - 5.37		
(c)	1000	MT – 117.28	1 → 2 - 44.8	1 → 2 - 4.8		1 → 2.38
			1 → 3 - 70.1	1 → 3 - 10.1		
(d)	1500	MT – 175.9	1 → 2 - 44.8	1 → 2 - 4.8		1 → 61
			1 → 3 - 70.1	1 → 3 - 10.1		

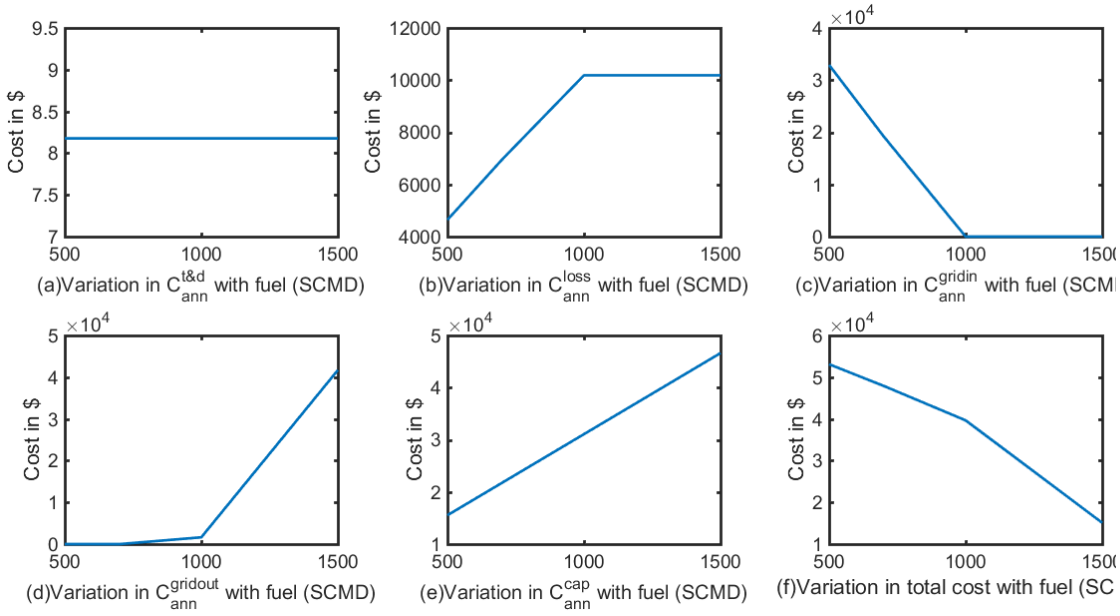

Figure 3-6 Cost Variation with respect to fuel

It can be observed from Figure 3-6*(a)* that line cost is constant because path selection is same in all cases. Cost associated with power loss Figure 3-6 *(b)* first increases and then remains constant, because initially fuel is deficient and therefore less power is transferred to satisfy power demand at site-3. So associated power loss is also less. Later, the fuel becomes excess. Therefore, power transfer to satisfy power demand at site-2 and site-3 is not changing. The same is the case with associated power loss. The cost of grid-in power Figure 3-6 *(c)* is decreasing as fuel is increasing because latter the fuel becomes sufficient to meet the power demand. Cost of grid-out power Figure 3-6 *(d)* increases as fuel increases from 1000 to 1500 SCMD because the excess power produced is sold to grid. It is very much intuitive that as the amount of fuel availability increases, the cost incurred in purchasing the power from the utility decreases, and the profits incurred by selling off the surplus power to the grid increase. This is proved in Figure 3-6 *(c)* and Figure 3-6 *(d)* as the cost of grid-in power and cost of grid-out power are complementary. Power Equipment cost (Figure 3-6 *(e)*) increases with increased fuel availability because generation capacity will also increase. In Figure 3-6 *(f)*, total cost decreases rapidly in the later part because fuel becomes surplus after 1000 SCMD. After meeting the power demand requirements, the excess power is sold to the grid, which is an income for the community. It can be concluded that the objective function formulated in this work assures full utilization of available natural gas to satisfy the power demand, and in addition to it, surplus power is sold off to grid in order to earn profit from the available

resources.

3.3.3 Analysis of different parameter with variable demand

This case is also based on the design given in case study I (*Figure 3-3*and *Figure 3-4*). It can be observed from ***Table 3-3***, in scenario (a) –(c) fuel is same, so generation capacity is also same. But reciprocating turbine is selected of 300 kW whereas microturbine is selected of 111.8 kW, because microturbine has maximum capacity constraint of 300 kW. In both (a) and (b), fuel is same but sold power is different because thermal capacity of wire is higher in case of (b). Therefore, sufficient power is transfer to satisfy the demand and the rest power is sold to grid.

Table 3-3 Variation of generation capacity, power transfer and loss with respect to available fuel and demand

Scenario	***Fuel (SCMD)***	***Demand (kW)***	***Max Thermal capacity of wire (kW)***	***Generation Capacity (kW)***	***Power transfer (kW)***	***Power loss (kW)***	***Pgrid_In (kW)***	***Pgrid_ Out (kW)***
(a)	3000	2 – 150 3 – 80	100	MT – 111.8 RT – 300	1 → 2 - 100	1 → 2 – 10.71	2 → 60.71	1 → 218.38
					1 → 3 – 93.47	1 → 3 – 13.47		
(b)	3000	2 – 150 3 – 80	200	MT – 111.8 RT – 300	1 → 2 – 168	1 → 2 - 18		1 → 150
					1 → 3 – 93.4	1 → 3 – 13.4		
(c)	3000	2 – 150 3 – 200	200	MT – 111.8 RT – 300	1 → 2 - 168	1 → 2 – 18	3 → 28.8	
					1 → 3 - 200	1 → 3 – 28.8		
(d)	4000	2 – 150 3 – 200	300	MT – 229 RT – 300	1 → 2 - 168	1 → 2 – 18		1 → 127.4
					1 → 3 – 233.7	1 → 3 – 33.7		

3.3.4 Analysis of a system with two well source

Here a second well source of 500 SCMD is added near to both demand sites (6.3 km from wellsite 2 to demand site 3 and 4.6 km from well site 2 to demand site 4 as shown in Figure 3-8. Thermal capacity constraint of transmission line is 100 kW. As it is closer to demand site 4 than demand site 3, it is providing all its power to demand site 4, i.e., 58.6 kW. And remainingpower demands are met by well source 1. The capacity of well source is now increased to 700SCMD. Here it can be seen that after meeting the power demand of site 4, the remaining power(14.17 kW) is sent to site 3. Well site 1 send 30 kW power to demand site 2 to meet all the power demands. Now the capacity is increased to 1000 SCMD, which is sufficient to producethat much power which is needed to meet demands. Well source 1 is producing power and selling all the power to the grid.

Justification of taking wt_o as 0.9 is shown in Figure 3-7. When both Pgridini and Pgridouti is given equal weightage, well site 2 is not transferring the power to the nearest source, demand site 4 as shown by Figure 3-7 (b). In this whole process, the priority to minimize is given to power exchange with grid. So, power demand is being satisfied via well site 1 instead of well site 2. Because it will be extracting slightly more power than it would use to be if the transfer would happen via well site 2. When slightly less weightage is given to Pgridouti (wto = 0.9), total power sold becomes 126.07 kW which is greater than 121.55 kW (105.82+15.73) as shown in Figure 3-7 (a). But total power loss decreases, which is one of the prime objectives.

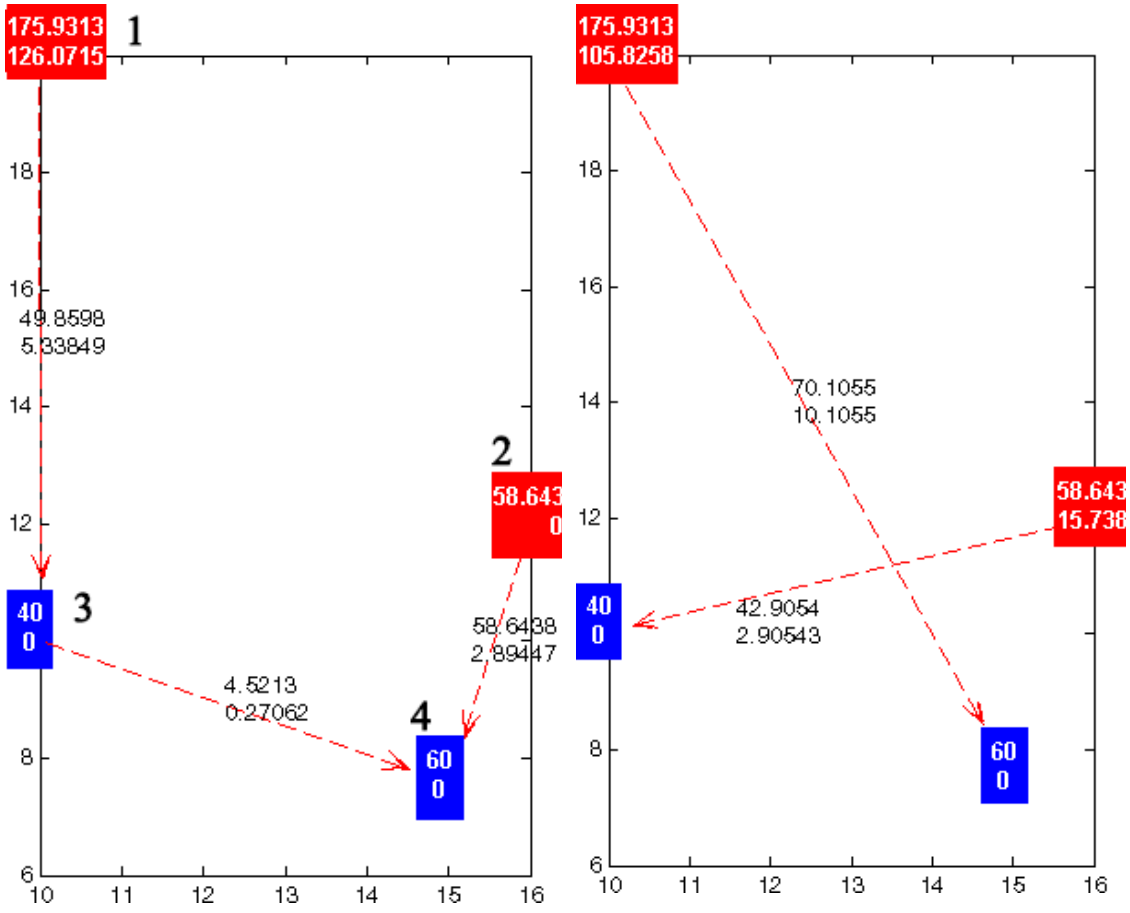

(a) $wt_o = 0.9$ (b) $wt_o = 1$

Figure 3-7 Variation of network with respect to wto, weightage to Pgridout

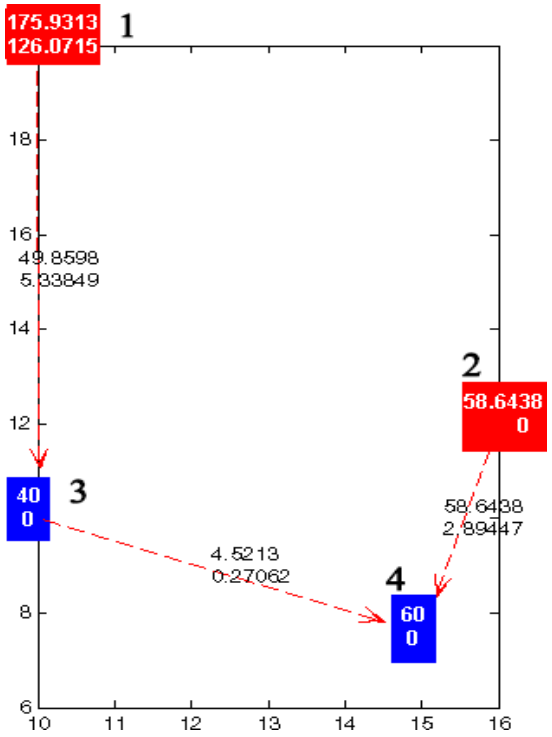

(a) Fuel at Well-2 = 500 SCMD

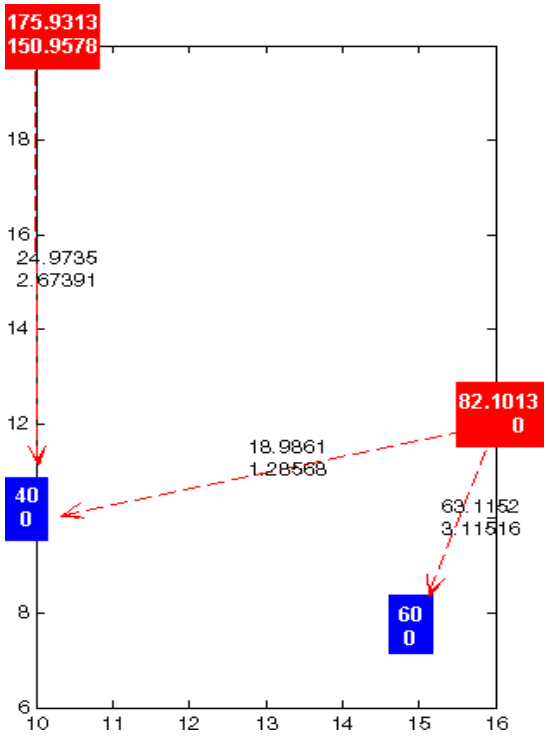

(b) Fuel at Well-2 = 700 SCMD

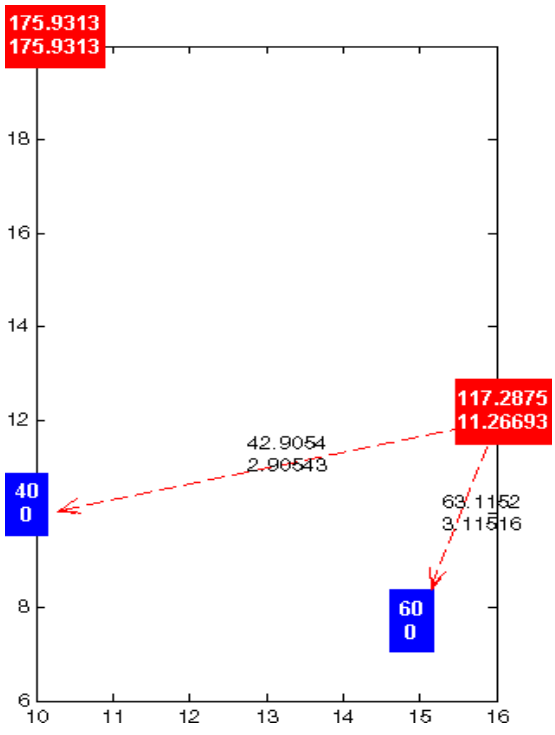

(c) Fuel at Well-2 = 1000 SCMD

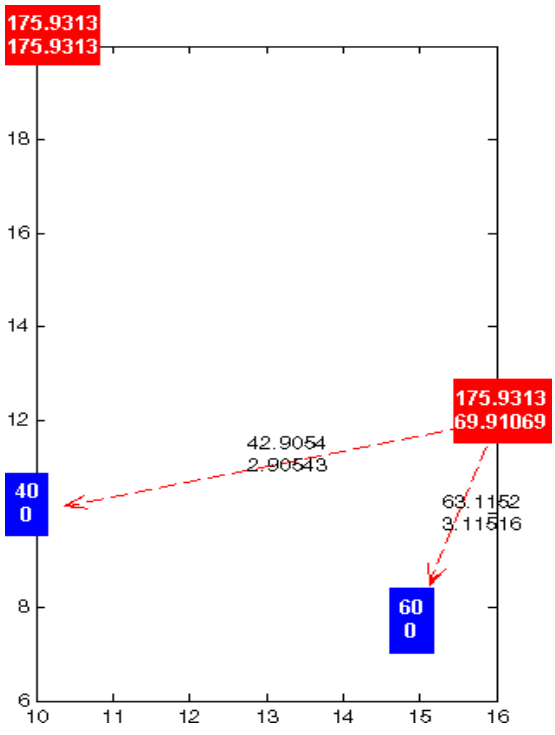

(d) Fuel at Well-2 = 1500 SCMD

Figure 3-8 Optimized network design with respect to capacity of second well

***Power generation and Pgridout is represented in red box; Power demand and Pgridin is represented in blue box; Power transfer and loss is representedbeside the line*

3.3.5 Analysis with multiple source and demand

Here seven well sources and eight demand sites are considered. Their x and y co-ordinates (scale in km) are given in sequence as (1, 13), (7, 25), (8, 17), (8, 2), (11, 12), (15, 24), (15, 3), (2, 3), (3, 21), (3, 13), (6, 7), (11, 7), (13, 16), (17, 11), (22, 20). Available capacity (in SCMD) of gas well site 1 to 7 is as follow: 1000, 2000, 3000, 2000, 4000, 2000, and 2000. Power demand (in kW) at site 8 to 15 is as follow: 100, 80, 110, 350, 200, 150, 300, and 250. Thermal capacity constraint of wire is taken as 100 kW. Results are presented in *Table 3-4*.

Table 3-4 Variation of different parameter for case-4

Sending node	Receiving node	Power transfer (kW)	Power loss (kW)
1	10	91.83	1.97
1	11	25.45	2.13
2	9	85.16	5.16
2	15	25.60	4.33
3	10	21.61	1.48
3	11	100.00	10.92
3	13	97.95	5.35
3	14	100.00	11.58
3	15	61.33	9.40
4	8	100.00	6.51
4	11	100.00	5.77
4	12	34.58	2.16
5	8	7.54	1.03
5	11	100.00	7.57
5	12	100.00	5.35
5	13	90.64	4.34
5	14	100.00	6.51
5	15	100.00	14.56
6	15	100.00	8.63
7	11	56.94	6.00
7	12	77.64	4.70
7	14	100.00	8.83
13	14	28.91	1.98

Power sold to grid at well site 2 and 6 is 123.82 kW and 134.58 kW respectively (figure 6.5). And any power exchanges with grid at other sites are zero. Total power demand which is met via microgrid is 1540 kW

Table 3-5 Selection of technology and their capacity

Well site	Power Generating Technology (kW)
1	MT – 117.29
2	MT – 234.57
3	MT – 80.89 GT – 300
4	MT – 234.57
5	MT – 198.18 GT – 300
6	MT – 234.57
7	MT – 234.57
Total Power (kW)	1934.7

It is seen from *Table 3-5*, that for well site 3 and 5, gas turbine is also chosen. Because here power production exceeds 300 kW which is maximum power capacity constraint for microturbine (*Table **3-1***). Cost of distribution line is $ 636.31/yr. Cost of equipment and production of power which include operating and maintenance cost is $ 557,547.06/yr. Total earning after selling to local users and grid at rate of $ 0.1075/kWh, is $ 1693553.28/yr.

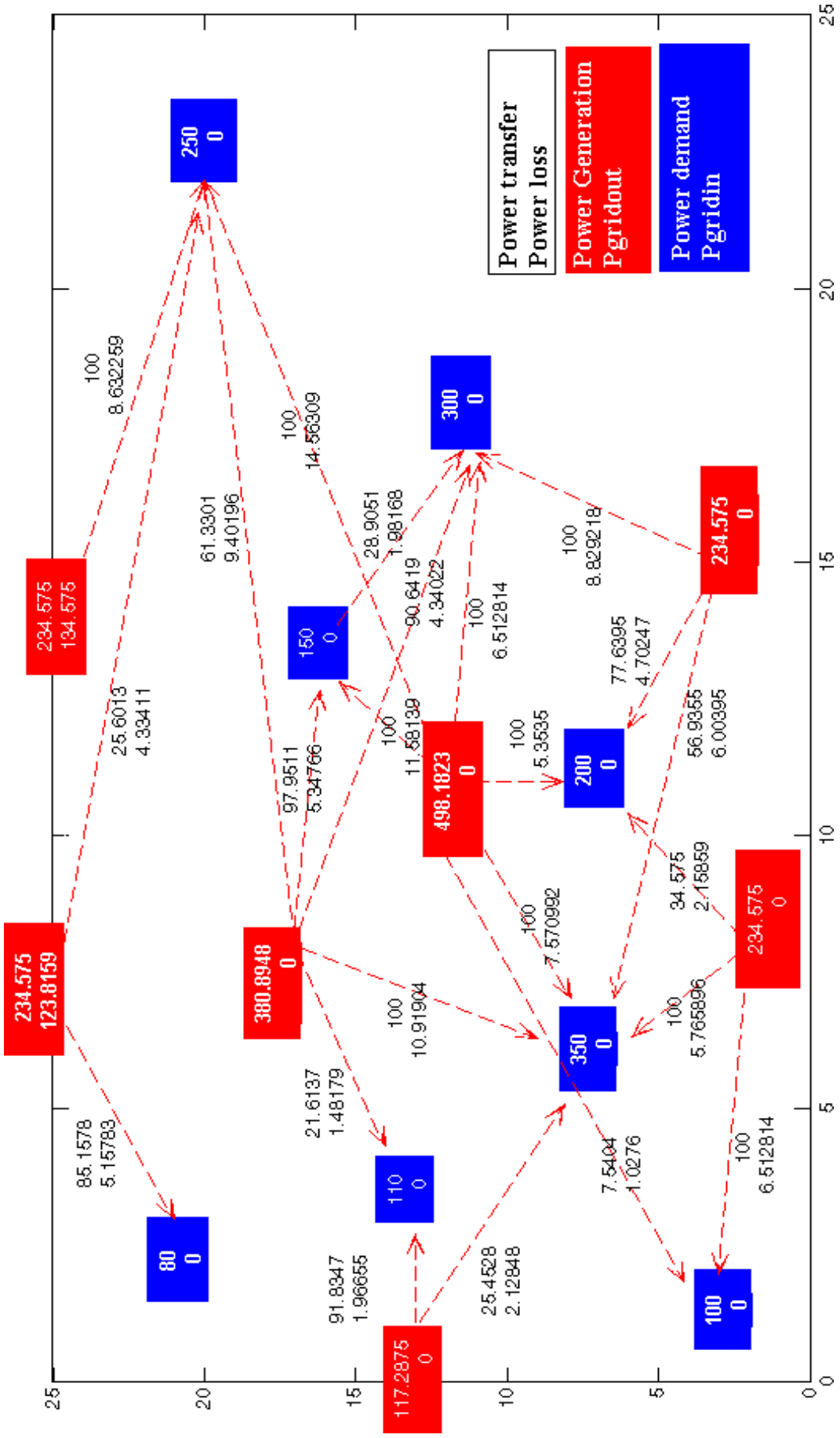

Figure 3-9 Optimized network graph of multiple source and demand

3.4 CONCLUSION

This chapter introduces a framework for implementing distributed power generation from flare gas as an attractive option in energy production. This work presented an idea that flared natural gas in upstream oil and gas sector is rather a potential source of energy. A new developed optimization model is implemented successfully to estimate capacity of power generator and best network to distribute power. The formulated model follow a hard constraint which assures full utilization of available fuel to satisfy power demand and sold remaining power to grid if any. The model also minimize power loss and power exchange with grid. Weightage parameter associated with the power sold to the grid, wt_o largely affects the network. The effect of variation of wt_o on network configuration and various power transfers is also studied. It is observedthat higher capacity technology will be selected only when there is a higher demand and poweremanating from a source exceeds the power capacity of that technology. Efficiency and equipment cost affect the generation capacity of a particular technology. The developed calculation framework is based on resource allocation and network design problem. Non-linear behavior of power loss makes it a mixed integer quadratic problem with quadratic constraint which complicates the problem; therefore, an assumption is taken to linearize the problem. By simulating various scenarios, it is seen that the assumption doesn't affect the optimal path.

Chapter 4

Solar Energy Prediction Using Machine Learning

4.1 Foreword

For utmost utilization of available resources, oil and gas well based Microgrids should also encorporate locally available renewable energy sources for power generation. Solar energy is considered most promising and abundant renewable resource for bulk power generation. But forecasting renewable resources requires addressing several challenges. All renewable energy sources are dependent on weather and meteorological parameters, and therefore the power generated using them cannot be fully controlled. The integration of solar energy with an electrical network intensifies the complexity of grid management. In the event of inaccurate forecasting, unexpected fluctuations in renewable power generation can cause significant impacts on the daily operation of the entire grid and may even negatively affect the daily lives of the consumers. Forecasting of the solar power generation allows the operators to schedule the load demand in order to maintain a supply-demand balance in the power system. Therefore, accurate forecasting of solar generation is required for the effective operation of the power grid for optimal management of energy fluxes occurring in the system. Almost all of the machine learning methods used for prediction and forecasting out-perform the simple classical methods. This chapter compares various machine learning techniques and presents a comprehensive discussion on solar PV power prediction.

Due to the time-varying weather conditions affecting renewable energy sources, it is very difficult to provide a stable, continuous power supply. The necessity to accurately predict the quantity of electricity that must be generated by solar PV systems, to feed into the grid 24 hours in advance, is as crucial as is the requirement to have precise weather forecasts. This forecast is used by the system operator to balance the supply-demand in the grid. Major energy corporations may incur cost overruns when electrical grids are not precisely balanced. Therefore, occurs the need for a machine learning algorithm that is capable enough of assisting microgrids with instantaneous control.

4.2 Methodology

Machine learning techniques extract features from the data, train the prediction models, observe validation accuracy on the training dataset, and evaluate the pre-trained model for the test dataset. The dataset imported would be pre-processed to make it suitable in format, free of anomalies, such as null values, outliers, missing values, and erroneous data values in the exploratory data analysis stage. Further, the machine learning techniques investigated in this paper are supervised learning methods, which include learning in input-output mappings from the empirical data. Figure 4-1 presents the flowchart of the proposed model.

The workplan includes mainly five steps:

1. In the first step, historical weather data for modeling was collected from NASA weather repository.
2. Data wrangling is the stage where data cleaning and dimensionality reduction are performed. The weather data was imported for processing, and missing or null values were eliminated or replaced from the dataset.
3. In the third step, the correlation matrix is formed. The outcome of the investigation discards useless features from the dataset reducing its dimension and exploring forecasting model accuracy. This step is crucial to get meaningful analysis from numeric values on an hourly basis on pre-processed data obtained from the second step to train the model.
4. The fourth step involves deploying various boosting tree algorithms for prediction, comparing these algorithms' performances, and identifying the algorithm that provides the most accurate prediction.

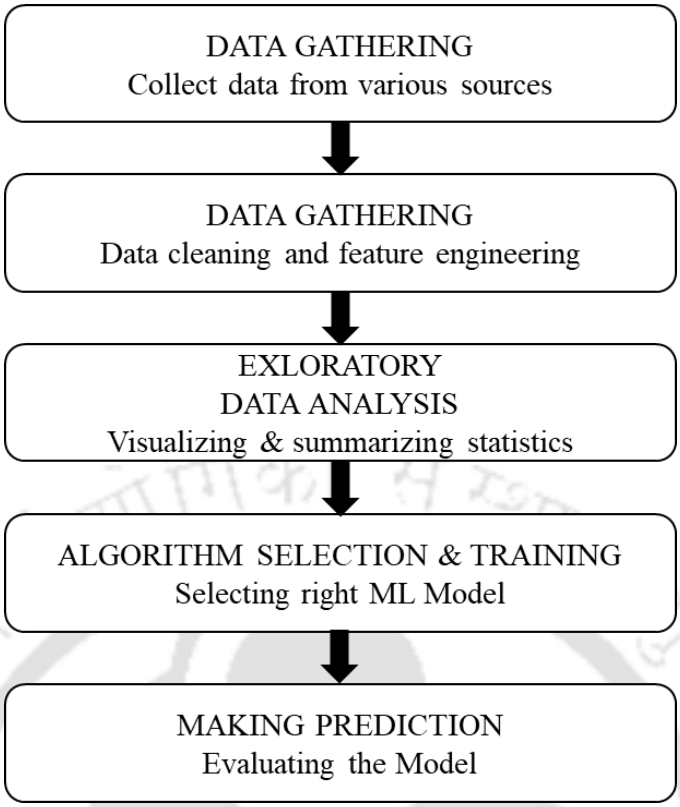

Figure 4-1Workflow for the prediction model

5. Finally, to ensure the model's accuracy, the error analysis methods like R-squared score, root mean squared error (RMSE) are used to calculate the model's performance accuracy.

In boosting algorithm, boosting refers to reducing the error of a weak learning model [135]. Boosting apparently works by repeatedly running a given weak learning model on different training data distributions and combining their outputs. At each iteration, the distribution of training data depends upon the performance of the previous iteration [136]. The process of calculating the distribution of the training data and combining the predictions from each model is different for different boosting methods (Solomatine). The ability of ensemble models to retain the bias of their learners while decreasing their individual variance has long made them quite attractive in several classification and regression problems [138].

4.2.1 Data Gathering

Data collection is the most critical step in solving any supervised machine learning problem, as along with other factors, the accuracy of the prediction model also depends on the dataset provided as input to the model. The machine learning techniques studied in this research function on the time-series climatological data to construct forecasting

models. The solar power generation data has been obtained from open source web-based libraries as there were no missing values in the data, and it covered a broad range of weather parameters which made the study of the impact of parameters on the forecasting models accurate and easier.

The global horizontal irradiance (GHI), which is the total daily solar radiation incident on a horizontal surface, for the chosen oil and gas field location in Nazira Assam asset (27° 1.8′ N, 94° 52.4′ E) was obtained from NASA surface meteorology and solar energy website [139]. The annual average solar radiation in the region is 3.92 kWh/m^2/day. Figure 4-2 shows the average monthly values of the Clearness index (left axis) and GHI (right axis) for 22 years (July 1983 – June 2005). The clearness index (surface radiation & the extraterrestial radiation ratio) is the measure of the clarity of the atmosphere and is a dimensionless quantity varying between 0 and 1. The clearness index is high in winters, whereas GHI is higher in summer months. Both these indices are used to calculate the flat-plate SPV output. Apart from solar irradiance data, solar photovoltaic panel parameters and datasets were obtained from HOMER software repository. These solar photovoltaic panel parameters include - Generic flat plate SPV Solar Altitude °, Generic flat plate PV Solar Azimuth °, Generic flat plate PV Angle of Incidence °, Generic flat plate PV Incident Solar (kW-m^2), Generic flat plate PV Power Output (kW). The data indicating weather dependency of solar energy was also considered for the analysis. This weather data included – cloud coverage, visibility, temperature, dew point, relative humidity, wind speed, station pressure and altimeter reading. Table 4-1 Solar data dependent on weather presents the weather dependent solar data.

Table 4-1 Solar data dependent on weather

	Hour	Cloud coverage	Visiblity	Tempe-rature	Dew Point	Relative Humidity	Wind Speed	Station Pressure	Altimeter	Solar Energy
0	6	0.00	9.92	0.37	-0.01	89.12	4.72	29.19	29.98	0.00
1	7	0.00	10.00	0.47	-0.04	90.08	6.00	29.20	29.99	84.29
2	8	0.14	9.92	0.89	0.30	92.00	2.76	29.22	30.01	531.00
3	9	0.92	10.00	1.97	0.41	86.12	5.56	29.24	30.04	923.75
4	10	0.46	10.00	3.15	1.07	82.48	2.12	29.27	30.06	1947.75

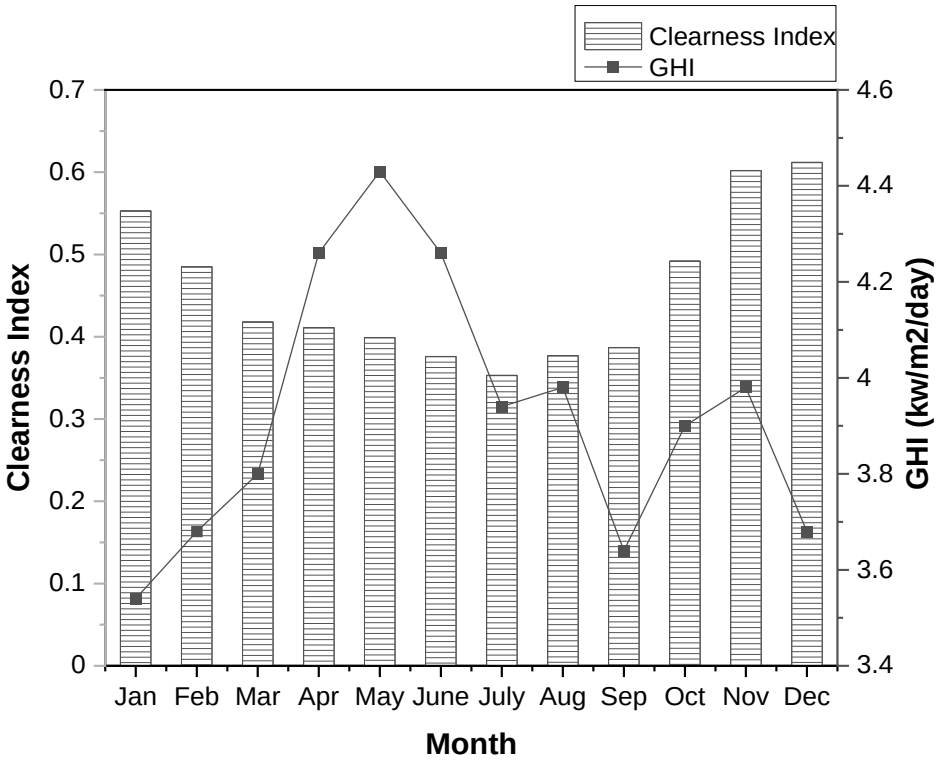

Figure 4-2 Global horizontal Index and clearness Index of solar energy forecast

4.2.2 Data Wrangling and Exploratory Data Analysis

Data wrangling involves pre-processing of data where the imported data is scrutinized for null values or duplicates. In this stage, the categorical values are converted into quantitative variables. Finally, features are scaled to match the rest of the features. Suitable python libraries are imported for data wrangling.

Exploratory Data Analysis (EDA) is a preliminary step for the exploration of the data to understand more about its characteristics. Data exploration mainly focuses on

i. Summarizing statistics
ii. Visualization

In correlation analysis, a correlation matrix helps in finding the strength of the relationship between two features. A high value of correlation coefficient between them means a positive linear relationship with each other.

Figure 4-3 shows the heat map taking the entire feature variable from the weather data. From the correlation study depicted in Figure 4-3, the importance of the rest six parameters with respect to solar energy generation can be judged.

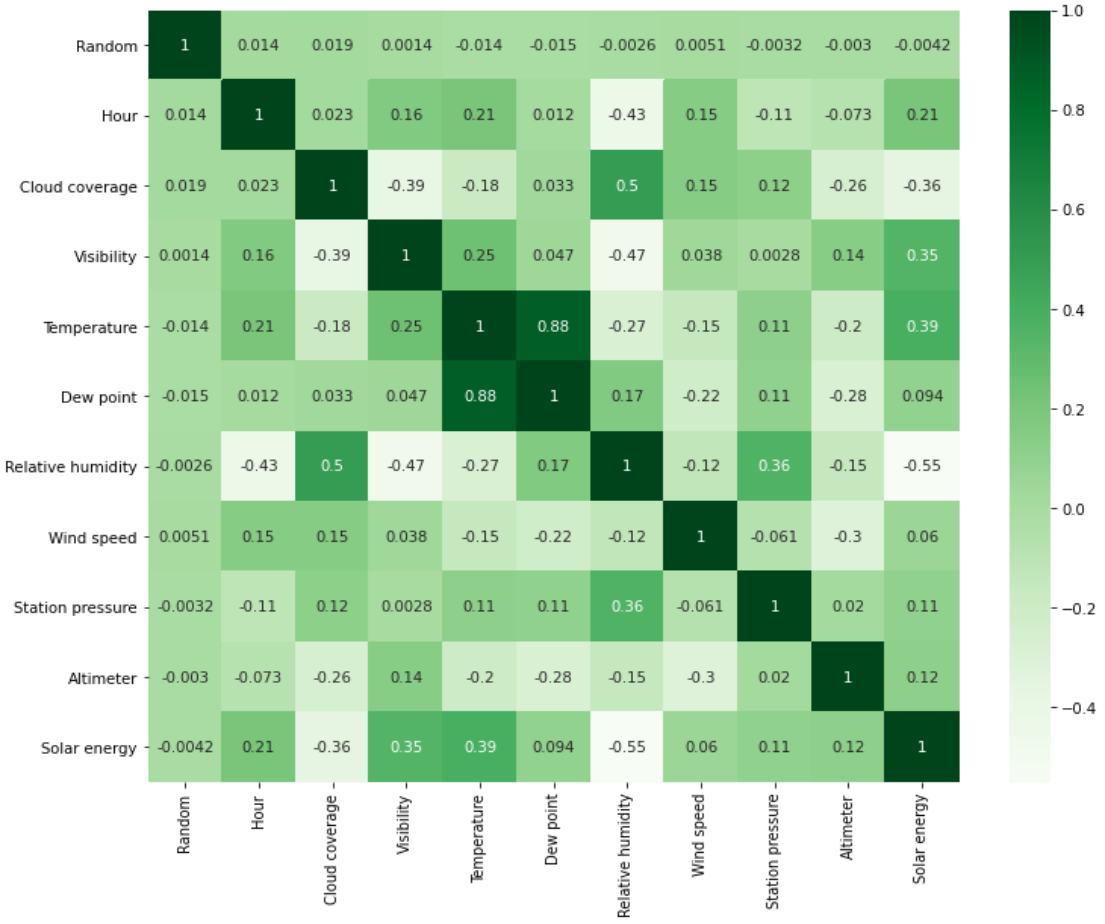

Figure 4-3 Pearson correlation heatmap for the SPV panel at energy generation

The following observations are made from this analysis:

- Relative humidity negatively correlates with solar intensity, and its value does not indicate solar PV panel power generation or solar intensity.
- Temperature correlates with solar intensity at higher values. If the temperature is high, the solar intensity is also likely to be high.
- However, if the dew point or temperature tends to be low, the solar intensity exhibits a much more significant variation between high and low values.

The results obtained in this study corroborate the previous findings [140].

Linear regression attempts to fit the best fit line on the data with weather parameters such as temperature, relative humidity, visibility and dew point, etc. Figure 4-4 demonstrates the regression plot for temperature in Celsius with respect to solar energy in kWh. A positive linear relationship between temperature and solar power

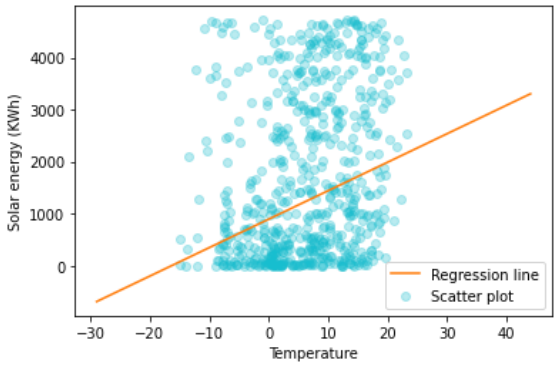

Figure 4-4 Linear relationship plot between temp & solar energy

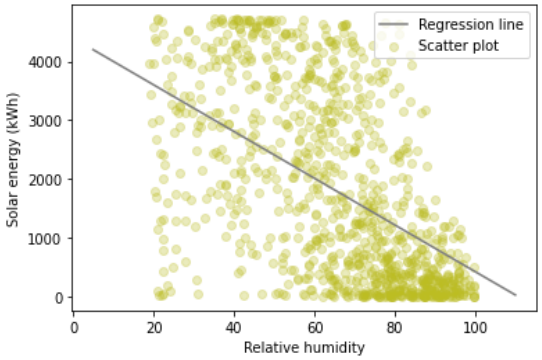

Figure 4-5 Inverse linear relationship plot between relative humidity & solar energy

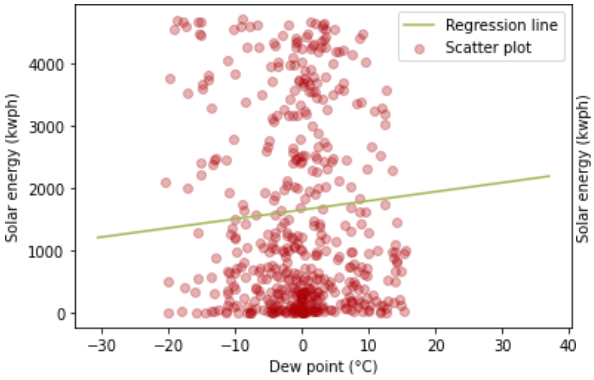

Figure 4-6 Linear Regression Plot of Solar Energy Vs. Dew Point

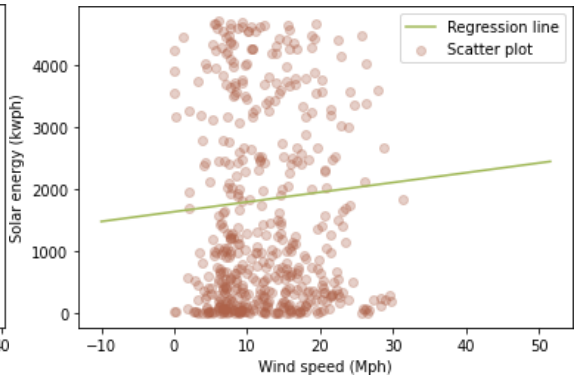

Figure 4-7 Linear Regression plot of wind speed Vs. Solar Energy

generation can be observed. Figure 4-5 demonstrates the regression plot for relative humidity with respect to the solar energy generated. In this graph, it can be observed that solar energy generation tends to increase as relative humidity decreases. Figure 4-6 and Figure 4-7 indicate the linear relationship of solar energy generation with respect to dew point and wind speed. The graphs show that solar energy generation increases with an increase in dew point and wind speed, but the slope is lesser as compared to the increase in case of temperature or decrease in case of wind speed.

4.3 Accuracy Estimating Index Metrics

In order to comprehensively evaluate the feasibility and effectiveness of the proposed solar and wind power forecasting models, two widely used performance evaluation metrics are used in this chapter. They are - determination coefficient or R Squared score (R^2) and Root Mean Squared Error (RMSE). The coefficient of determination is usually represented in percentages. It gives an idea of the number of data

points falling within the results of the line fitted by the regression equation. The higher the coefficient, the higher percentage of points the line passes through when the data points and line are plotted. R^2 score is the amount of variation in the output-dependent attribute, which we predict from the input-independent variable(s). The RMSE is used to measure the average amplitude of the error and gives a higher weight to the relatively large error. This means that RMSE is suitable for identifying significant prediction errors in the prediction process. The formula for RMSE and R^2 score is given by eq (1) and (2).

$$RMSE = \sqrt{\sum_{i=1}^{n} \frac{(\hat{y}_i - y)^2}{n}} \tag{1}$$

$$R^2\ score = 1 - \frac{SS_{res}}{SS_{tot}} = 1 - \frac{\sum_i (y_i - \hat{y}_i)^2}{\sum_i (y_i - \hat{y})^2} \tag{2}$$

Where $(\hat{y}_i - y)^2$ is the square of the difference in the actual value (y_i) and the forecast value ($\hat{y}_i$). The total number of data points is represented by n. The R^2 score or coefficient of determination is given by eqn (2) where SS_{res} is the sum of squares of residues, and SS_{tot} is the total sum of squares.

4.4 Implementation of Models

The presented study compares the performance of multiple linear regression, AdaBoost, and XgBoost for solar and wind power prediction. This section discusses hyperparameters chosen for improving model prediction accuracy and robustness. The performance of each model is evaluated, and finally, the best-performing model is suggested for solar power forecasting.

4.4.1 Multiple Linear Regression

Multiple linear regression is a kind of supervised learning that aims to model the linear relationship between independent and dependent variables. The purpose of simple regression analysis is to evaluate the relative impact of a predictor variable on the outcome. Linear regression is based on explaining the change in one variable through changes in other variables. It allows the modeling of a linear relationship between two or more explanatory variables (model inputs) and a response variable (solar energy generation) through a fitting procedure. The regression equation hypothesis function is a straight-line equation given by (3) [141].

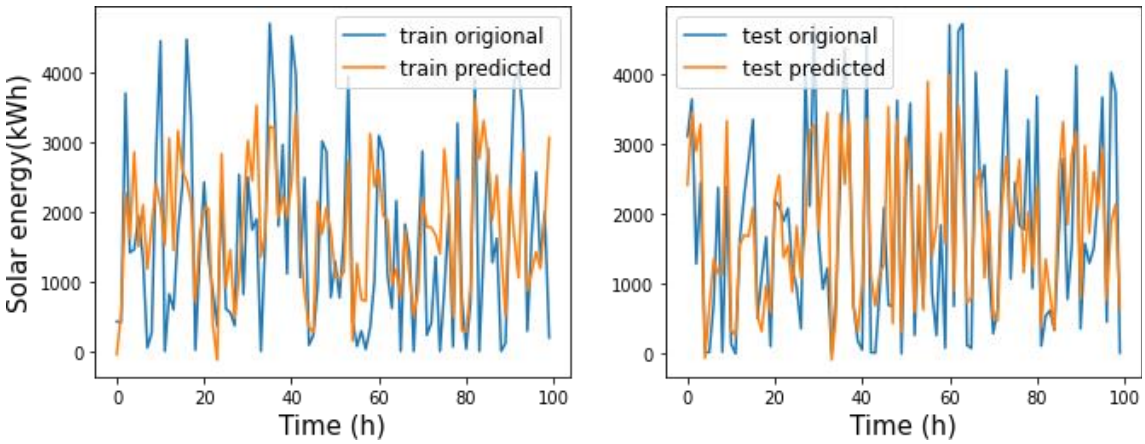

Figure 4-8 Solar Energy Prediction using Multiple Linear Regression
Train R2 score= 0.4576 and Test R2 score= 0.453

$$y = mx + c \tag{3}$$

Where y is the dependent variable or called the output variable; m is the gradient slope; x denotes the independent variable or the input variable, and c represents the intercept of the line.

The data is split into the test and train datasets, and the regression model is fitted to the training set. Using the training dataset, the results of the developed model are predicted. The intercept coefficients are calculated, and finally, the model prediction accuracy is evaluated.

It can be seen from Figure 4-8 that the training accuracy for the training dataset is 46% and for the testing dataset 45%. The RMSE of training set is 1099.493 and that of testing set is 1076.682.

4.4.2 Adaptive Boosting

Adaptive boosting, also known as AdaBoost in short, boosts the model's performance. It is best used with weak learners. This algorithm accepts weights on training data and decision trees with a single split, called decision stumps, used as the base learner [142]. Weak models are added sequentially and trained using the weighted weather training data. This process iteratively happens until the complete training data fits without any error or until a specified maximum number of estimations are attained.

An accuracy of 64% is observed from the training and testing dataset using the ada-boost algorithm. The RMSE for the training dataset was 897.1505, and that of the test data was 869.58.

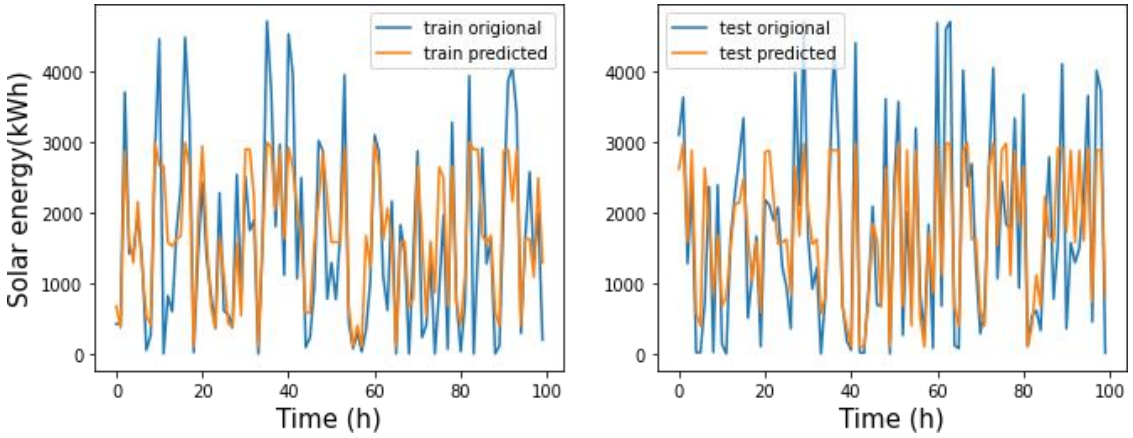

Figure 4-9 Solar Energy Prediction using Ada-Boost
Train R2 score - 0.6388 and Test R2 score - 0.643

4.4.3 Gradient Boosting

Gradient boosting is considered the most powerful technique for building predicting models. Tuning its parameters, i.e., the number of estimators and depth of the graph is required to get the best results. This technique employs the logic in which the subsequent predictors learn from the mistakes of the previous predictors [143][144]. The predictions of each tree are added together sequentially. The measure of the hypothesis function's accuracy is estimated using a cost function presented in (4) [145]. Gradient descent is the general function for minimizing a cost function. Gradient boost considers additive forward model training in a stage-wise manner of form.

$$F_m(x) = F_{m-1}(x) + h_m(x) \quad (4)$$

Where $h_m(x)$ is the basis function referred to as a weak learner. The basic functions h_m are small regression trees of a certain fixed size. The model $F_m(x)$ is a sum of *m* small regression trees. With each boosting *m* iteration, a new regression tree is added sequentially to the model. *x* is the set of input variables for the model [146][147]. This function is otherwise called the "Squared error function". The gradient descent function is minimized using (5), and equations (6) and (7) are repeated until convergence.

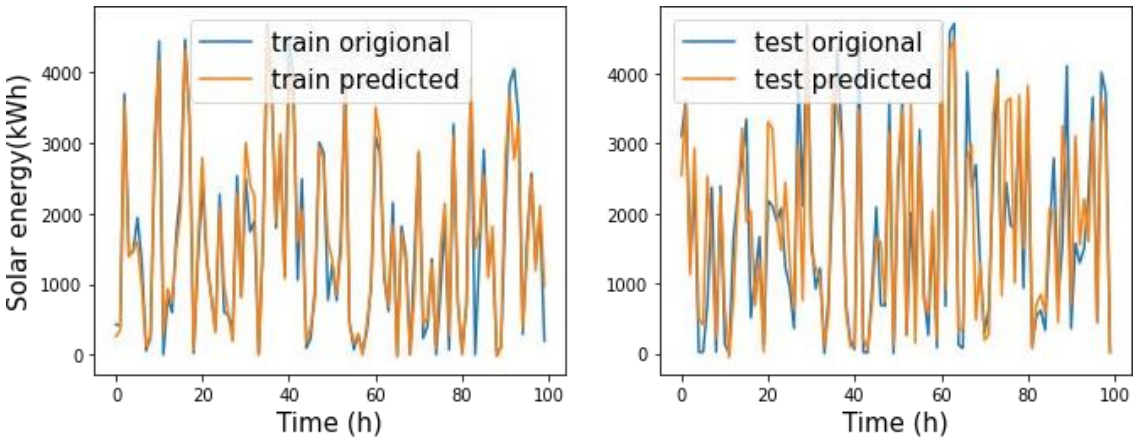

Figure 4-10 Solar Generation Prediction using Gradient boost algorithm: Train R^2 score = 0.954 and Test R^2 score = 0.784

$$\theta_j = \theta_j - \alpha \frac{\partial}{\partial \theta_j} J(\theta_0, \theta_1) \tag{5}$$

$$\theta_0 = \theta_0 - \alpha \frac{1}{m} \sum_{i=1}^{m} (h_\theta(x^{(i)}) - y^{(i)}) \tag{6}$$

$$\theta_1 = \theta_1 - \alpha \frac{1}{m} \sum_{i=1}^{m} (h_\theta(x^{(i)}) - y^{(i)}).x^{(i)} \tag{7}$$

It is observed that the R2 score for train dataset is 0.954 and testing dataset is 0.784. The RMSE of training dataset was found to be 317.45 and that of testing dataset was 676.097. Figure 4-10 presents the prediction results using gradient boost algorithm.

4.4.4 XG Boost Algorithm

eXtreme Gradient Boosting is in short known as XGBoost. It belongs to the family of boosting algorithms which works on the principle of ensemble learning technique. This algorithm combines a set of weak learners and delivers a much-improved prediction accuracy. Training data is used to get the model parameters. Validation data is used to pick the best hyperparameter. Testing data helps in determining the best value for the hyperparameters used in data to estimate how the model performs in the real world.[148].

Figure 4-11 shows the solar energy prediction results for training and tsting dataset using Xg boost algorithm. It is observed that with training dataset xg boost demonstrates an R2 score of 0.98, whereas with testing dataset it is 0.785. The RMSE of training set is 206.775 and that of testing set is 674.74.

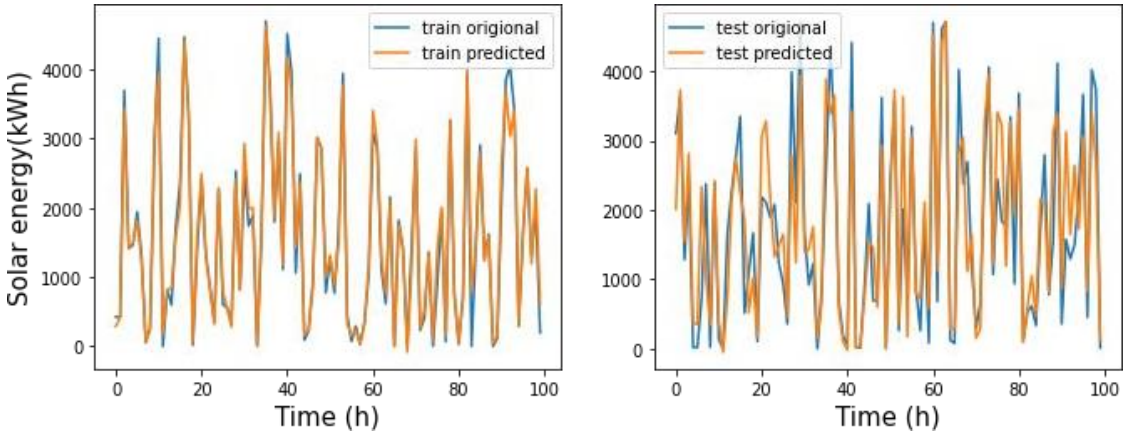

Figure 4-11 Solar Energy Prediction using Xg Boost algorithm
Train R2 score- 0.98, Test R2 score - 0.785

4.5 Comparative Study of Models

This section presents and compares the results of MLR, XgBoost, AdaBoost, and gradient boost for solar energy predictions. Table 4-2 shows the performance (on one-year long dataset) of prediction models in terms of RMSE and R^2 score.

A comparison of prediction efficiency of various machine learning algorithms is provided in Figure 4-12. The test original with marker represents the original solar energy series. From the plot, it is quite clear that gradient boost and XgBoost algorithms can be deployed to provide the best prediction. Linear regression performs the worst due to

Table 4-2 Comparison of Accuracy Estimation Indices of Various Algorithms

Algorithms	Solar Energy	
	RMSE	R^2 score
Multiple linear regression	1076.68	0.453
Ada Boost algorithm	869.58	0.643
Gradient boost algorithm	676.09	0.784
XgBoost algorithm	674.74	0.785

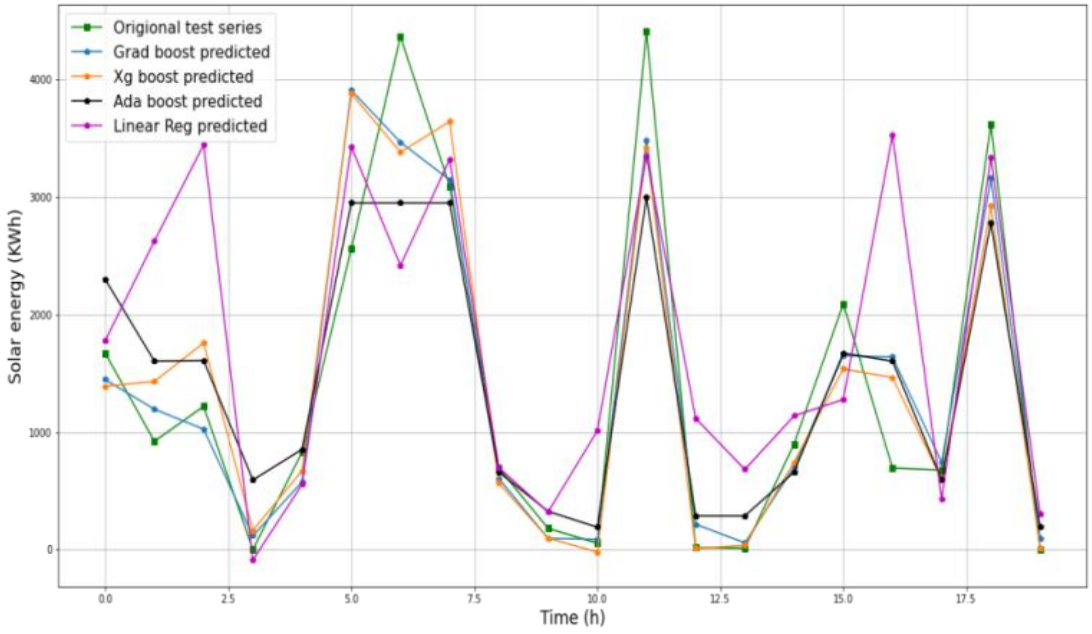

Figure 4-12 Comparion of various Ensemble learning models for solar power prediction

heteroscedasticity present in the data violating the assumption of homoscedasticity. In heteroscedasticity, the size of the error term differs significantly across values of an independent variable which is undesirable.

4.6 Conclusion

A day ahead prediction of renewable power generation is essential for scheduling dispatch and last-minute optimization of supply-demand balance to maintain stability in the microgrid power system. The proposed model ensures to keep the system both flexible and resilient using the most accurate available machine-learning algorithm to forecast renewable energy output and make the best predictions. The research presented in this chapter compares four different machine learning models to estimate solar power generation. In this research, widely known machine learning algorithms were analyzed and tested in different scenarios to investigate their suitability and accuracy of prediction. From the analysis, it can be concluded that for solar energy prediction eXtreme gradient boost algorithm gives the most accurate forecast of 78.5% accuracy. The ensemble machine learning methods presented in this chapter have a great scope of robust representation and interpretability in the future.

Chapter 5

Novel MCDM Algorithm for HRES installation Site-Selection in oil and Gas Fields

5.1 Foreword

In any oil and gas production site, multiple gas flaring locations varying from tens to hundreds in numbers are present. Each gas flaring location has different demography, flare gas availability, electricity requirements, and other resource availability. Therefore, to ensure the productivity and efficiency of the HRES throughout its lifetime, selecting the most appropriate location for HRES installation is essential. Several researchers have applied a variety of multi-criteria decision-making algorithms either to select the HRES mix or to select the site for HRES installation. However, any study on site selection for oil and gas well based HRES is still lacking. One of the critical concerns while dealing with oil and gas well based HRES is the unavailability of precise data. The existing MCDM approaches are insufficient as they either work on entirely quantifiable data or qualitative data. This chapter presents a novel combinational multi-criteria decision-making approach for site selection, which deals with the ambiguous data issue prevalent in oil and gas fields.

The content in this chapter is published in the following research paper:

- Deepika Bishnoi and Harsh Chaturvedi, 'Optimised Site Selection of Hybrid Renewable Installations for Flare Gas Reduction using Multi-Criteria Decision Making', Energy Conversion and Management X, 2022. https://doi.org/10.1016/j.ecmx.2022.100181.

For the analysis in this chapter, nine gas flaring sites falling under the Lakwa, Geleky, and Rudrasagar GGSs of Assam asset, India, are considered (Figure 5-1). Medium to reasonably dense settlements comprising tea gardens, hospitals, schools, colleges, churches, temples, and shops are located around the oil and gas well sites. There are substations as well as rivers Disang and Dikhow near gas flaring sites. There is a possibility of installing hydrokinetic generators in the river tributaries. The Brahmaputra river tributaries, Disang and Dikhow, have annual streamflow of 5.08 m/s and flow close to four gas flaring locations. The gas flaring locations considered for the analysis are mapped in *Figure 5-1*. The flare gas availability (annual average for the year 2020) and the geographical details for the study area are provided in Table 5-1.

5.2 Methodology

The process flow for the site selection for HRES installation to reduce gas flaring and electricity production at oil and gas fields is elaborated in Figure 5-2. The illustration presents a comprehensive structure of weight determination for assessment criteria and further steps involved in merging primitive TOPSIS with three different weight determination methods. The steps involved in site selection using the proposed MCDM process are described in the following paragraphs.

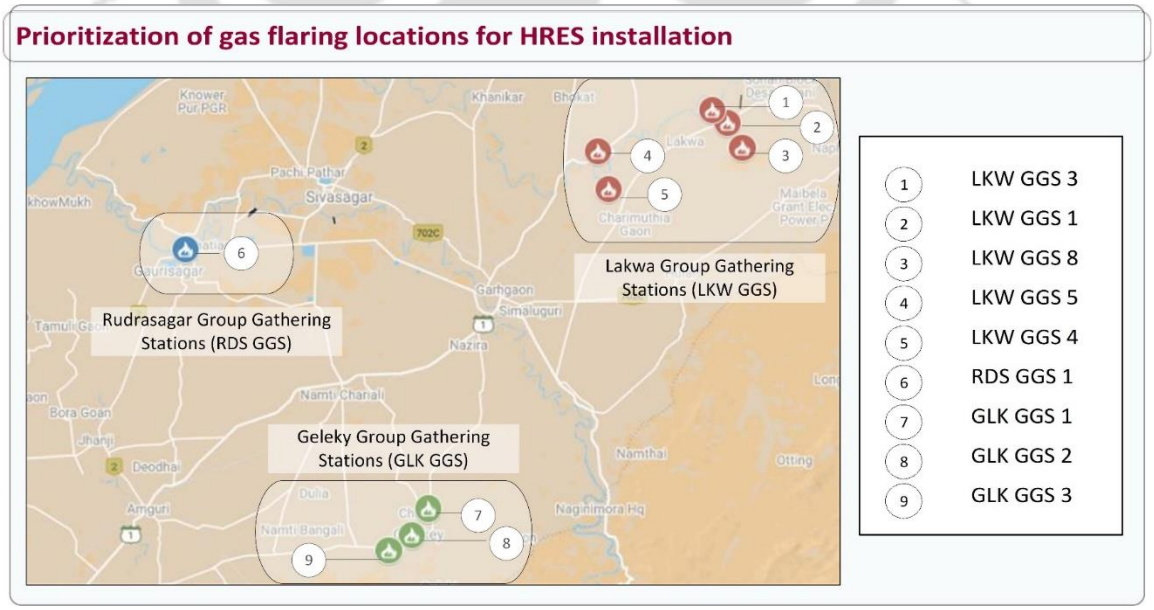

Figure 5-1 The model for selection of gas flare locations for the three HRES installation; In map – Nazira Assam Asset

Table 5-1 Gas flaring details of Assam asset

Area	Installations	Latitude	Longitude	Availability of waste gas flares (MMSCM) per day (annual average of 2018)	Distance from the river (m)	Distance from Grid (km)
Geleki	GLK GGS 1	26.81	94.6975	94	Very high	30.6
	GLK GGS 2	26.795	94.6867	5025	Very high	32.6
	GLK GGS 3	26.7865	94.6727	90	Very high	34.2
Rudras--agar	RDS GGS1 & 4	26.9531	94.546	489	214	38.3
Lakwa	GGS1	27.0228	94.8837	4	1130	4.57
	GGS3	27.0304	94.8735	0	378	6.13
	GGS4	26.9869	94.8094	630	544	12
	GGS5 (Lakhmoni)	27.0079	94.8023	26634	805	12.9
	GGS8	27.0098	94.8924	155	Very high	4.45

5.3 Data Collection

An assessment of the gas flaring location in ONGC Assam asset was conducted after site visits and online meetings (via google meet) with the engineers working with ONGC, APDCL, tea garden workers, and local people in business. The gas flaring sites were identified, and the data of flare gas quantity (in MMSCM – million metric standard cubic meters) at each GGS and GCP was obtained from oil and gas company (ONGC) officers. The latitude-longitude coordinates of the gas flare sites were obtained, which were useful in determining the exact distance of the gas flare locations from the nearby rivers; Disang and Dikhow, the substation (grid connection), and the demand site (settlements/shops/ tea gardens/ schools/ hospitals/ worship places/ industries etc.).

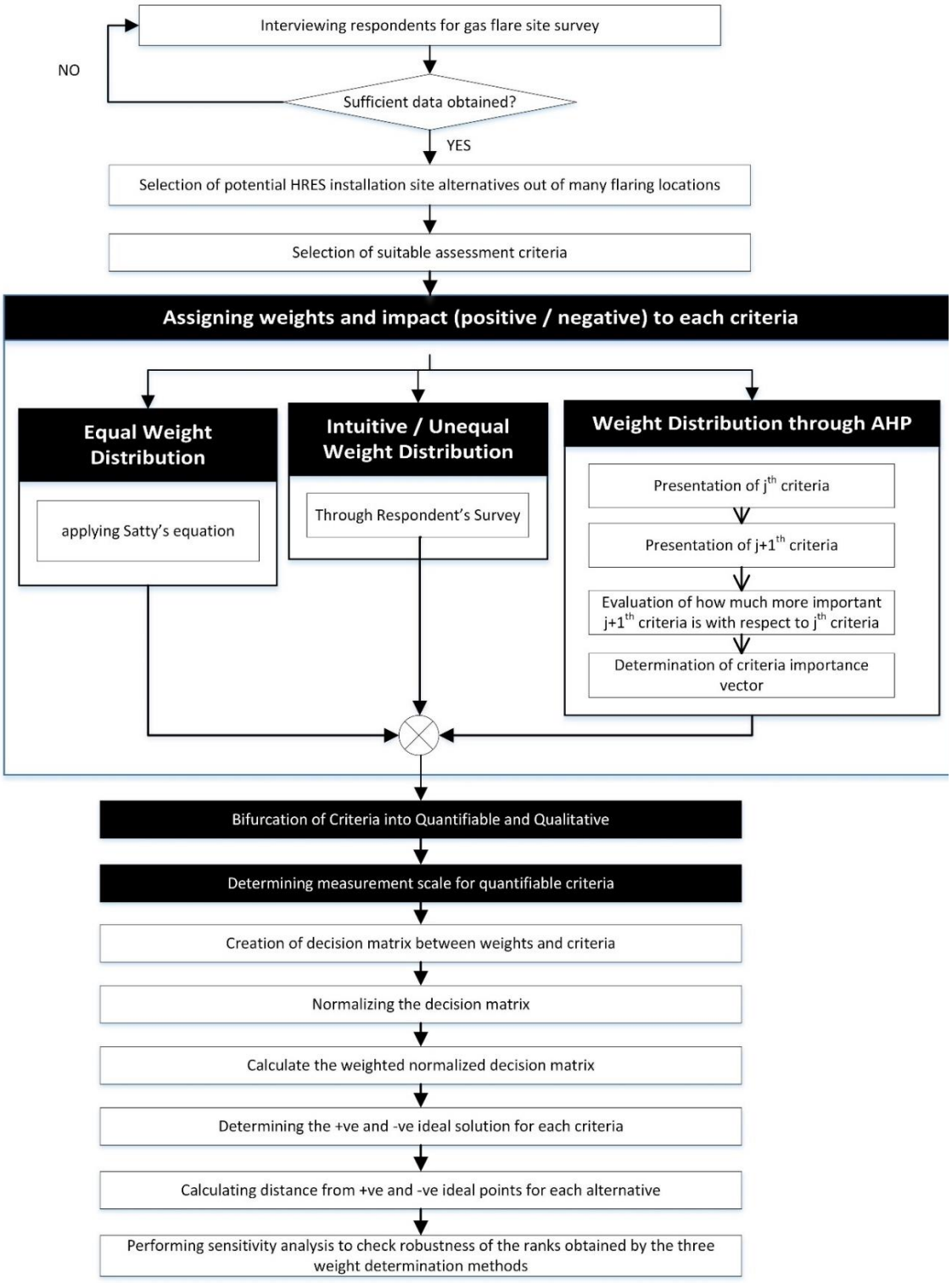

Figure 5-2 Methodology Flowchart

5.4 Alternative Selection

Gas microturbines cannot be installed at every well site to reduce gas flaring as all well-sites are not pure gas wells. Oil and gas flow jointly at most well-sites. To separate the gas, separators are required at every well site, which is techno-economically not possible.

However, microturbines can be installed at GGSs, and GCPs mentioned in Table 5-1, are selected based on the availability of gas separation and processing facility. The listed GGS/GCP will be ranked using the proposed MCDM algorithm for HRES installation.

5.5 Selection of Suitable Assessment Criteria

Nine different criteria were selected, as mentioned in *Table 5-2*. The criteria are a mix of resource availability and technical, environmental, and social indicators. Based on these indicators, a questionnaire was prepared, and weights were assigned based on the answers provided by ONGC engineers in an online meeting. The criteria can be classified into two categories:

- Quantifiable Criteria: This category involves criteria that can be measured on a tangible scale. The amount of flare gas availability, solar radiation, distance from the river, distance from the substation, and the distance from the demand site falls under this category.
- Qualitative Criteria: This category involves indeterminate criteria, which essentially do not have a well-defined unit. The criteria, such as technical maturity, land availability, social acceptability, and the effect of progress on the surrounding region, fall in this category.

5.6 Assigning Weight and Impact to the Assessment Criteria

The weights and impacts (positive or negative) of each criterion were derived using three different sets of processes:

1) Equal Weights for all Criteria

2) Unequal weights are taken as an average of judgment by three decision-makers

3) Weights assigned using AHP (Analytic Hierarchy Process) [149].

In all three cases, Satty's equation (eq. (1)) of the sum of all weights equal to 1 is satisfied [149].

$$w_j = \frac{1}{n} \qquad (1)$$

where, w_j is the weight assigned to j^{th} criteria and n is the total number of criteria.

Table 5-2 Criteria Characteristics

#	Criteria Category	Name of selected criteria	Criteria classification	Type	Equal Weights (w_2)	Intuitive Weights (w_1)	Weights using AHP
1	Resource Availability	Availability of Gas flares (C1)	Quantifiable	+	0.111	0.212	0.201
2		Availability of Solar Radiation (C2)	Quantifiable	+	0.111	0.211	0.153
3		Distance from the river (C3)	Quantifiable	-	0.111	0.211	0.130
4	Technical	Distance from grid connection (C4)	Quantifiable	-	0.111	0.211	0.114
5		Distance from demand site (C5)	Quantifiable	-	0.111	0.111	0.124
6		Technical maturity (Presence of gas separation facility) (C6)	Quantifiable	+	0.111	0.011	0.070
7	Environmental	Land Availability (C7)	Quantifiable	+	0.111	0.011	0.081
8	Social	Effect of progress on surrounding region (C8)	Qualitative	+	0.111	0.011	0.069
9		Social Acceptability (C9)	Qualitative	+	0.111	0.011	0.059

In the first case, all criteria are rated equally. In the second case, a priority list of the criteria is generated based on the assessment by the ONGC (Oil and Natural Gas Corporation) personnel involved in decision-making. Since the availability of gas flares, distance from the river, and grid connection have more critical roles in site selection decision-making, they are given higher priority than other criteria. The weights are assigned according to the formula given in eq. (1) and then modified to justify the criteria's hierarchical position, keeping the sum of all weights limited to 1. In the third case, a pairwise comparison of all criteria is made for assigning weights using the AHP technique. A total of 36 comparisons were made between - availability of gas flares (C1), availability of solar radiation (C2), distance from the river (C3), distance from the grid connection (C4), distance from demand site (C5), technical maturity (C6), land availability (C7), the effect of progress on surrounding region (C8), and social acceptability (C9). A scale of 1 to 3 has been used to make the pairwise comparisons,

where 1 indicates equal importance, 2 indicates moderate importance, and 3 indicates the strong importance of one criterion over another. The resulting weights (shown in *Table 5-2*) are based on the principal eigenvector of the decision matrix shown in Table 5-3. As shown in Table 5-3, C2, C3, and C4 are three times more important than C1. Whereas C5, C6, C7 are as important as C1. The rest of the table can be interpreted in the same manner. These comparisons were made with the help of engineers working at the gas flaring locations during an online meeting.

5.7 Determining Measurement Scale for Quantified Criteria

Since it is challenging to obtain exact data for all the GGSs and GCPs due to the uncertainties associated with new well developments and the amount of waste flare gas availability at each well site, the quantifiable criteria like – availability of gas flares, distance from the river, and distance from the grid connection are converted to a scale of 0 to 5 according to the scale presented in Table 5-4. The same scale of 0 to 5 is used to rate all alternatives against the qualitative criteria. This step distinguishes the conventional TOPSIS algorithm from the proposed modified TOPSIS algorithm and is performed based on the inputs from stakeholders involved in the project's decision-making.

Table 5-3 Eigen-vector matrix created for pairwise comparison of criteria

	C1	C2	C3	C4	C5	C6	C7	C8	C9
C1	1	3.00	3.00	3.00	1.00	1.00	1.00	2.00	3.00
C2	0.33	1	2.00	2.00	2.00	3.00	1.00	2.00	2.00
C3	0.33	0.50	1	1.00	1.00	2.00	3.00	3.00	3.00
C4	0.33	0.50	1.00	1	2.00	2.00	2.00	1.00	2.00
C5	1.00	0.50	1.00	0.50	1	3.00	2.00	2.00	2.00
C6	1.00	0.33	0.50	0.50	0.33	1	1.00	1.00	1.00
C7	1.00	1.00	0.33	0.50	0.50	1.00	1	1.00	1.00
C8	0.50	0.50	0.33	1.00	0.50	1.00	1.00	1	1.00
C9	0.33	0.50	0.33	0.50	0.50	1.00	1.00	1.00	1

Table 5-4 Assortment of Quantifiable Criteria

	Unavailability	**Very Low**	**Low**	**Medium**	**High**	**Very High**
	0	**1**	**2**	**3**	**4**	**5**
Gas Flaring (in MMSCMD)	0	<100	100-500	500-5000	5000-10,000	>10,000
Distance from River (in meters)	NA	<400	400-700	700-1000	1000-2000	>2000
Distance from Grid (in meters)	NA	<10 km	10-20 km	20-30 km	>30 km	NA

5.8 The Mathematical Formulation

All the m alternatives; $A_1, \ldots, A_m$ are examined against n criteria; $x_1, \ldots x_n$, expressed with positive numbers x_{ij}. The criteria $x_1, \ldots x_k$ have a positive impact and criteria $x_{k+1}, \ldots x_n$ have negative impacts associated with them. Weights w_j of the criteria x_j are decided such that $\sum_{j=1}^{n} w_j = 1$ [150]. For better visibility, all the elements of the decision-making problem are arranged in Table 5-5.

Table 5-5 Initial table for TOPSIS

Criteria	x_1	x_2	…	x_n
Weights	w_1	w_2	…	w_n
A_1	x_{11}	x_{12}	…	x_{1n}
A_2	x_{21}	x_{22}	…	x_{2n}
A_m	x_{m1}	x_{m2}	…	x_{mn}

Taking weights associated with each criterion with different measuring units into account, the numbers x_{ij} of the criteria x_j are replaced by normalized vectors.

The following formula is used for the normalization:

$$r_{ij}(x) = \frac{x_{ij}}{\sqrt{\sum_{i=1}^{m} x_{ij}^2}} \quad i = 1, \dots, m \;\; ; j = 1, \dots \;\; , n \tag{2}$$

Where, r_{ij} is the normalized number belonging to the open interval (0, 1).

After this, the normalized matrix is multiplied by the criteria-weight to obtain the weighted normalized numbers given by v_{ij} (eq. 3):

$$v_{ij}(x) = w_j r_{ij}(x) \quad i = 1, \dots, m \;\; ; j = 1, \dots \;\; , n \tag{3}$$

The weighted normalized number a_{ij} is given by:

$$a_{ij} = w_j r_{ij} = w_j \frac{x_{ij}}{\sqrt{\sum_{i=1}^{m} x_{ij}^2}} \tag{4}$$

a_{ij} belonging to the open interval (0,1).

The weighted normalized matrix obtained for the three methods is presented in the appendix in Table 5-6 and analyzed in the results and discussion section.

The TOPSIS method aims to calculate the distance of each alternative from the positive and negative ideals. The following formula is used to determine the positive and negative ideal solutions: [151]

$$A^+ = (v_1^+, v_2^+, \dots, v_n^+) \tag{5}$$

$$A^- = (v_1^-, v_2^-, \dots, v_n^{-+}) \tag{6}$$

So that,

$$v_j^+ = \left\{\left(\max v_{ij}(x) \middle| \, j \epsilon j_1\right), \left(\min v_{ij}(x) \middle| \, j \epsilon j_2\right)\right\} \; i = 1, \dots, m \tag{7}$$

$$v_j^- = \left\{\left(\min v_{ij}(x) \middle| \, j \epsilon j_1\right), \left(\max v_{ij}(x) \middle| \, j \epsilon j_2\right)\right\} \; i = 1, \dots, m \tag{8}$$

where j_1 and j_2 denote the negative and positive criteria, respectively. TOPSIS method lists each alternative based on the relative degree of closeness to the positive and negative

ideals. This step calculates the distances between each alternative and the positive-negative ideal solutions using the following formulas: [151]

$$d_i^+ = \sqrt{\sum_{j=1}^{n}[v_{ij}(x) - v_j^+(x)]^2} \quad , \quad i = 1, \dots, m \tag{9}$$

$$d_i^- = \sqrt{\sum_{j=1}^{n}[v_{ij}(x) - v_j^-(x)]^2} \quad , \quad i = 1, \dots, m \tag{10}$$

Finally, the approximate ratio of each option to the correct solution is obtained by eq. (11). Suppose the degree of closeness for a particular alternative is near to 1. In that case, it signifies a shorter distance from the positive ideal solution and a longer distance from the negative ideal solution for that particular alternative [151].

$$C_i = \frac{d_i^-}{(d_i^+ + d_i^-)} \quad , \quad i = 1, \dots, m \tag{11}$$

5.9 Result and Discussions

The proposed modified TOPSIS algorithm (with three different weight determination strategies) was applied to the three HRES configurations as mentioned in [152]:

- HRES Combination# 1: River turbine, Solar Photovoltaics, Gas microturbines, and Grid.
- HRES Combination# 2: Solar Photovoltaics, Gas Microturbines, and Grid
- HRES Combination# 3: Gas Microturbines and Grid

The first combination requires a location close to the river due to the presence of a river turbine (refer to the map in Figure 5-1, Rudrasagar and Lakwa GGS are close to rivers Disang and Dikhow). In contrast, the 2nd and 3rd combinations can be installed on locations far from the rivers as well. Thus, the study is divided into three parts:

A. Considering all sites irrespective of their distance from the rivers.
B. Considering sites in proximity of the rivers for the installation of HRES having a river turbine (i.e. Combination# 1)
C. Considering sites away from the river only.

5.10 Validation

For testing the deviation in the ranking of HRES installation location alternatives, three different methods have been used to determine the weights of the criteria. In the first case,

an equal weight of 0.111 was selected for all criteria. In second, unequal weights reflective of the relative importance of the criteria, and in the third case, weights determined through AHP were considered. (Refer to Table 5-2 for the weights assigned to the nine criteria using three different schemes). A sensitivity analysis is performed to understand the effect of changes in weights of the criteria on the research outcome. The aim is to establish the robustness in the decision to finalise the HRES installation location. Table 5-6 provides a normalised decision matrix with weights used for sensitivity analysis in the three methods.

A. In the first case, when all sites, irrespective of their distances from the rivers, were considered, it was observed that Lakwa GGS 5 is the most preferred location irrespective of the scheme of assignment of weights. However, the ranks of preferred locations vary from each other rank two onwards based on different schemes. A comparison of the priority of different locations for the three schemes is provided in Figure 5-3. The ranks obtained using AHP weighted TOPSIS and intuitively weighted TOPSIS are very much similar to each other. This proves the accuracy of the presented modified TOPSIS algorithm in selecting Lakwa GGS 5 as the best possible location for installing a gas microturbine-based hybrid energy system. The closeness to the ideal solution index (Ci) for Lakwa GGS 5 exceeds the average of all other locations by 96%. This could be because of an abundance of waste flare gas availability at that location. Other assessment criteria do not seem to affect the result as much as the availability of gas flares to select suitable gas flare locations for the installation of HRES proposed for oil and gas fields.

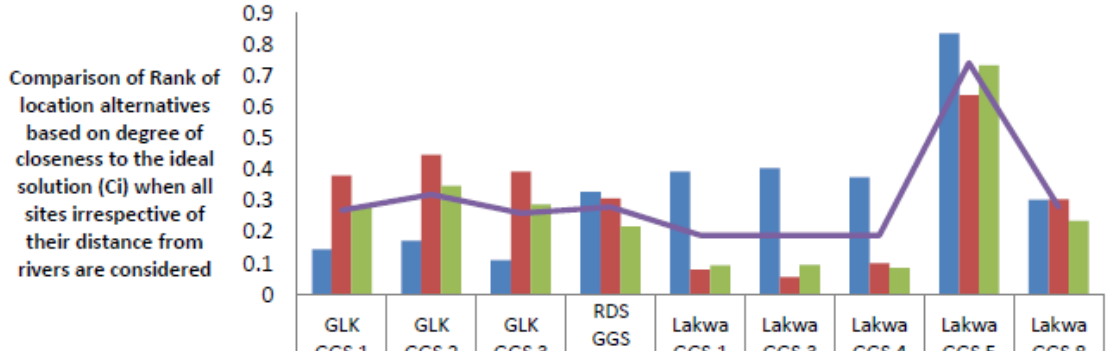

	GLK GGS 1	GLK GGS 2	GLK GGS 3	RDS GGS 1&4	Lakwa GGS 1	Lakwa GGS 3	Lakwa GGS 4	Lakwa GGS 5	Lakwa GGS 8
Ci (equal weights)	0.144	0.173	0.111	0.328	0.393	0.404	0.376	0.835	0.303
Ci (unequal weights)	0.38	0.447	0.393	0.307	0.079	0.057	0.1	0.638	0.305
Ci (AHP weights)	0.28	0.348	0.289	0.218	0.094	0.095	0.085	0.733	0.236
Average	0.27	0.32	0.26	0.28	0.19	0.19	0.19	0.74	0.28

Rank (equal weights)	8	7	9	5	3	2	4	1	6
Rank (unequal weights)	4	2	3	5	8	9	7	1	6
Rank (AHP)	4	2	3	6	8	7	9	1	5

Figure 5-3 Ranking of locations based on the novel multi-criteria decision-making approach when only locations in the proximity of the river are considered for the analysis

Table 5-6 Weighted normalised Matrix for sensitivity analysis of the effect on change in weights of decision criteria on the HRES site selection

Location	Availability of gas flares			Availability of solar radiation			Distance from the river			Distance from grid connection			Distance from demand site			Technical Maturity			Land Availability			Social Acceptability			Effect of Progress on Surrounding Region		
	1	2	3	1	2	3	1	2	3	1	2	3	1	2	3	1	2	3	1	2	3	1	2	3	1	2	3
GLK GGS 1	.001		.001	.073	.039	.053	.105	.055	.064	.091	.048	.049	.037	.037	.041	.004	.041	.026	.004	.036	.027	.004	.04	.025	.003	.034	.018
GLK GGS 2	.039	.021	.037	.075	.04	.055	.105	.055	.064	.097	.051	.052	.037	.037	.041	.003	.027	.017	.003	.032	.023	.004	.04	.025	.003	.034	.018
GLK GGS 3	.01	0	.001	.065	.034	.047	.105	.055	.064	.102	.054	.055	.041	.041	.046	.004	.041	.026	.003	.032	.023	.004	.04	.025	.003	.034	.018
RDS GGS 1&4	.004	.002	.004	.069	.036	.05	.004	.002	.002	.114	.06	.062	.033	.033	.037	.005	.048	.03	.004	.036	.027	.004	.04	.025	.004	.04	.021
Lakwa GGS 1	0	0		.071	.038	.052	.02	.01	.012	.014	.007	.007	.041	.041	.046	.004	.041	.026	.004	.041	.03	.003	.035	.022	.003	.034	.018
Lakwa GGS 3				.071	.038	.052	.007	.003	.004	.018	.01	.01	.041	.041	.046	.003	.027	.017	.005	.05	.037	.003	.035	.022	.004	.04	.021
Lakwa GGS 4	.005	.003	.005	.073	.039	.053	.009	.005	.006	.036	.019	.019	.037	.037	.041	.003	.034	.022	.004	.036	.027	.003	.035	.022	.003	.034	.018
Lakwa GGS 5	.208	.109	.197	.065	.034	.047	.014	.007	.009	.038	.02	.021	.029	.029	.032	.003	.034	.022	.004	.036	.027	.003	.035	.022	.004	.043	.023
Lakwa GGS 8	.001	.001	.001	.067	.035	.049	.105	.055	.064	.013	.007	.007	.037	.037	.041	.003	.034	.022	.003	.027	.02	.003	.035	.022	.004	.04	.021

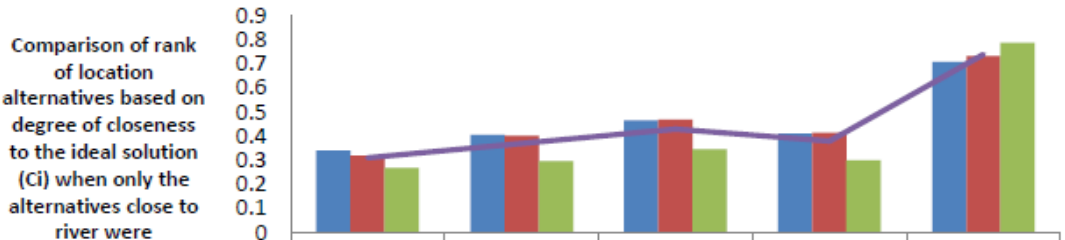

	RDS GGS 1&4	Lakwa GGS 1	Lakwa GGS 3	Lakwa GGS 4	Lakwa GGS 5
Ci (equal weights)	0.34	0.405	0.465	0.41	0.71
Ci (unequal weights)	0.32	0.403	0.469	0.415	0.734
Ci (AHP weights)	0.269	0.296	0.346	0.301	0.789
Average	0.31	0.37	0.43	0.38	0.74

Rank (equal weight)	5	4	2	3	1
Rank (unequal weight)	5	4	2	3	1
Rank (AHP weight)	5	4	2	3	1

Figure 5-4 Ranking of locations based on the novel multi-criteria decision-making approach when all sites, irrespective of their distance from rivers, are considered for the analysis.

B. In the second case, the three variations of TOPSIS were applied on the locations close to the river only (refer Figure 5-1); i.e. RDS GGS1&4, Lakwa GGS1, Lakwa GGS3, Lakwa GGS4, and Lakwa GGS5. In this case, Lakwa GGS 5 was chosen as the bestpossible location for installing a hybrid renewable energy system involving a river turbine. There were slight variations in the degree of closeness to the ideal solution indexing (Ci) owing to the three different criteria weighing schemes considered. However, the ranks obtained by the three different weighing schemes were precisely the same. This proves the accuracy of the proposed multi-criteria decision-making algorithm in selecting the right location for the installation of HRES involving a river turbine. In contrast to the first case, the difference in Ci values of Lakwa GGS 5 and the remaining locations was a marginal value of 1.32% only. This shows a tough competition between locations close to the river for the installation of HRES comprising a river turbine.

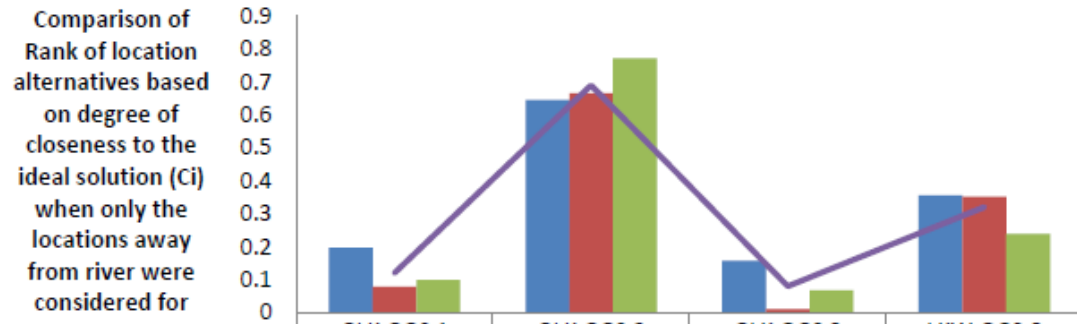

	GLK GGS 1	GLK GGS 2	GLK GGS 3	LKW GGS 8
Ci (equal weights)	0.196	0.645	0.158	0.356
Ci (unequal weights)	0.078	0.665	0.01	0.351
Ci (AHP weights)	0.099	0.771	0.068	0.238
Average	0.12	0.69	0.08	0.32
Rank (equal weight)	3	1	4	2
Rank (unequal weight)	3	1	4	2
Rank (AHP weight)	3	1	4	2

Figure 5-5 Ranking locations based on the novel multi-criteria decision-making approach when only locations far from the river are considered for setting up a hybrid energy system that does not involve a river turbine

C. In the third case, the three variations of TOPSIS were applied only to the locations situated far away from rivers, i.e., Geleky GGS 1,2,3 and Lakwa GGS 8. This was done to select the optimum location for the installation of a hybrid energy system comprising a gas microturbine, solar photovoltaics, and a Grid. Just like in the second case, in the current case as well, slightly varying C_i index, but the same rank values were obtained using the three different weight determination methods. As a result of the sensitivity analysis, Geleky GGS 2 emerged as the most suitable site for installing the mentioned hybrid renewable energy system using the proposed algorithm. The obtained location result also holds suitable for any combination of the hybrid energy system that does not involve a river turbine but involves a gas microturbine that utilizes energy from waste natural gas to generate power. The average C_i value for Geleky GGS 2 supersedes the remaining three locations by 198.07%. It can be concluded from the results that after Lakwa GGS5, Geleky GGS 2 is the suitable location for installation of any combination of HRES which does not involve a river turbine.

The results depicted in *Figure 5-3*, *Figure 5-4*, and *Figure 5-5* show the comparative C_i values (degree of closeness to the ideal solution) after applying the modified TOPSIS algorithm for all the different site combinations (A, B, and C). The consensus of results by three weight determination algorithms proves the effectiveness of the modified TOPSIS algorithm for site selection for HRES installation at oil and gas fields.

5.11 Analysis of Weighted Normalized Decision Matrix

In figures 5-7 to 5-14, W1 indicates an equal distribution of weights, W2 indicates intuitive assignment, and W3 implies weights assigned through AHP. It can be seen from Figure 5-6 that the flare gas availability for Lakwa GGS 5 is abundant (26634 MMSCMD as mentioned in Table 5-1) that the weighted normalized score appears to be zero for the rest of the locations for this particular criterion. For most of the criteria (C2, C3, C5, C6, C7, C8), the weighted normalized score value calculated using AHP is intermediate between equal and intuitive distribution (Fig 5-8, 5-9, 5-11, 5-12, 5-13, 5-14). The present findings corroborate those reported by [42], proving the effectiveness of AHP in weight calculation for optimum site selection. It can be interpreted from *Figure 5-8* that four sites, namely – Lakwa GGS 8, GLK GGS1, GLK GGS 2, GLK GGS 3, are situated away from the river, whereas rest of the locations lie close to rivers. Intuitively (W2), as well as using AHP (W3), less importance is being given to the criteria – 'C3 – Distance from river' and 'C4 – Distance from grid connection'.

In contrast to the resource availability, geographical and technical criteria (C1 to C4), the Social and environmental criteria, such as – C6, C7, and C8, are given more importance intuitively (W2). However, in these four criteria (C5 – 'technical maturity, C6 – 'Land availability', C7 – 'Social acceptability', and C8 – 'effect of progress on surrounding region') as well, AHP is the intermediate value just like that of the criteria pertaining to resource availability (C1) and geographical factors (C2, C3, C4). The fact that the order

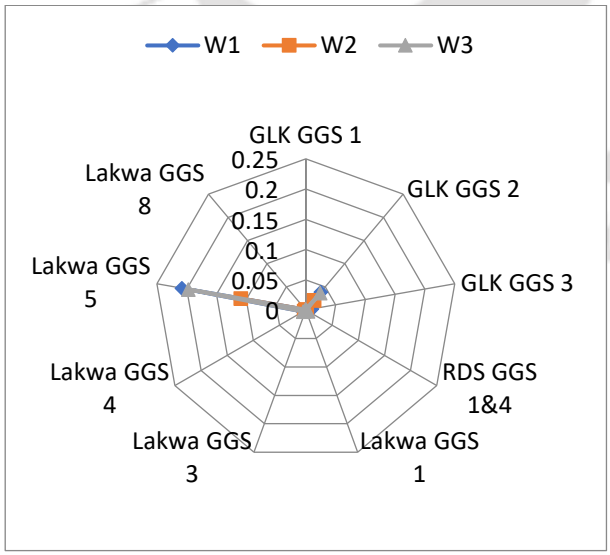

Figure 5-6 Comparison of the three weighted normalised scores for 'C1 - Availability of gas flare'.

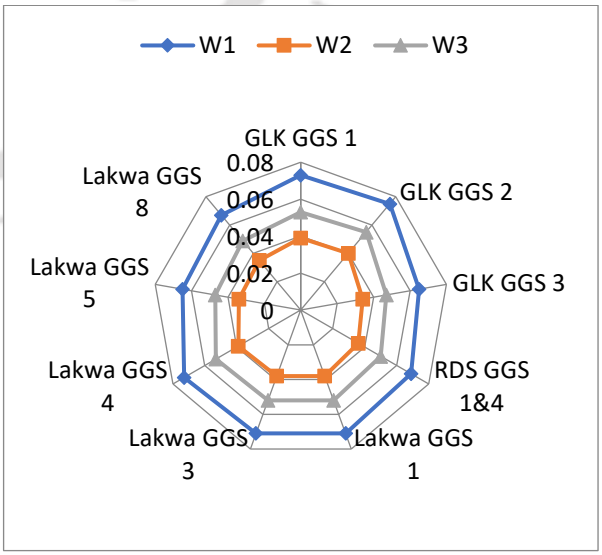

Figure 5-7 Comparison of the three weighted normalized scores for 'C2 - Availability of solar radiation.

of preference of alternatives is the same using all three methods and AHP gives an intermediate value for all criteria indicates that weight determination through AHP followed by alternative selection through TOPSIS is an effective tool for consistent decision making. The present result findings uphold the method suggested by Mohamed et al. [153].

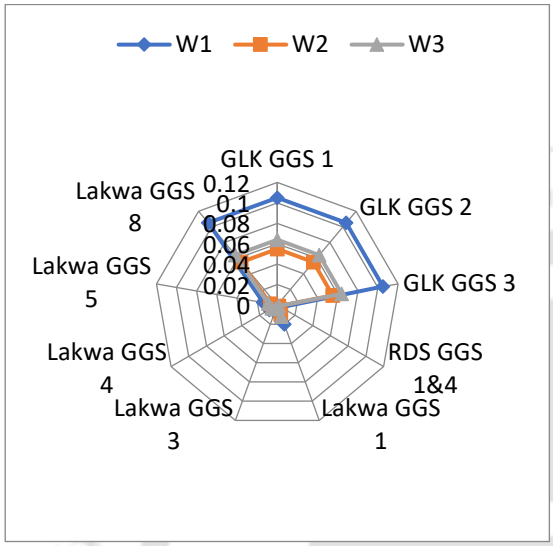

Figure 5-8 Comparison of the three weighted normalised scores for 'C3 - Distance from river'

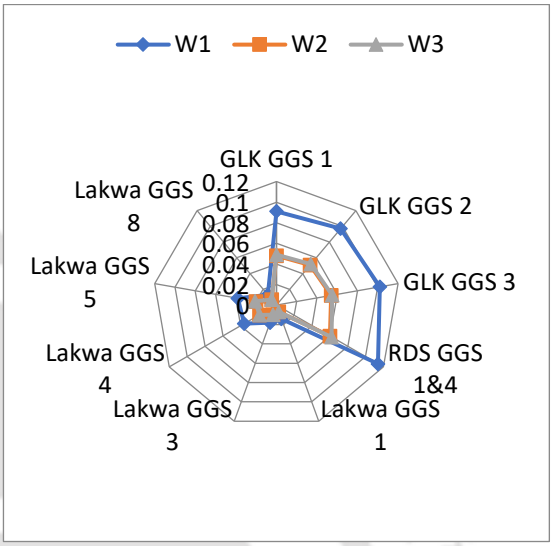

Figure 5-9 Comparison of the three weighted normalised scores for 'C4 - Distance from grid connection'

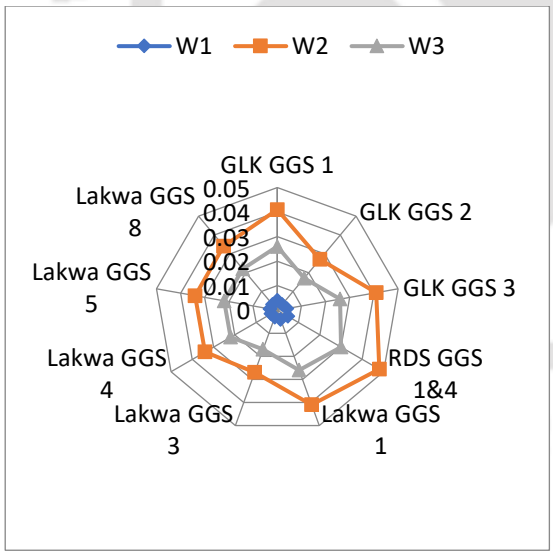

Figure 5-10 Comparison of the three weighted normalised scores for 'C5 - Technical Maturity'.

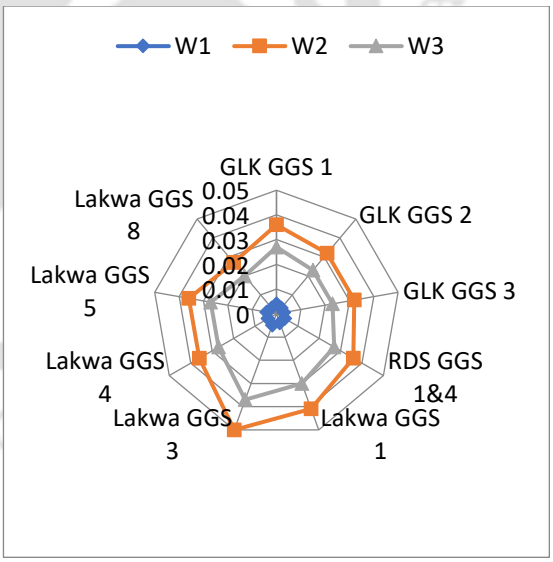

Figure 5-11 Comparison of the three weighted normalised scores for 'C6 - Land Availability'.

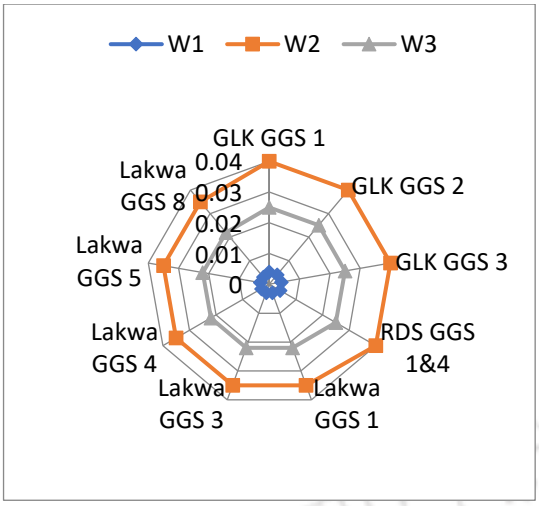

Figure 5-12 Comparison of the three weighted normalised scores for 'C7 - Social Acceptability'.

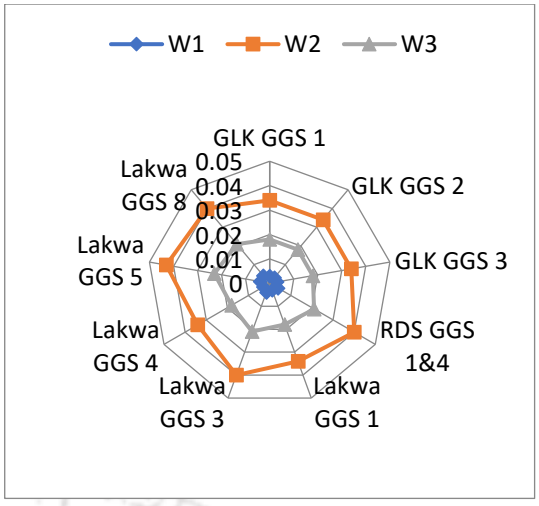

Figure 5-13 Comparison of the three weighted normalised scores for 'C8 - Effect of progress on surrounding region'.

The limitation of this study is that the existing algorithms have been modified to suit the requirements of oil and gas fields. However, advanced algorithms may be developed and explored to obtain the exact results.

Determination of the appropriate location is a crucial step in installing HRES as it ensures the complete utilization of available geographical and technical resources. If the location is not found correctly, it will result in the inefficient performance of the HRES and insufficient production of electricity. Thus, the present study aids in improving the electricity production, power management, and overall performance of HRES and hence the operation of the oil and gas field industry. The study proposes the utilization of wasted gas flares for electricity generation, which is a step towards the United Nations' sustainable development goal – 'Affordable, reliable, sustainable and modern energy for all' [154].

5.12 Conclusion

In order to cut down the drawbacks associated with gas flaring and enhance electricity production at oil and gas field areas, this investigation uses combinational multi-criteria decision-making to rank gas flaring locations for the installation of a Hybrid Renewable Energy System (HRES) that utilize locally available renewable energy sources like solar energy, and hydro-kinetic energy along with waste gas flares to generate power. The site selection criteria included ecological, technical, and sociological parameters to select the best alternative. The multivariable decision-making algorithm was developed using three different methods to determine weights of the criteria, namely – equal, intuitive, and

Analytical Hierarchy Process (AHP). The contributory aspect of this study is - 1) a modification in the existing TOPSIS algorithm to suit the requirements of oil and gas field locations. 2) Validation of the developed algorithm using three different weight determination methods.

The results collected from the current study were compared to past similar investigations proving the efficiency of combining AHP and TOPSIS in identifying locations for HRES installation at oil and gas fields. Lakwa GGS 5 is the most appropriate choice for installing all combinations of hybrid energy systems that use waste flare gas to generate power out of the analyzed locations. The 'degree of closeness to the ideal solution' (C_i) values exceed by over 50% compared to other location alternatives in both the cases; 1) when all location alternatives were considered, 2) when only locations close to the river were considered. However, Geleky GGS 2 is a superior choice amongst sites having a distance of more than two kilometers from the river, with C_i values 40% greater than the rest of the locations for installing a hybrid energy system that uses gas flares with any combination of renewables except river turbines. The results also conclude that the integrated TOPSIS-AHP approach is a more powerful tool for site-suitability purposes than TOPSIS with equal or random weights.

The presented integrated approach can offer helpful information to the authorities at the management level for planning energy management and flare gas waste reduction in oil and gas fields in Assam – India, as well as across the globe. The analysis may need to exclude or include assessment criteria as per the requirements of other utilities or countries.

Chapter 6

Hybrid Energy System Designing and Scheduling Algorithm for Oil and Gas Fields

6.1 Foreword

For effective minimization of operational costs and optimal utilization of all DERs (whether renewable or non-renewable), mathematical modeling of all the DERs plays a crucial role. This chapter presents a framework to design hybrid energy systems (HES) which utilize the gas flare wastes and locally available renewable energy sources to generate electricity. A novel dispatch strategy to suit the requirements of the oil and gas fields has been used for real-time simulations and optimization of the HES. As a test case, six different hybrid energy configurations, modeled for two gas flaring sites: Lakwa and Geleky in Assam – India, were analyzed and compared based on economic and environmental factors. The best suitable configuration comprised 2000 kW solar photovoltaic (SPV) panel sets, one 200 kW gas microturbine, two 30 kW gas microturbines, and grid connection. The proposed system economically outperformed the existing power system in the area by 35.52% in terms of the net present cost. Moreover, it could save 850 tons of carbon-di-oxide emissions annually and has a renewable fraction of 93.7% in the total energy generation. Owing to these merits, the presented technique would be a promising option for generating electricity from flare gas wastes and mitigating pollution.

The content in this chapter has been published in the following paper:

- Deepika Bishnoi and Harsh Chaturvedi, 'Optimal Design of Microgrid Power Management System for Economic and Environmental Sustainability of Onshore Oil and Gas Fields', Energies 2022. https://doi.org/10.3390/en15062063.

6.2 HRES Configuration

In this chapter HRES systems are designed for two gas flaring locations in oil and gas fields of Nazira Assam Asset, namely – Lakwa and Geleky. These locations have been selected as an outcome of the research presented in chapter 5. Apart from natural gas, these locations are rich in solar energy and hydel power. Therefore, hybrid energy systems involving solar photovoltaic panels, gas microturbines, hydrokinetic river turbines, and the requird ancilliary services are designed in the current chapter. Figure 6-1 summarizes the framework for optimal design, planning, and techno-commercial analysis of the hybrid renewable energy systems.

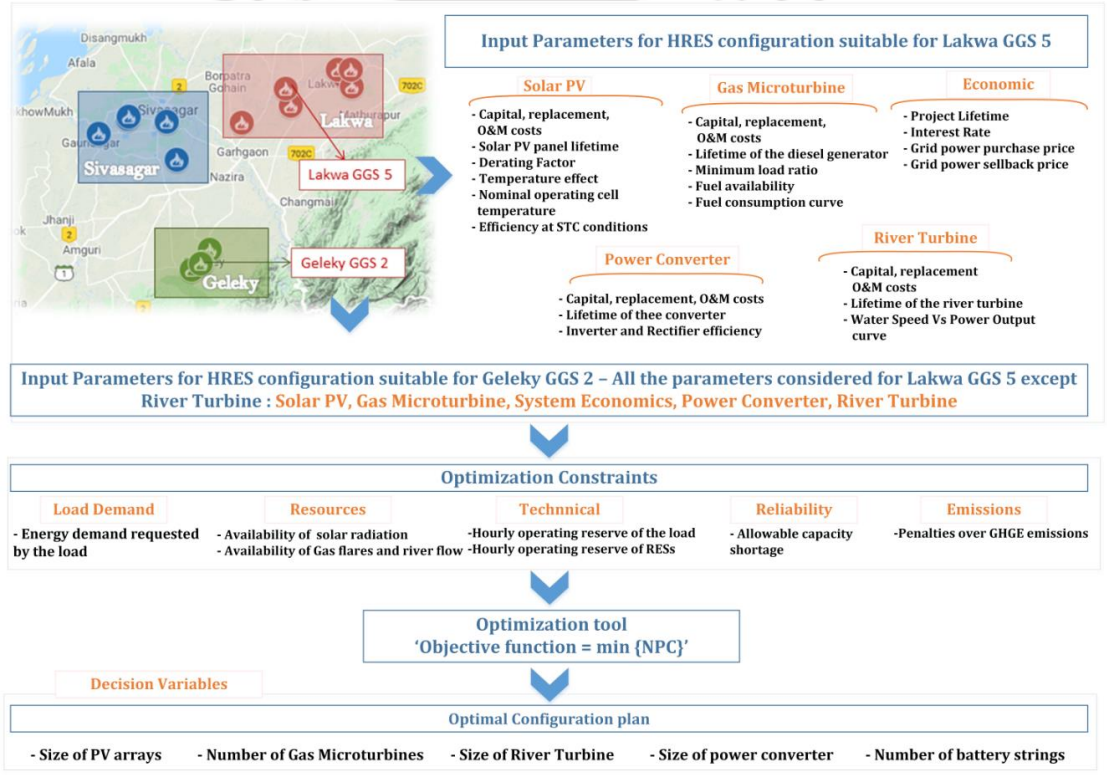

Figure 6-1 Framework for optimal design, planning, and techno-commercial analysis of Hybrid Renewable Energy Systems

6.8.1 Solar Photovoltaic

For selecting the right SPV panel, cost efficiency, tolerance to variation in power, conversion efficiency, and temperature coefficient are crucial factors. To estimate the performance of SPV generators, IEC standard 61,724 and international energy agency PVPS task II guidelines are practiced [86]. Accordingly, CanadianSolar MaxPower CS6X-325P PV modules were chosen for the current study. As quoted by the seller and verified from the literature [155], the capital cost, replacement cost, and operation &

maintenance cost of the SPV panels were estimated to be 714 $/kW, 700 $/kW, and 14 $/kW, respectively. The capital cost is more than the replacement cost as it includes the cost of cables, inverters, installation, and substation charges. The selected SPV modules had a derating factor of 88%, an efficiency of 16.94%, and a nominal operating cell temperature (NOCT) of 45°C[155]. The derating factor compensates for losses in the solar PV caused by dust, elevation and drop in temperature, cable losses, etc., and makes the performance of rated SPV close to real-life operation[156]. The efficiency of a PV panel decreases linearly with an increase in temperature[157]. The manufacturer's rated performance was tested at 25°C with NOCT of 45°C, and the resultant 20°C increase causes a reduction in rated power output[158]. Therefore, ambient temperature effects were considered while calculating the power output of the SPV generation system using Eqn(1) [159]:

$$P_{PV} = Y_{PV} \times d \times \frac{I_T}{I_{T,STC}} \times [1 + \alpha_p(T_c - T_{c,STC})] \quad (1)$$

where Y_{PV} is the rated capacity of the SPV module (kW), d is the derating factor, I_T is the incident solar radiations at actual conditions, $I_{T,STC}$ is the solar insolation on the SPV panel at standard test conditions (STC) (1 kW/m^2). $\alpha_p$is the temperature coefficient of power (%/°C), which accounts for the ambient temperature effects, and T_c and $T_{c,STC}$ are the SPV cell temperatures (°C) at real-time and STC, respectively. The real-time SPV cell temperature can be calculated using the following equation [156]:

$$T_C = T_a + (T_{C,NOCT} - T_{a,NOCT}) \times \left(\frac{I_T}{I_{T,STC}}\right) \times \left[1 - \left(\frac{\eta_{mp}}{\tau\alpha}\right)\right] \quad (2)$$

$$\eta_{mp} = \eta_{mp,STC} \times [1 + \alpha_p \times \left(\frac{T_C}{T_{C,STC}}\right)] \quad (3)$$

where T_a is the ambient air temperature (°C), $T_{C,NOCT}$ is the nominal operating cell temperature, $T_{a,NOCT}$ is the ambient temperature at which $T_{C,NOCT}$ is calculated (°C), $T_{C,STC}$ is the SPV cell temperature at STC of 25°C and η_{mp} and $\eta_{mp,STC}$ are maximum power point efficiencies (in %) of the SPV array at real-time and STC, respectively, α is the coefficient of absorption of SPV panel (%), and τ is the transmittance associated with the SPV panel cover (%).

6.8.2 River Turbine

Hydrokinetic River Turbines (HKRT) require a lesser amount of civil engineering and construction work as compared to hydel power stations and dams [160]. The planned installation locations (Lakwa GGS5 and Geleky GGS2) are swept by rivers Dikhow and Disang, tributaries of the Brahmaputra, and have average river heads varying from 2 to 5 m [161]. The most common problem with such low river heads is rotor blockage due to debris deposition; axial flow turbines with blades that swing back and shed off the debris are considered the most effective to deal with this problem [162]. Deployment of an HKRT becomes difficult in deep and high flow velocity rivers, and Darreius turbines are a good fit for such cases [162]. Since the river head in the present case is low (2 to 5 m), and flow velocity is as low as 3.152 m/s in the summers and as high as 19.8 m/s in the rainy season, axial flow Schottel hydrokinetic turbine (Figure 6-3) manufactured by GmbH Germany is the most suitable fit [162], [163]. It has a rotor diameter of 3 m, rated power of 70 kW, rated water velocity of 3.8 m/s, cut-in speed of 0.9 m/s, and a cut-out speed of 6.75 m/s [164]. The lifetime of the selected turbine is 25 years [164]. The hydrokinetic turbine power curve in Figure 6-2 derived from the manufacturer datasheet [163] shows that the maximum output is obtained if the water speed is between 3.75 and 6.75 m/s, and a water speed above 0.89 m/s will start giving exponentially increasing power output. Figure 6-3 shows the installation of a Schottel Hydrokinetic turbine.

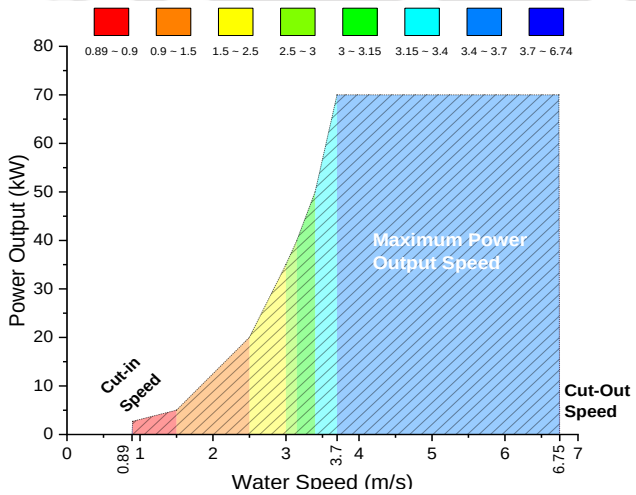

Figure 6-2 Power Output vs water speed curve for hydrokinetic river turbine

Figure 6-3 Installation of Schottel hydrokinetic river turbine

The hydro turbine's nominal power output is given by Eqn (4) [156].

$$P_{hyd} = \eta_{hyd}\rho_{water}gh_{net}Q_{turbine} \quad (4)$$

where η_{hyd} is the turbine efficiency, ρ_{water} is the density of water, g is the gravitational acceleration, h_{net} is the net head, and $Q_{turbine}$ is the flow rate through the turbine [165] expressed as,

$$Q_{turbine} = \frac{1}{2}.\frac{C_T.\ A.v^3}{g.\ h_{net}} \quad (5)$$

where C_T is the coefficient of power of the hydrokinetic turbine, A is the swept by turbine blades, and v is the velocity of river water in m/s [164]. Therefore,

$$P_{hyd} = \frac{1}{2}.\eta_{hyd}.\rho_{water}.C_T.\ A.v^3 \quad (6)$$

6.8.3 Converter

The converter works as a coupling between DC and AC systems and can facilitate the bidirectional power flow. Since the proposed model has solar PV and river turbine modeled on the DC bus, and gas microturbine, grid, and load modeled on the AC bus, a bidirectional converter having an input efficiency of 95% and rectifier input efficiency of 97% was considered [166].

6.8.4 Gas Microturbine

The average annual flaring of natural gas in the area under consideration is 2958.25 MMSCM (million metric standard cubic meters) daily [166]. The gas flaring amounts to 11.833 million tons of CO_2 emissions and a loss of $59165 annually [167]. The aim of this study was to utilize the waste flare gas to produce electricity, thereby reducing carbon emissions and the electricity problem in an economically optimal way. Therefore, three Capstone's gas microturbines were employed for the hybrid renewable energy system design: two 30 kW gas MTs with a fuel curve intercept of 1.50 m^3/h and a 200 kW gas MT with a fuel curve intercept of 10.0 m^3/h. Both types of gas MTs have a fuel curve slope of 0.29 m^3/h/kW (Figure 6-4) [166].

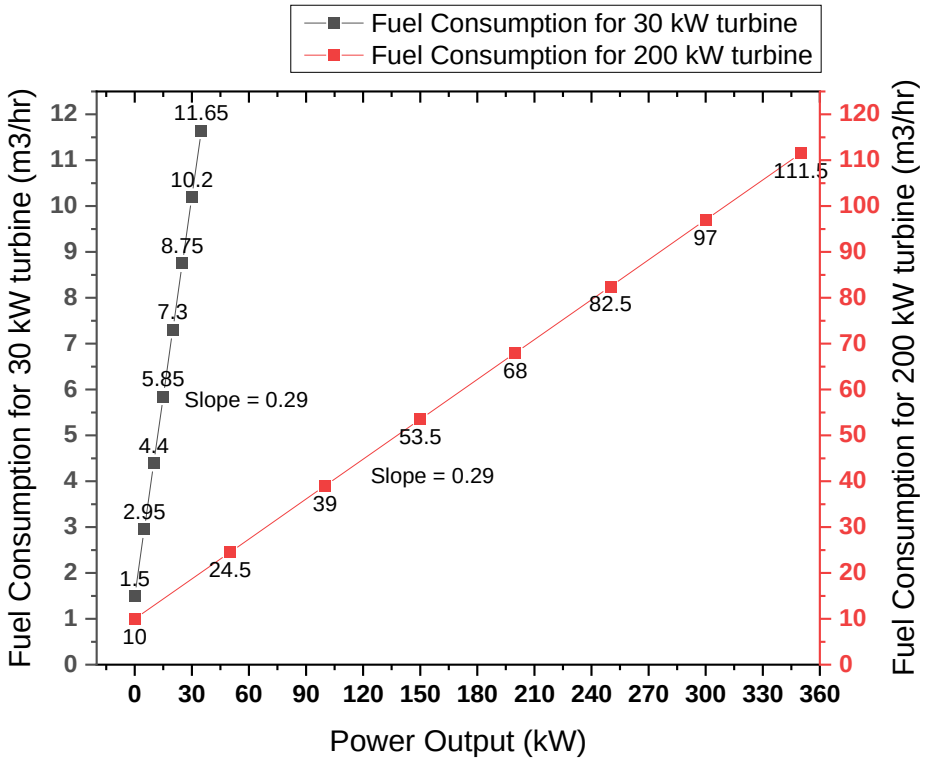

Figure 6-4 Fuel consumption curves for 30 kW and 200 kW Gas Microturbines

The fuel curve, as shown in Figure 6-4, is a straight line with a y-intercept, and it uses the following equation for the fuel consumption of the generator:

$$F = F_0 Y_{gen} + F_1 P_{gen} \tag{7}$$

where F_0 is the fuel curve intercept coefficient, F_1 is the fuel curve slope, and Y_{gen} is the rated capacity of the generator (in kW).

The fixed and marginal energy costs of the generator are estimated by Eqs. (8) and (9), respectively, were used for simulating the system operation. The fixed cost is simply the cost of running a generator without generating electricity, whereas the marginal cost is the additional cost per kilowatt-hour of electricity produced by the generator:

$$C_{gen,fixed} = C_{om,gen} + \frac{C_{rep,gen}}{R_{gen}} + F_0 Y_{gen} C_{fuel,eff} \tag{8}$$

where $C_{om,gen}$ is the operation and maintenance cost (in \$ per hour), $C_{rep,gen}$ is the replacement cost in \$, R_{gen} the lifetime of the generator (in hours), $F_0$is the fuel curve intercept coefficient or the quantity of fuel per hour per kilowatt, Y_{gen} is the capacity of the generator (in kW), $C_{fuel,eff}$ is the valid fuel price (in \$ per quantity of fuel).

$$C_{gen,mar} = F_1 C_{fuel,eff} \quad (9)$$

where F_1 is the fuel curve slope is the quantity of fuel/hour/kW, and $C_{fuel,eff}$ is the effective price of fuel in $/quantity of the fuel.

6.8.5 Grid

The grid was modeled as a component that allows micropower systems to purchase and sell AC electricity in case of a power shortage or surplus production. Whether the power will be sold to the utility or purchased from it is decided using the dispatch strategy discussed in section 6.6, page 115. The rate of selling back power to the grid was set as 0.108 $/kWh, and the power purchase price is set to 0.081 $/kWh [168]. The capacity ratings and cost specifications of various components used have been summarized in Table 6-1.

Table 6-1 Various costs, lifetime, type, and rating details of various components involved in the HES design [163]

Component Name	Type	Rating	Quantity	Capital Cost	Replacement Cost	O&M Cost	Lifetime
Gas Microturbine	Capstone	200 kW	1	200,000 $	200,000 $	0.005 $/operational hour	40,000 hours
		30 kW	2	30,000 $	30,000 $	0.005 $/operational hour	40,000 hours
Solar Photovoltaics	CanadianSolar MaxPower	2000 kW	SPV arrays arranged in series and parallel	0.08 $/kWh	0.08 $/kWh	-	25 years

Hydrokinetic River Turbine	Schottel	70 kW	1	57,000,000 $	57,000,000 $	6,290,000 $	25 years
Converter	Free size	10,455 kW[1]	1	375 $	375 $	10 $	25 years

6.3 Load Demand Estimation

The Assam Power Distribution Company Limited (APDCL) supplies power to residential customers, commercial customers, and industries in the study area. Hence, the site has a mixed hourly load profile as shown in Figure 6-5. The average annualized load demand of the Nazira oil and gas field region is 16,500 kWh/day, with a peak load of 2040.49 kW for the year 2019 as obtained from APDCL. The regional power grid operates on a power factor of 0.85 and a load factor of 0.34. To make the load data more accurate, typical daily load profiles for all months were specified, and then the randomness was added to synthesize the data. A daily variability of 10% was selected at every 20% variation in the

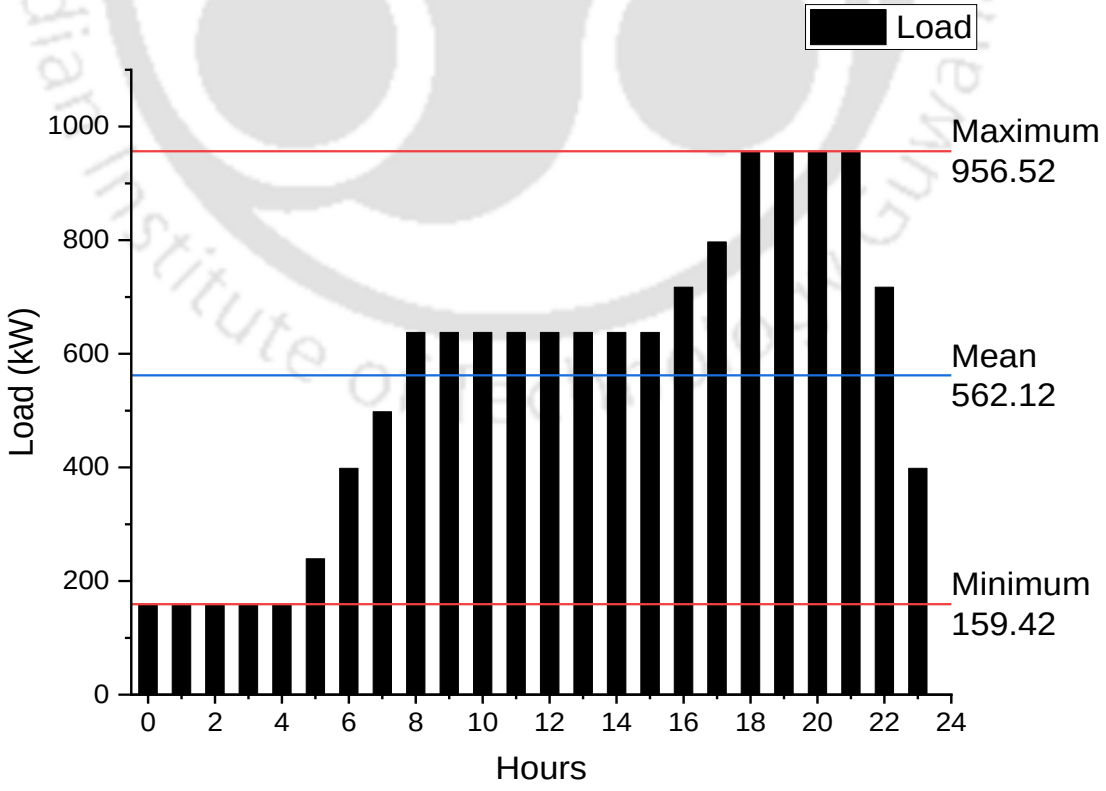

Figure 6-5 Annual average hourly load profile of Nazira oil and gas field

time-step [169]. It can be seen from Figure 6-5 that loading occurs mostly between 7:00 AM to around 11:00 PM, and peak load occurs between 6:00 PM to 11:00 PM. The remaining hours of the day experience light loads. The grid-connected microgrid power management system has to be scheduled accordingly.

6.4 Economic Modelling and Objective Function

The net present cost (NPC) incurred during the project lifetime is the best indicator of the suitability of a given HRES design. The NPC calculation considers all possible factors: interest rate, inflation, discount rate, capital costs, operation & maintenance costs, replacement, and salvation costs. The objective function minimizes the NPC; the expression for which is given by [170]:

$$Obj\ Fn = \min(NPC) = \min\left(\frac{C_{tot,ann}}{CRF\ (d,\tau)}\right) \tag{11}$$

where $C_{tot,ann}$ is the total annualized cost of the system ($/year) and CRF is the capital recovery factor, which depends on discount rate (d) and project lifetime (τ,years) as expressed by Eqn(12):

$$CRF\ (d,\tau) = d \times \frac{(1+d)^{\tau}}{[(1+d)^{\tau}-1]} \tag{12}$$

where d is expressed as,

$$d = \frac{(d'-f)}{(1+f)} \tag{13}$$

where d' is the nominal discount rate, and f is the expected inflation rate.

The capital cost of each component is converted to the annual cost by amortizing it over the component's life using the actual discount rate. The total annualized cost of the system was estimated by Eq. (14):

$$C_{tot,ann} = \sum_{k \in PV,GMT1,GMT2,RT,Converter} C_{cap,k} + C_{O\&M,k} + C_{repl,k} - C_{salv,k} \tag{14}$$

where Cs_{alv} is the salvage cost, C_{cap} is the capital cost, $C_{O\&M}$ is the operation and maintenance cost, C_{repl} is the replacement cost, and k denotes the system components – SPV, GMT, RT, and converter.

The salvage cost of a system component is directly proportional to its remaining life and is dependent on the component's replacement cost rather than capital investment cost. The salvage cost is given by Eq. (15) [166].

$$C_{salv,k} = C_{repl,k}\left(\frac{T_{rem,k}}{T_{com,k}}\right) \tag{15}$$

Here T_{rem} is the remaining life of the component in years, and T_{com} is the component lifetime in years. The system with a minimum life-cycle cost ultimately results in a system with a minimum Levelized cost of energy (LCOE). LCOE is the average cost per kWh of the useful electricity generated by the system and is given by [166] –

$$LCOE = \frac{C_{tot,ann}}{E_{tot,ann}} \tag{16}$$

$E_{tot,ann}$ is the total amount of energy used in meeting the load demands per year (kWh/year). Additionally, the return on investment (ROI) is another crucial indicator that determines the profitability or economic viability of the HES as an investment, as expressed in Eq. (17) [170]:

$$ROI = \frac{\sum_{i=1}^{\tau}\left(C_{i,ref} - C_{i,sel}\right)}{\tau \times \left(C_{cap,sel} - C_{cap,ref}\right)} \tag{17}$$

where, $C_{i,ref}$ and $C_{i,sel}$ are the nominal annual cash flow of the base/reference and selected systems, respectively, and $C_{cap,ref}$ and $C_{cap,sel}$ are the corresponding capital costs. In the present study, since grid connectivity and a 200 kW gas microturbine exist in Lakwa, the base case was considered a 'grid + 200kW Gas MT' for Lakwa, whereas it was 'Grid only' for Geleky. Three different systems were selected for the analysis: 1) SPV/RT/GMT/Grid, 2)SPV/GMT/Grid, 3)GMT/Grid.

6.5 Environmental Suitability Indicators

Renewable fraction (RF) and amount of CO_2 emitted (A_{CO2}) were chosen as the sustainability indicators as expressed by Eqs. (18) [171] and (19) [170], respectively:

$$\mathrm{RF} = 1 - \frac{\mathrm{Enon\_ren}}{\mathrm{Etot,ann}} \tag{18}$$

where Enon_ren is the non-renewable generation in kWh/yr, and Etot, ann is the total electrical load served (in kWh/yr), which included gas MT and Grid in the present case.

$$\mathrm{A_{CO2}} = 3.667 \times \mathrm{m_f} \times \mathrm{LHV_f} \times \mathrm{CEF_f} \times \mathrm{X_c} \tag{19}$$

Where m_f is the amount of diesel fuel (L), LHV_f is the fuel heating value (MJ/L), CEF_f is the factor related to carbon emission (ton carbon / TJ), and X_c is the oxidized carbon fraction, where each 3.667 gm of CO_2 includes 1 gm of carbon.

6.6 Dispatch Strategy

A dispatch strategy is a logical sequence of instructions that govern the operation and flow of energy between various HRES components. After accounting for the current power/energy status of the component, it determines which equipment must operate at that instant. HOMER Pro software uses cycle-charging (CC) and load-following (LF) strategies by default [156]. In both strategies, renewable-source-based generators are given top priority while meeting the load. The basic difference between CC and LF is that in CC, the generator is used to meet the load as well as charge the battery, while it is used only to meet the load in LF. The battery is charged using surplus renewable in the case of LF, depending on the renewable availability [172]. Since the use of the generator is lesser in LF, it is more effective in minimizing environmental pollution and overall system operating costs (as the cost of fuel will be reduced) [173]. But in the current case, as the natural-gas-based generator uses flare gas wastes to generate electricity, the gas-microturbines are considered equivalent to renewable-source-based generators. Therefore, the dispatch strategy has been customized to suit the requirements of the presented case study. The following equations explain the dispatch strategy:

$$P_{Ren} = P_{PV} + P_{RT} + P_{MT} \tag{9}$$

$$P_X = P_L - P_{Ren} \tag{10}$$

where, P_{Ren} is the total renewable generation, which is the sum of the power produced by solar PV (P_{PV}), hydrokinetic river turbine (P_{RT}), and gas microturbine (P_{MT}); P_X is the outstanding power requirement after utilizing P_{Ren} to meet the load demand (P_L). Thus, decisions must be made depending on the value of P_X, as illustrated in Figure 6. $P_X = 0$

indicates P_L was fully met by renewables, while $P_X > 0$ means there Is outstanding power requirement, which has to be met from the grid. However, $P_X < 0$ indicates availability of surplus renewable power, which can be fed to the grid.

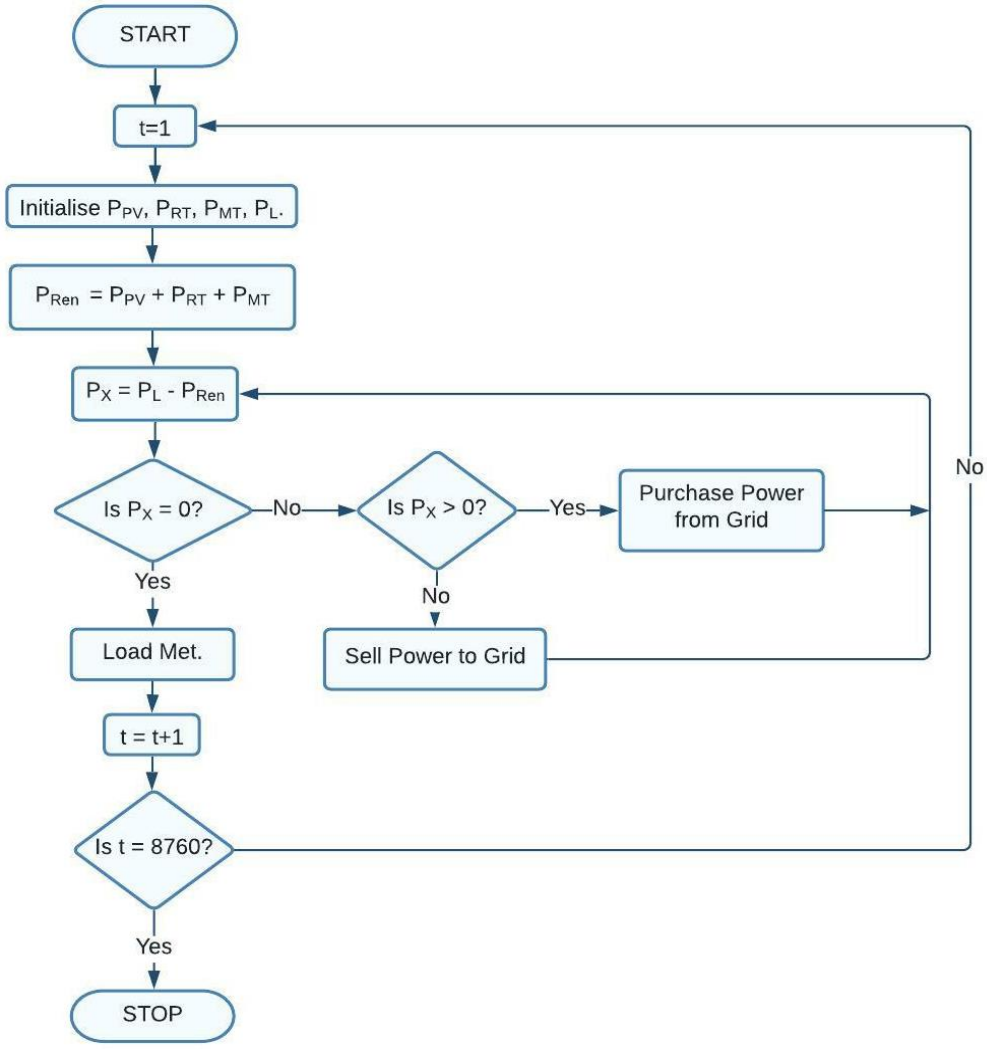

Figure 6-6 Flowchart of the dispatch strategy used for the modeled hybrid energy system.

The algorithm shown in Figure 6-6 runs for the entire year and makes hourly calculations for real-time dynamic power dispatch between various components (8760 hours in a year). Whenever the system is deficient in power, it can fetch power from local generation and the grid using the proposed dispatch strategy, making the system robust and reliable.

6.7 Optimization Constraints

The following constraints and assumptions were followed in the present case study:

1) Resource constraints: The selected study location has annual solar radiation of 3.14 kWh/m^2/day [139], and an annual average river flow of 3.152 m/s and 19.8 m/s in summers and winters, respectively.

2) Economic: Nominal discount rate determines the present lump sum value of future cash flows. A nominal discount rate of 8% was considered for the present study. Considering the scale of the current operational project in ONGC Nazira [174] and the availability of the natural gas reserves in the area [175], a project lifetime of 25 years was considered.

3) Technical: An operating reserve of 10% was selected as a percentage of the load. This accounts for abrupt changes in load patterns, and an active operating reserve of 50% was considered for solar photovoltaics to deal with the intermittent weather conditions.

4) Reliability: To ensure high levels of power supply reliability, the 'caidi' index – the average number of interruptions per year- was considered 0%.

5) Emission: Currently, there is no law on emission penalties in Assam. Therefore, the emission penalties for CO_2, nitrogen oxides, carbon monoxide, particulate matter, and sulphur dioxides, were assumed to be zero.

6.8 Results and Discussion

Six configurations of HES were selected for two different locations: Lakwa and Geleky. Since Geleky GGS2 is away from river stream, configurations devoid of hydrokinetic river turbines were selected for Geleky GGS2, while configurations having a river turbine were suggested for Lakwa GGS4 owing to its vicinity to the river stream. The six configurations were compared on the basis of a) Cost: NPC, LCOE, Operating expenses, and b) Environmental suitability: Total Fuel Consumption, Renewable Fraction, as shown in Table 6-2.

Table 6-2 Comparison of the selected HES based on cost and environmental sustainability

#	Configuration	Cost Parameters			Environmental Sustainability		
		NPC	LCOE	Operating Cost	Renewable Fraction (%)	Total Fuel Consumption (m3/yr)	Suggested Location
1	**SPV/GMT/RT/G**	-$2.32B	-$2.72	-$187M	93.8	774,384	Lakwa
2	**GMT/RT/G**	$571B	$7.16	$39.8M	1.99	774,384	Lakwa
3	**SPV/RT/G**	-$2.14B	-$2.56	-$173M	95.6	0	Lakwa
4	**SPV/GMT/G**	-$2.45B	-$2.87	-$192M	93.7	774,384	Geleky
5	**GMT/G**	$445M	$5.61	$34.4M	0	774,384	Geleky
6	**SPV/G**	-$2.27B	-$2.72	-$178M	95.5	0	Geleky

Configuration numbers 2 and 5 – GMT/ RT/ G and GMT/ G have exorbitant Net Present, Operating costs as well as Levelized Cost of Energy (LCOE) (NPC $571B and $445M, Operating Cost: $39.8M and $34.4M, LCOE: $7.16 and $5.61). It is observed from Table 6-2 that all systems except GMT/RT/G and GMT/G (G denotes grid) are profitable as they have negative cash flows. Lower cost values (less positive and more negative) imply more grid export [176]. Furthermore, the renewable fraction available in these two systems is negligible (1.99% and 0%). Therefore, GMT/ RT/ G and GMT/ G were excluded from the viable options, and a cost comparison of the remaining four systems was made, as shown in Figure 6-7. The NPC represents the overall lifecycle cost of the system, with all the future cashflows discounted back to the present [152]. Out of all the four systems, SPV/GMT/G has the lowest NPC. It may be noted from Table 6-2 that all four systems have almost equal renewable fractions. Therefore, SPV/GMT/G is the best suitable system economically and environmentally for the considered oil and gas field location.

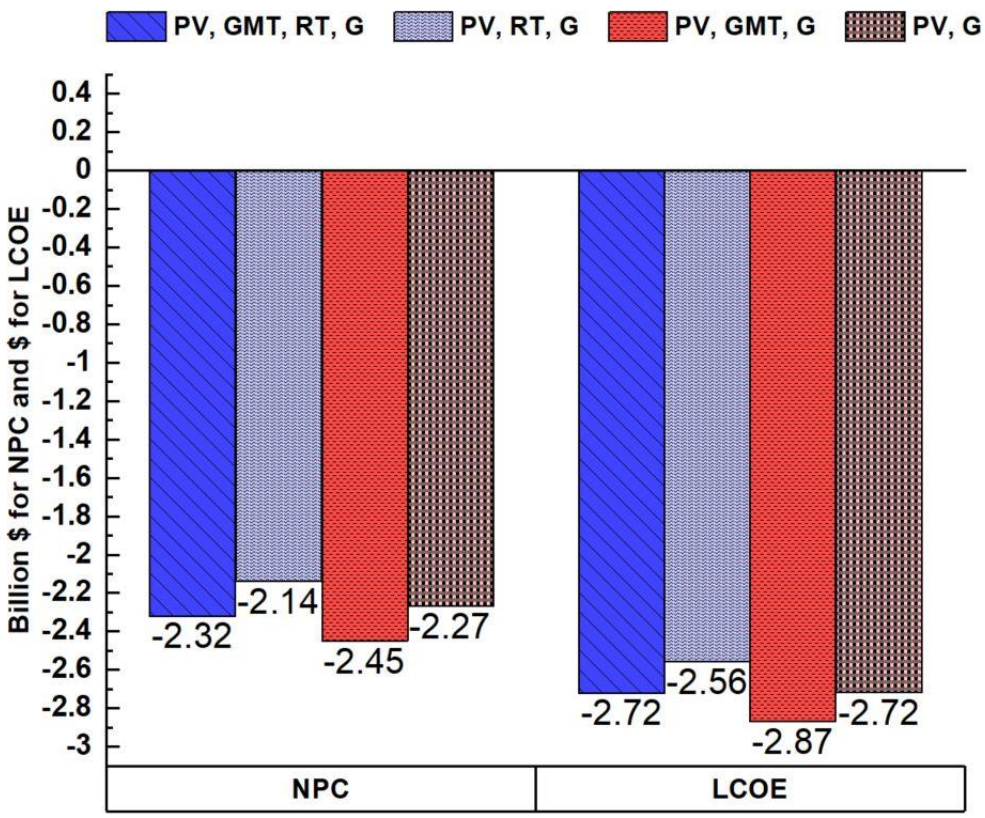

Figure 6-7 Cost comparison of SPV/ GMT/ RT/ G, SPV/ RT/ G, SPV/GMT/ G, and SPV/ G configurations.

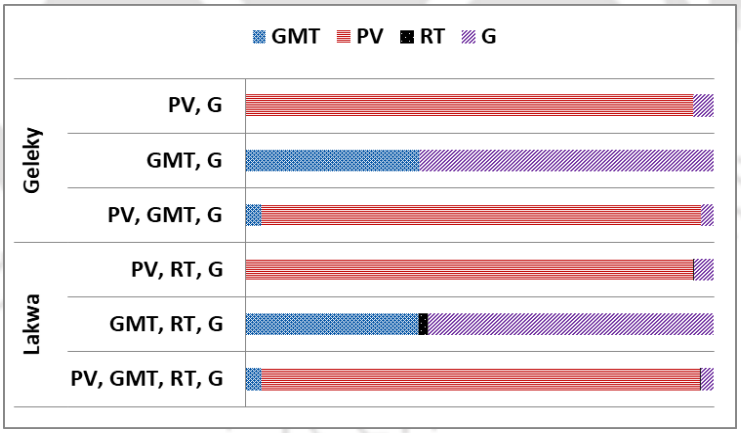

Figure 6-8 Share of electrical power consumption by each component of the selected HES

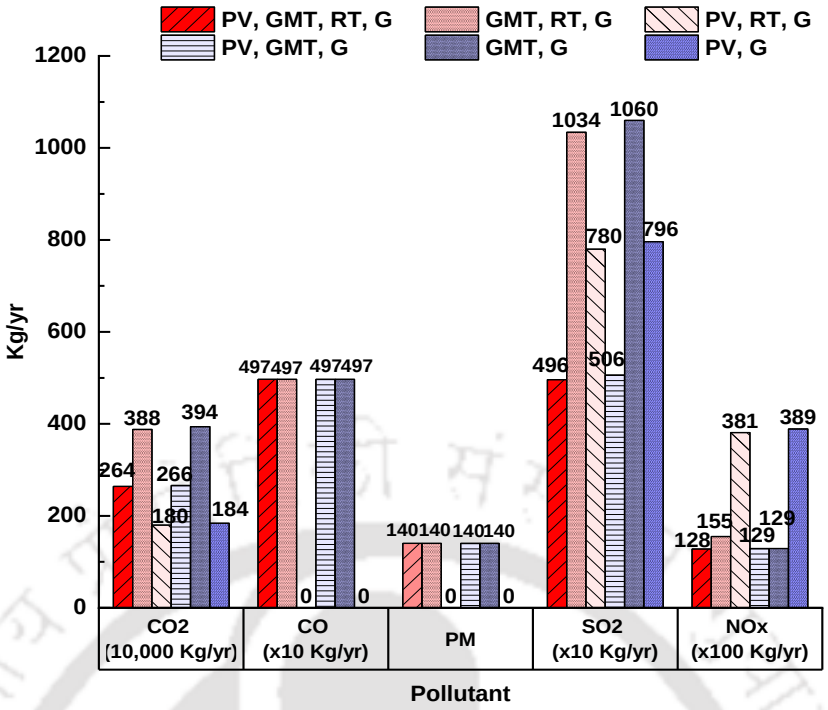

Figure 6-9 Comparison of level of pollutants from the six systems.

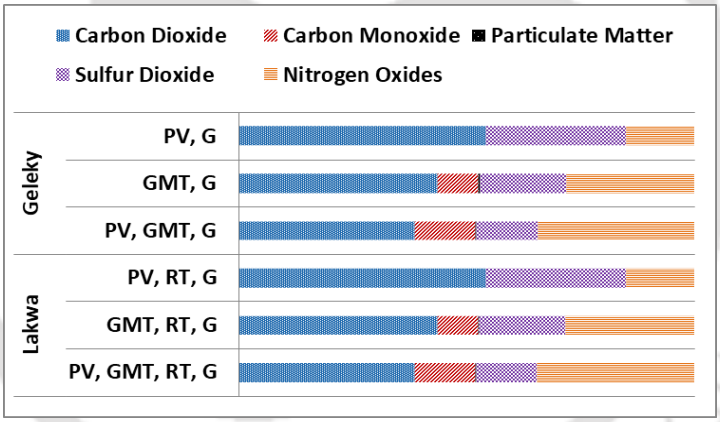

Figure 6-10 Share of pollutants by all HES during 25 years of operation

Further, an analysis of the component-wise electrical power consumption and emissions from the operation of the six HES for a lifetime of 25 years was performed, and the results are shown in Figure 6-8, Figure 6-9, and Figure 6-10, respectively. Figure 6-8 shows that the presence of RT does not have any significant impact on the share of emissions in any HES. It also depicts that the proportion of CO_2, CO, and nitrogen oxides is almost constant for SPV/G -- SPV/ RT/ G, GMT/G -- GMT/ RT/ G, and SPV/ GMT/ G -- SPV/ GMT/ RT/ G.

It can also be observed from Figure 6-8 that the electrical power production from RT in the systems having RT is negligible, whereas the distribution of power produced by GMT, SPV, RT, and G is almost constant for SPV/G - SPV/ RT/ G, GMT/G - GMT/ RT/ G, and SPV/ GMT/ G - SPV/ GMT/ RT/ G systems. A detailed analysis of emissions from the six systems is provided in Figure 6-9. It is observed that both GMT, G and GMT, RT, G cause the highest amount of overall emissions, making them unfit for the environment. With respect to overall emissions, SPV, GMT, G, and SPV, GMT, RT, and G had the lowest. However, by considering the nominal contribution of RT in the total electrical power production, SPV, GMT, and G could be finalized as the most viable configuration for both locations.

6.8.1 Production Analysis of the most Optimal Solution (SPV/ GMT/ G)

A combination of solar PV, two 30 kW and one 200 kW GMTs, and a grid was observed to be the most optimal configuration. Figure 6-11 provides the monthly component-wise electrical power production summary of the SPV/ GMT/ G system. The maximum power

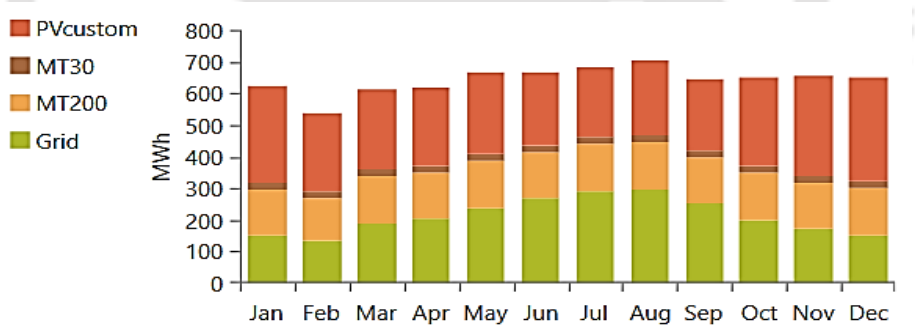

Figure 6-11 Monthly electrical production of the designed system components

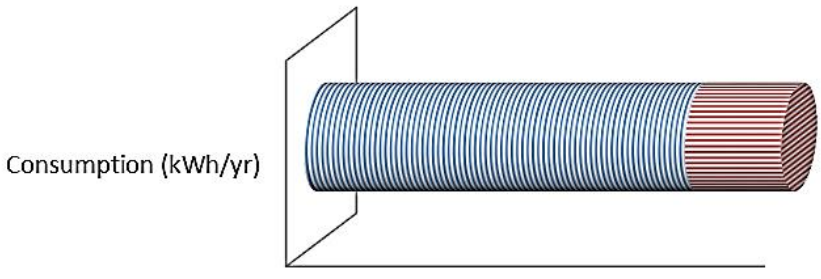

	Consumption (kWh/yr)
AC Primary Load	60,22,500
Grid Sales	15,20,326

Figure 6-12 Electrical power Consumption summary of the designed system

is generated in August, followed by July, May, June, and January. Likewise, the maximum power exchange with the grid also occurs in mid-year (i.e., June to August). The electrical penetration by SPV in the entire system comes out to be 52.3%. Figure 6-12 depicts that the load consumes 79.8% of energy, whereas 20.2% is sold off to the utility power grid. Figure 6-13 provides a detailed image of the energy exchange with the grid by the winning system architecture. It is observed that the load demand is comparatively less in the winter months (Nov, Dec, Jan, Feb) than in the other months. Therefore, surplus energy is sold to the grid during the winter months. However, the peak demand is the highest (2,036 kW and 2,093 kW) in the summer months (June-July). It is also observed that the energy cost is maximum in August. Figure 6-14 shows that power has to be purchased from the grid to meet the surplus load, mainly during night hours (5:00 PM to 11:00 PM), and surplus energy is sold back to the grid during the daytime (6:00 AM to 5:00 PM).

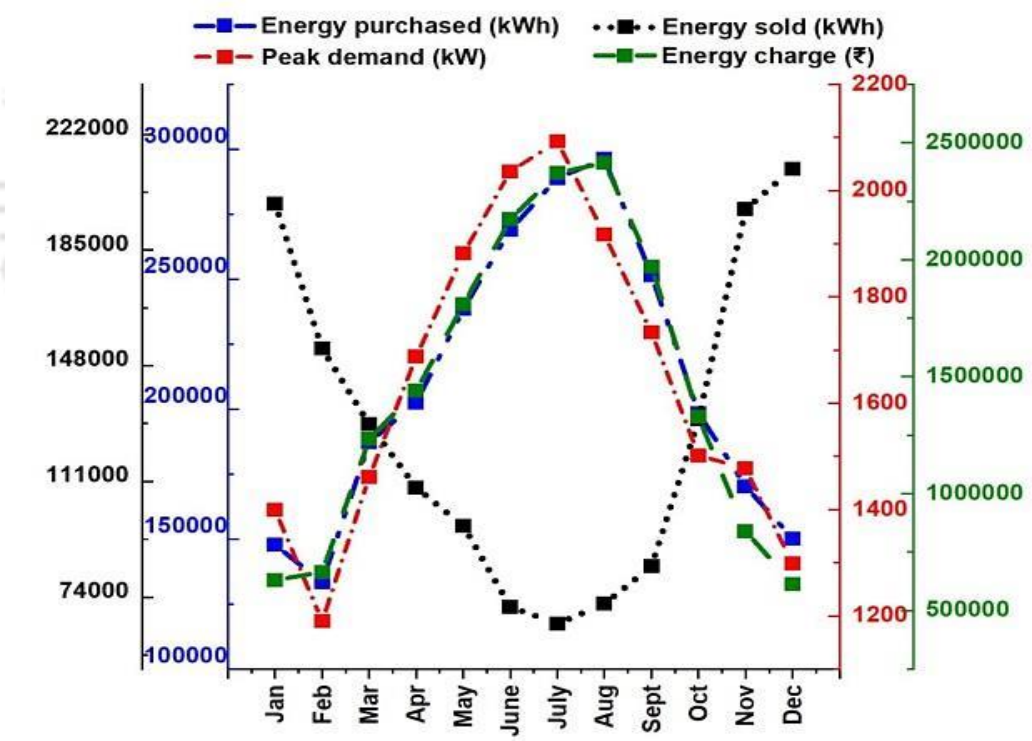

Figure 6-13 Annually averaged monthly energy metrics

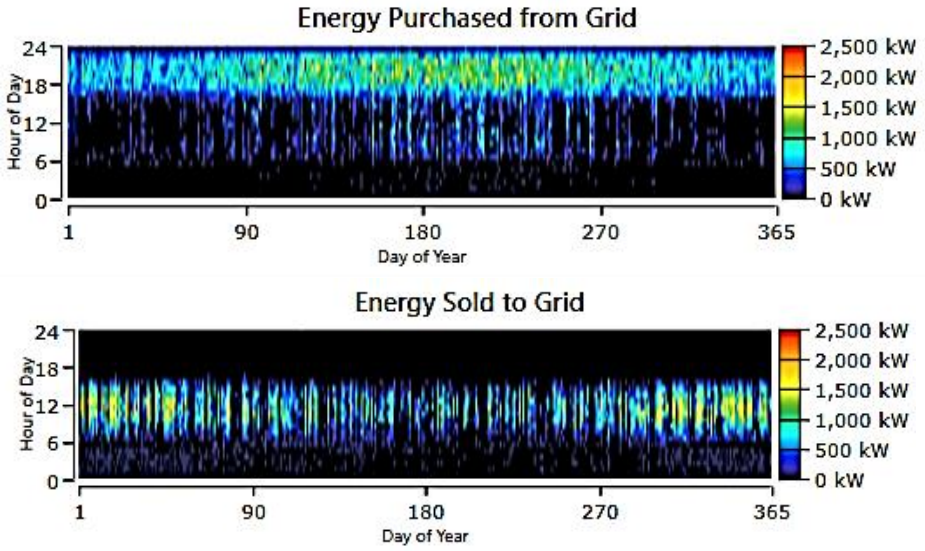

Figure 6-14 Annually averaged hourly energy Density Map

6.8.2 Comparison of the proposed system with the existing power system.

Compared to the existing power system, the proposed GMT/ SPV/ G design is 35.54% economically ($ 5.9M reduction in NPC) and 50% ecologically (decrease of 850 tonnes of CO_2 per year) more sustainable. Figure 6-15 shows a comparison of the cumulative as well as annualized cash flows by the two systems. The downward slope of the cumulative nominal cash flow graph indicates expenditures. A lesser negative slope implies that setting up a hybrid system in the Nazira area is more profitable than the existing grid power supply, calculated for 25 years.

After a payback period of 7.8 years, the designed hybrid system proved to be profitable, with an ROI (return on investment) of 11%. The lifetime for GMT is 40,000 hours, and hence there occurs a replacement cost for the gas microturbines after completing 40,000 hours, so there will be a replacement cost for GMT after this period (5^{th} year). Therefore there would be a spike in the annual nominal cash flow for both the proposed and existing systems in the 5^{th} year. The existing system's yearly cash flow becomes higher as ₹40 million per year must be spent for operation and maintenance throughout the lifetime of the project (25 years). Consequently, the overall cost of the existing system supersedes that of the proposed hybrid system.

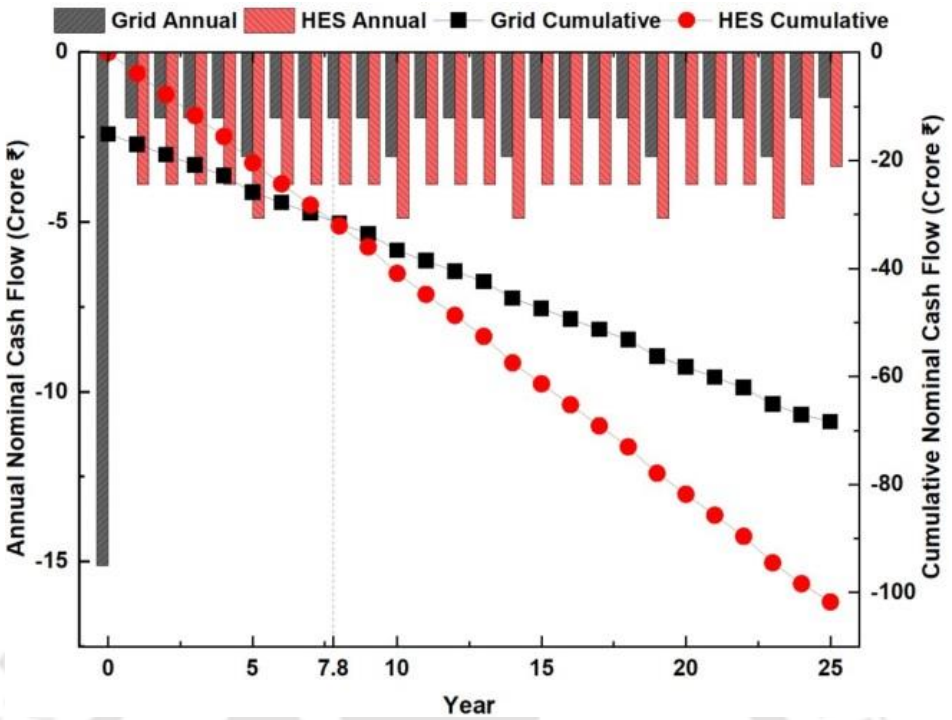

Figure 6-15 Comparison of annual and cumulative nominal cash flows of the proposed hybrid energy system and the existing system

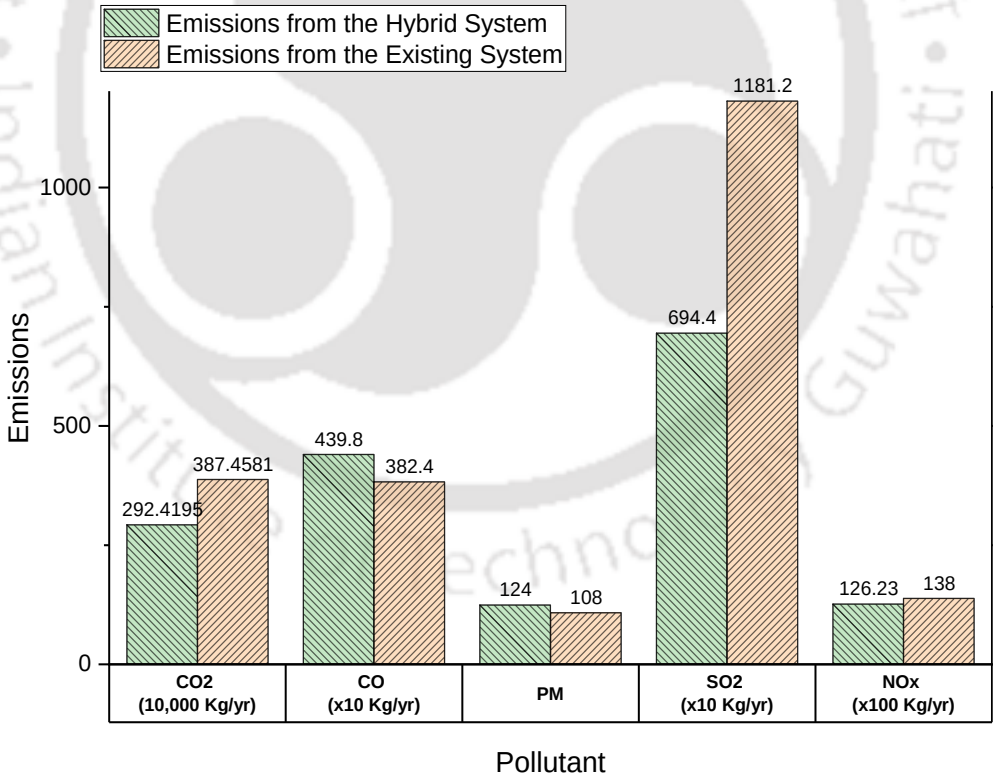

Figure 6-16 Pollutant wise comparison of emissions from the proposed hybrid energy system and the existing power system

Major emissions from the natural gas generators and the designed system include CO_2, CO, unburnt hydrocarbons, particulate matter, sulfur dioxide, and nitrogen oxides. Figure 6-16 provides an exact statistical comparison of emissions from the hybrid system with the existing system. Compared to the existing system, the emissions of CO_2, CO, particulate matter, sulfur dioxide, and nitrogen oxides were reduced by 24.52%, 13.05%, 12.90%, 41.21%, and 8.52%, respectively. The CO_2 emissions from the proposed hybrid system is up to 50 % less than that from direct flaring (statistics of the CO_2 emissions from direct flaring provided in [177]). Therefore this study proves that the combination of gas micro turbines with SPV to generate electricity from natural gas reduces emissions by 40-50 %.

6.9 Conclusions

Due to gas flaring at oil and gas fields, the flora – fauna and human health of settlements around the flaring site are adversely affected. Another issue is the lack of a reliable and robust power supply in the oil and gas field area. This research work has proposed a hybrid energy system (HES) that utilizes waste gas flares to generate electricity, thereby solving both the aforementioned problems. A systematic framework was established to suggest the optimal size and design of the HES. A novel dispatch algorithm was used to simulate the real-time operation of the HES to suit the requirements of the oil and gas fields. The techno-commercial and environmental viability of six HESs was analyzed for two different gas flaring sites. A system comprising two 30 kW gas microturbines, a 2000 kW solar PV panel set, and a grid connection could save 35.52% net present cost and reduce gas flaring by up to 50%. This research is in line with the United Nations sustainable development goals and can be beneficial for the engineers and researchers who aim to improve productivity while reducing gas flaring in oil and gas fields.

Chapter 7

Multi-Microgrid Power and Energy Management

7.1 Foreword

The Generation and utilization within a single microgrid are localized. The energy generated within a microgrid system is utilized in the following ways: consumption by local loads, stored in batteries and selling back to the utility. Presented research proposes an energy-efficient alternative to use the produced energy when multiple microgrids are situated in the vicinity of each other. The idea is to share the power surfeit amongst multiple microgrids dynamically. A mixed-integer linear problem (MILP) is formulated for transactive energy management between multiple microgrid systems and solved using CPLEX solver by TOMLAB in MATLAB. The uncertainty in solar and wind production is modeled using beta and Weibull distributions, respectively. Monte Carlo simulation clubbed with a fast-forward selection method is used for scenario generation. The results suggest that as the number of microgrids in the collaborative multi-microgrid network is increases, the overall cost of the system decreases. As multiple gas flaring locations are situated in the vicinity of each other in any oil and gas field, forming a collaborative network will multifold the benefits of establishing a distributed generation system to reduce natural gas flaring in oil and gas fields.

Transactive Energy Management (TEM) and trading can be used in Microgrids to facilitate the integration of distributed energy resources (DERs) in the existing network. The TEM establishes a distributed information system architecture that can be used to coordinate various components of the system[178]. It is a set of economic and control mechanisms that allows the dynamic balance of supply and demand across the entire electrical infrastructure using value as a key operational parameter. This means that all the operational objectives and constraints of the complete electrical system can be described in terms of their value or cost. The transactive energy system considered in this research is responsible for managing distributed energy resources (DERs) belonging to multiple microgrids. It enables and incentivizes the DER owners to participate in the energy market.

In any microgrid or multi-microgrid network, the total power generation should be greater than or equal to the power demand of the network. This constraint, put up by the equation of Balance of Power (BOP) and Balance of Energy (BOE), should be kept in mind while reconfiguring the integrators for optimal sharing of resources so as to avoid overloading of any one of the generating units. The principal aim of the optimization problem presented in this chapter is to minimize the operational costs of the multi-microgrid network.

The impact of collaboration amongst microgrids on cost saving is studied in three different scenarios.

In the first case, a single microgrid is considered in the collaborative network. Multiple Microgrids do not share any connection with each other in the first scenario. Here, a microgrid can only take energy from the grid in case of a deficit.

In the second case, transactive energy management between four Microgrids is considered. In this case, four microgrids trade energy with each other to reduce dependency on the primary grid.

A third case is proposed to check the scalability of the algorithm. In the third case, ten Microgrids participate in the TEM network.

-

-

7.2 The Multi-Microgrid Architecture

Each microgrid participating in the TEM for a multi-microgrid network comprises solar photovoltaics systems (SPV), wind turbines (WT), BESS, load, grid, and connections with the Local Energy Market (LEM) for taking power in from the LEM or sending power to the LEM. The block diagram of the multi-microgrid architecture is presented in *Figure 7-1*. In this connection scheme, the LEM can have a bidirectional exchange of power/energy with BESS. It can take power from both renewable sources - wind turbines and solar panels, and the surplus power from all Microgrids participating in the collaborative network can be transferred to the load. Both solar and wind have only

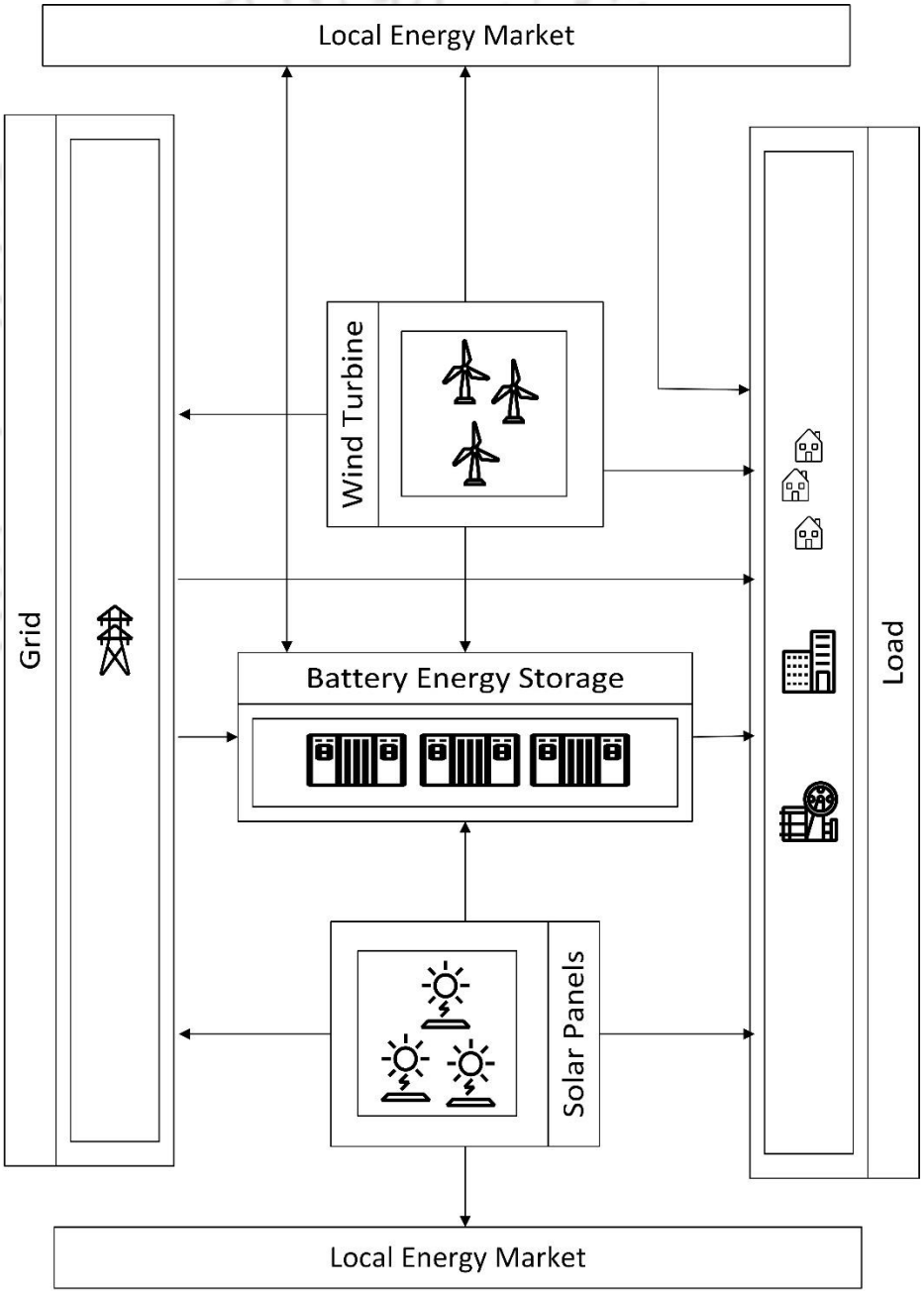

Figure 7-1 Schematic diagram of microgrid connections

outgoing connections to LEM, BESS, Load, and grid. BESS can take power from the grid, LEM, and renewable resources and supply power only to load. The load has only incoming connections from all components. This sign convention is followed in the entire collaborative multi-microgrid network, where there is a possibility of more than one microgrid sharing the same LEM.

The battery energy storage discharges to meet the load when wind and solar are not sufficient or it discharges to meet the demands of other Microgrids via LEM while maintaining its state of charge (SOC).

The suggested architecture enables many forms of energy trading in microgrids. For instance, the energy demand can initially be met by the energy generated by the RESs inside the microgrids. If the energy demand is more than the energy produced within a single microgrid, then the shortfall can be mitigated by supplying energy from other Microgrids via the LEM (Local Energy Market). LEM is designed to satisfy the broad definition of transactive energy standards. In order to lessen microgrids' reliance on the main grid and to perform dynamic energy balancing, LEM is taken into consideration. This is done while boosting cost-saving in market interactions and minimizing the overall energy cost of microgrids. In the last step, energy can be traded with the main power grid in case LEM does not have sufficient energy to meet the demands of the participating Microgrids. The designed architecture is economically (energy cost minimization) as well as ecologically (renewable power generation) suitable for oil and gas field applications wherein multiple Microgrids can be formed in the vicinity of each other. The proposed setup increases system reliability and demonstrates efficacy in meeting collaborative system load. The proposed system also reduces transmission losses as transmission losses in power exchanges with nearby Microgrids are far less than losses in exchange with a grid located far away.

7.3 Uncertainty Modelling

Wind speed and solar radiation are uncertain parameters. The Probability density function can be used to statistically characterize the erratic behavior of renewable resources. Wind speed is modeled with Weibull distribution[179], and solar radiation is modeled with beta distributions[180].

7.3.1 Weibull Distribution for Wind Speed Modeling

Weibull distribution is a widely used probability function in wind energy applications due to its simplicity. The following equation describes it:

$$\phi(V) = \frac{k}{c}.(\frac{V}{c})^{k-1} e^{-(\frac{V}{c})^{k}} \quad ; k>0 ; c>0 \qquad (1)$$

where V is the probability of wind being at speed v. It depends on two easily estimated parameters: k and c.

In short, $\phi(V) = weibull\ (k, c)$

k is known as the shape parameter. The higher the value of k, the higher the wind speed. It settles the shape of the Weibull function. C is known as the scale parameter. It has a velocity dimension (m/s). For the presented research, we have used MATLAB's *'wblrnd'* function to model the uncertainty in the wind speed.

7.3.2 Beta Distribution for Solar Radiation Modeling

Several methods are used for solar radiation modeling. [181] has used ANN for this purpose. However, [182]–[190] have used the beta distribution function for modeling solar radiation. Beta distribution function is apt for modeling solar irradiance and calculates the exact output power from the SPV module.

Beta distribution for solar irradiance (kW/m2) over time segment 't' is given by:

$$f_s^t(s) = \frac{\Gamma(\alpha^t+\beta^t)}{\Gamma(\alpha^t).\Gamma(\beta^t)} .(s^t)^{\alpha^t-1}.(1-s^t)^{\beta^t-1} \text{ for } \alpha^t > 0;\ \beta^t > 0 \qquad (2)$$

Where α^t and β^t are the shape parameters at 't'; and Γ represents Gamma function.

Shape parameters of Beta probability distribution function can be calculated using mean (μ_s^t) and standard deviation (σ_s^t) of irradiance for the corresponding time segment.

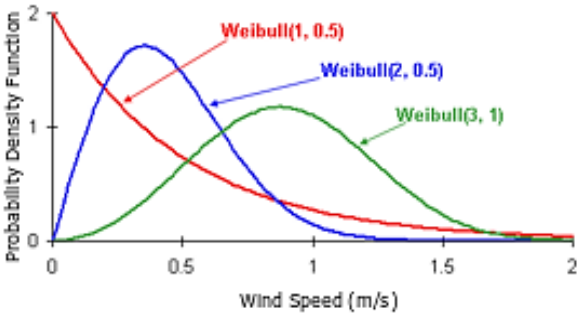

Figure 7-2 Weibull distribution function for wind speed modeling

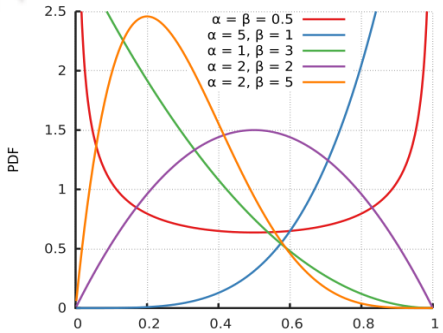

Figure 7-3 Beta distribution function for solar radiation modelling

$$\beta^t = (1-\mu_s^t).\left(\frac{\mu_s^t(1+\mu_s^t)}{(\sigma_s^t)^2}-1\right);\ \alpha^t = \frac{(\mu_s^t * \beta^t)}{(1-\mu_s^t)} \quad (3)$$

In short, the Probability density function to model solar irradiance is $f_s^t(s)$= beta(α, β). Unlike Weibull distribution, beta is more random and can have shape.

7.3.3 Uncertainty Modeling Approach using Monte Carlo and Fast Forward Selection:

Monte Carlo approaches random sampling to stimulate physical phenomena.[179], [180], [191]–[196] Used the monte Carlo formula to generate random values of solar radiation, which correspond quite closely with the observed values. The candidate scenarios with a high probability of occurrence are selected using the fast-forward selection method. So Monte Carlo is used for scenario generation and FFS for scenario reduction to reduce computation time. To model the uncertainty using Monte Carlo and fast forward selection, inputs are taken from Weibull and beta distributions, and each resultant data point is sampled individually. This process is repeated using fast forward selection to improve accuracy and reduce deflection from the formula. For this study, all uncertain parameters like load demand, wind speed, temperature, and solar irradiance are modeled using Monte Carlo and fast forward selection. The Monte Carlo simulation generates 200 scenarios, and fast forward selection reduces the final data points to 50.

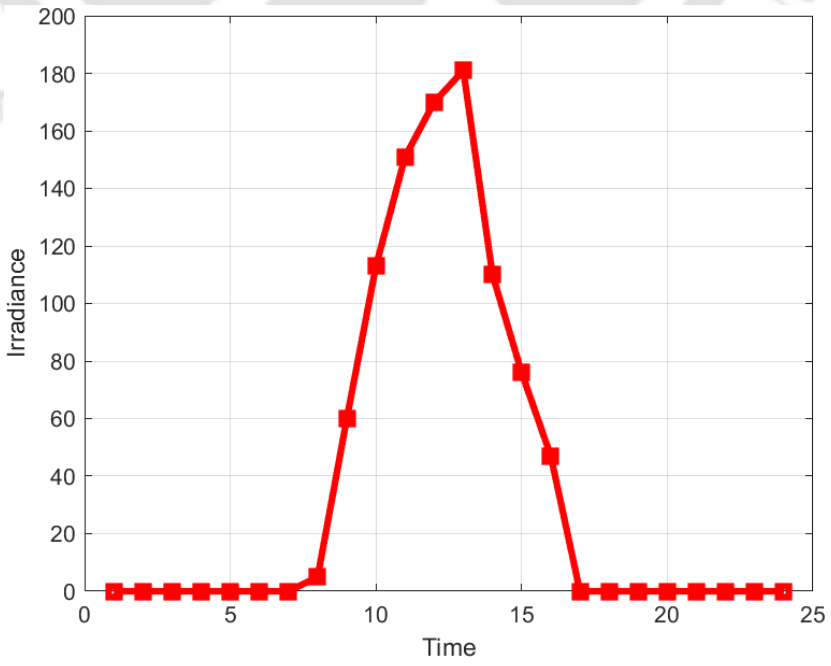

Figure 7-4 Solar irradiance data inputs using monte-carlo and fast forward selection

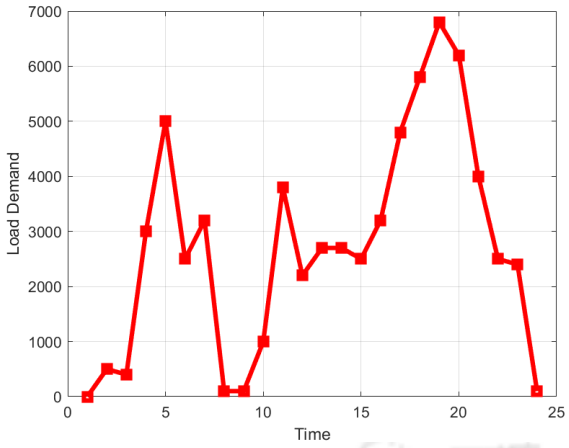

Figure 7-5 Load demand data inputs resulted from monte-carlo and fast forward selection process

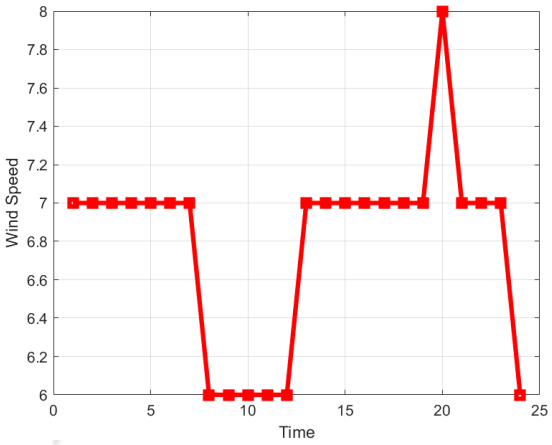

Figure 7-6 Wind speed data inputs resulted from monte-carlo and fast forward selection process

7.4 Mathematical Model of the Multi-Microgrid TEM Architecture

The prime objective of this chapter is to minimize the total energy cost of a Multi-Microgrid system. [197][102] have used MILP to schedule the DERs and multi-agent systems in Microgrid systems. This research also uses MILP (Mixed Integer Linear Programming) formulation to solve this optimization mix.

The total cost of energy for the multi-microgrid system is the cumulative difference in the cost of energy purchased and sold by all participating Microgrids.

It is given by -

Sum of 1 to i (Cost of Electrical Energy purchased by MG(i) at the time (t) - Cost of Electrical Energy Sold to the Power grid by MG(i) at the time (t))

i is the number of Microgrids and *t* is the time

$$FC_i = \sum_t Epm_{i,t} * P_{pm_t} - Emp_{i,t} * P_{mp_i} \quad \forall i \tag{4}$$

Where $Epm_{i,t}$ is the amount of electrical energy purchased from the power grid by microgrid i at time t. $Emp_{i,t}$ is the amount of electrical energy sold to the power grid by microgrid i at time t. Ppm_t is the price of purchasing electricity from the grid and Pmp_t is the price of selling electricity back to the grid

Along with the minimizing of the objective function, several operational and technical constraints should be followed.

1. Power-Demand Balance

The first constraint enforces the limitation of electricity balance. At every time step, the electricity generation should match the electricity demand for every microgrid in the collaborative microgrid network at every time instant.

$$E_{pm_{i,t}} + Ewt_{i,t} + Espv_{i,t} + Ebd_{i,t}.\eta_{bd} + Elm_{i,t} = E_{mp_{i,t}} + El_{i,t} + \frac{Ebc_{i,t}}{\eta_{bc}} + Eml_{i,t} \quad \forall i, \forall t \tag{5}$$

where,

$Ewt_{i,t} \longrightarrow Electricity\ generated\ by\ wind\ turbine\ in\ i^{th}\ microgrid\ at\ t^{th}\ time$

$Espv_{i,t} \longrightarrow Electricity\ generated\ by\ SPV\ in\ i^{th}\ microgrid\ at\ t^{th}\ time$

$Ebd_{i,t} \longrightarrow Battery\ discharging\ rate\ in\ i_{th}\ microgrid\ at\ t_{th}\ time$

$Ebc_{i,t} \longrightarrow Battery\ charging\ rate\ in\ i_{th}\ microgrid\ at\ t_{th}\ time$

$\eta_{bd} \longrightarrow constant\ parameter\ for\ Battery\ discharging\ efficiency$

$\eta_{bc} \longrightarrow constant\ parameter\ for\ Battery\ charging\ efficiency$

$Eml_{i,t} \rightarrow Electrical\ energy\ transmitted\ to\ integrator\ from\ i^{th}\ microgrid\ at\ t^{th}\ time$

$Elm_{i,t} \rightarrow Electrical\ energy\ transmitted\ from\ integrator\ to\ i^{th}\ microgrid\ at\ t^{th}\ time$

2. Solar PV model (Inequality Constraint)

In the past few years, solar photovoltaic panels have been widely employed as a clean power production technology. In this work, they are taken into consideration for each microgrid, and their output power limitation shall adhere to the following restriction:

$$E_{SPV\,i,t} \leq f_{PV\,i} Y_{PV\,i} sol_i \quad \forall i, \forall t \tag{6}$$

Where, $f_{PV\,i}$ is the efficiency of SPV panels for ith microgrid, $Y_{PV\,i}$ is the rated capacity or size of SPV panel, and sol_i is the amount of solar radiation at time t.

3. Wind Model (Equality Constraint)

The second most popular source of clean energy is wind power. The power output from a wind turbine depends primarily on wind speed. The wind model can be explained using the following equality constraint:

$$Ewt_{i,t} = \begin{cases} 0 & Vw_t < Vci_i, Vw_t > Vco_i \\ Pg_{t,max} \cdot \left(\frac{Vw_t - Vci_i}{Vr_i - Vci_i}\right)^3 & Vci_i \le Vw_t \le Vr_i \\ Pg_{t,max} & Vri_i \le Vw_t \le Vco_i \end{cases} \quad (7)$$

Where, $Ewt_{i,t}$ is the power output of wind turbine in i[th] Microgrid at t[th] time, $Pg_{t,max}$ is the rated power of wind turbine, Vw_t is the forecasted speed, Vr_i is the rated speed, and Vci_i is the cut in speed.

4. Battery Model

In general, battery storage devices work electrochemically to store electricity at different levels. The following are some logical and technical restrictions taken into account for these systems:

$$MBc_{i,t} + MBd_{i,t} \le 1 \quad \forall i, \forall t \quad (8)$$

$$Sb_i . \delta_{B,min} \le Eb_{i,t} \le Sb_i \quad \forall i, \forall t \quad (9)$$

$$Eb_{i,t} = Ibe + \left(Ebc_{i,t} - Ebd_{i,t}\right)\Delta t \quad \forall i, t = 1$$

$$Eb_{i,t} - Eb_{i,t-1} = \left(Ebc_{i,t} - Ebd_{i,t}\right)\Delta t \quad \forall i, \forall t \ge 2 \quad (11)$$

$$\delta_{Bc,min} . Sb_i . MBc_{i,t} \le Ebc_{i,t} \le \delta_{Bc,max} . Sb_i . MBc_{i,t} \quad \forall i, \forall t \quad (12)$$

$$\delta_{Bd,min} . Sb_i . MBd_{i,t} \le Ebd_{i,t} \le \delta_{Bd,max} . Sb_i . MBd_{i,t} \quad \forall i, \forall t \quad (13)$$

Where $MBc_{i,t}$ is the battery charging mode, $MBd_{i,t}$ is the battery discharging mode, Sb_i is the battey rating, $\delta_{B,min}$ is the coefficient of minimum limitation of battery, $Eb_{i,t}$ is the amount of stored electrical energy in battery of i[th] microgrid at t[th] time, Ibe is the initial electrical energy stored in the battery, Δt is the time interval which is 1, $\delta_{Bc,max}$ is the maximum charging limit, $\delta_{Bc,min}$ is the minimum charging limit, $\delta_{Bd,max}$ is the maximum discharging limit, $\delta_{Bd,min}$ is the minimum discharging limit.

5. Power Grid Constraints

In general, transmission lines are only capable of sending a certain amount of power to various nodes in the electrical power system. As a result, while modeling the networked microgrid problem, power grid constraints should be included. These restrictions are listed as:

$$P_{n,t}(\delta_t, V_t) + El_{n,t} = P_{n,t}^{Gen} \quad \forall n, \forall t \tag{14}$$

$$S_{n,m,t}(\delta_t, V_t) \leq S_{n,m}^{Up} \quad \forall n, \forall m, \forall t \tag{15}$$

$$V_t^{min} \leq V_{n,t} \leq V_t^{max} \quad \forall n, \forall t \tag{16}$$

$$-\pi \leq \delta_{n,t} \leq \pi \quad \forall n, \forall t \tag{17}$$

Where $P_{n,t}(\delta_t, V_t)$ is the active power injection at node n at time t, $P_{n,t}^{Gen}$ is active power production at node n at time t, $S_{n,m,t}(\delta_t, V_t)$ is the complex power flow between nodes n and m at time t, $S_{n,m}^{Up}$ is the maximum amount of power complex, $V_{n,t}$ is the voltage magnitude at node n at time t, $\delta_{n,t}$ is the phase angle at node n at time t, V_t^{min} is the minimum voltage at time t, V_t^{max} is the maximum voltage at time t.

6. Constraints for LEM

All other microgrids are considered as LEM (local energy market) for each microgrid. All microgrids share their surplus with the LEM, from where the deficit microgrid can withdraw. Microgrids can trade electricity with the power grid and with each other in a smart grid. The other microgrids are treated as LEM for each microgrid in this chapter.

The following set of operational restrictions should be satisfied for the energy trading between microgrids:

$$MElm_{i,t} + MEml_{i,t} \leq 1 \quad \forall i, \forall t \tag{18}$$

The above equation means that at a time, energy can either be transmitted from the LEM or received by the LEM

$$Elm_{i,t} \leq X.MElm_{i,t} \quad \forall i, \forall t \tag{19}$$

$$Eml_{i,t} \leq X.MEml_{i,t} \quad \forall i, \forall t \tag{20}$$

Above two equations model the electricity transaction limits

$$\sum_i Elm_{i,t} = \sum_i Eml_{i,t} \quad \forall t \tag{21}$$

The above equation is for the balance of supply and demand.

$MElm_{i,t}$ and $MEml_{i,t}$ are the modes of electrical energy transfer from LEM to MG and MG to LEM respectively. X is a big number used in Mixed Integer Programming

7.5 Analysis of Operational Cases

Three different operational cases were considered in order to test the correctness of the proposed algorithm and analyze the energy exchange control between multi-microgrids and the power grid. In the first case, the energy trading mode is turned off, and Microgrids cannot exchange energy with each other. The main grid is the only trustworthy option for microgrids to meet their electricity demands in case 1. Case 2 is set up to create the ideal conditions for microgrids to save money, with a focus on doing so while keeping the overall energy expenditure of microgrids to a minimum. In this situation, microgrids can share energy among themselves as well as with the electric grid, reducing reliance on the electric grid. The final case offered to assess the Case 2 model's scalability is Case 3. This example shows that the TE-based model may be successfully used in large-scale systems with numerous microgrids. Case 3's energy trading conditions are identical to Case 2 with the exception of the increase in the number of microgrids (from 4 to 10).

Case 1

In this case energy trading is not considered between multiple microgrids as LEM is not available and multiple microgrids do not have any connection with each other. The main grid is the only source to meet the power deficit of any particular microgrid. All Microgrids loaded with renewable energy sources trade energy individually with the primary grid.

In this case, the objective function is minimized subject to all the constraints with additional constraints to switch off the LEM mode.

The newly added constraints to turn off LEM will be as follows:

$$MElm_{i,t} = 0 \; \forall i, \forall t \tag{22}$$

$$MEml_{i,t} = 0 \; \forall i, \forall t \tag{23}$$

Therefore the mathematical formulation of the problem for this case is as follows:

$$\begin{cases} minFC_1 = \sum_i FC_{1,i} \\ s.t\ (5) to\ (23) \end{cases} \tag{24}$$

Here FC_1 is the total energy cost in Case 1; and $FC_{1,i}$ is the energy cost in Case 1 for microgrid I calculated by (4).

Case 2

In this case the microgrids can exchange energy with each other as well as with the main grid. Four Microgrids are considered for the analysis in this case. Any of the four microgrids can trade energy with the other three microgrids and the power grid. Transactive energy management is used to regulate the energy exchange, and it can reduce the microgrids' overall energy costs while also saving costs due to transmission losses. For this case, the problem formulation is as follows:

$$\begin{cases} minFC_2 = \sum_i FC_{2,i} \\ s.t\ (5) to\ (21) \\ with\ the\ following\ additional\ constraint: \\ FC_{2,i} \leq FC_{1,i}\ \forall i \end{cases} \quad (25)$$

Here FC_2 is the total energy cost in case 2 and $FC_{2,i}$ is the energy cost in case 2 for microgrid I calculated by (4).

Case 3

This case is considered just to test the scalability of case 2. With the same formulation, in this case, ten Microgrids are considered for the analysis instead of four.

7.6 Results and Discussions

Each of the microgrids considered for analysis in this study is equipped with a wind turbine of 1.5 kW capacity, solar PV, battery storage, and a load of varied capacity, as depicted in Figure 7-1. It is observed that with the increase in the number of collaborative microgrids in the network, the transactive cost of energy exchange with the grid decreases. *Table 7-1* and *Table 7-2* prove the efficacy of the proposed algorithm. The overall cost of energy exchange is reduced from case 1 to case 2 to case 3. This demonstrates that the proposed transactive energy exchange model can successfully be implemented on a large-scale multi-microgrid system as well.

Figure 7-7 presents the amount of electricity that Microgrids had to purchase from the main grid to satisfy their power demands in case 1 and case 2. It can be observed that the amount of electricity purchased from the main grid also drops from case 1 to case 2. This indicates that due to transactive energy exchange between multiple Microgrids, the dependency on the main grid is also reduces.

Table 7-1 Comparision of simulation results in case 1(no TEM) and case 2 (TEM between 4 microgrids)

Microgrid No.	Cost of Energy Exchange in Case 1	Cost of Energy Exchange in Case 2	Amount of cost saving	Percentage of cost saving
1	573.13	423.02	150.11	26.191
2	575.88	510.48	65.394	11.356
3	577.71	415.33	162.38	28.108
4	578.12	422.86	155.26	26.856
Total	Total Energy cost in Case 1	Total Energy cost in Case 2	Total amount of cost saving	Total percentage of cost saving
	2304.8	1771.7	533.14	23.131

In addition, the energy transferred to all the microgrid components participating in TEM is presented in Figure 7-8. The contribution of wind turbines, solar photovoltaics, LEM, and the main grid in meeting the load demand in case 2 and case 3 can be seen in Figure 7-8. In LEM, the energy exchange of microgrids minimizes reliance on the primary grid, particularly during peak load. Microgrids purchase electricity from the power grid at times when the energy price is low in order to reduce the energy cost as peak-load times have high electricity prices. Additionally, microgrids effectively sell energy to the main grid at peak demand, when the cost of energy is at its highest, by utilizing the vast capacity of wind energy for electricity production. The energy exchange

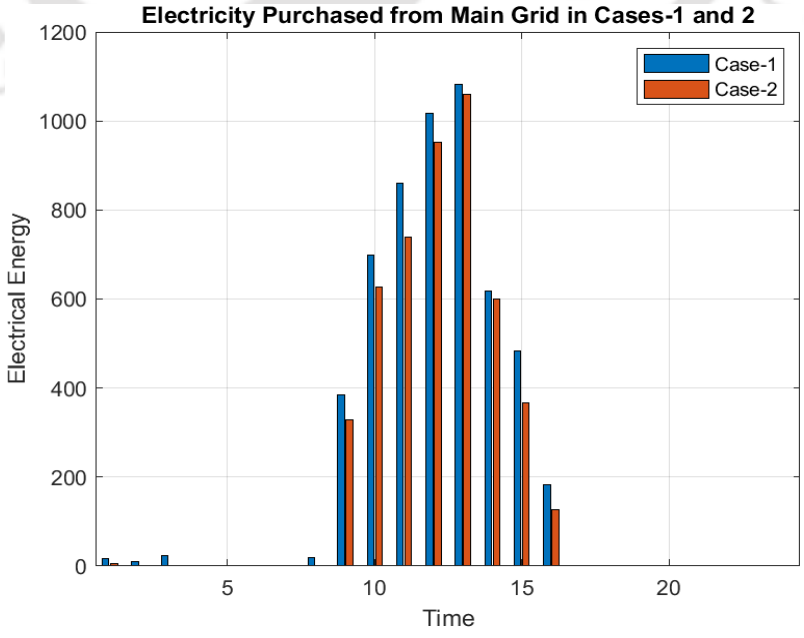

Figure 7-7 Comparison of electricity purchased from main grid in case 1 and case 2

operation of microgrids based on the TE paradigm maximizes the profit. However, due to the decreased output of wind turbines at night (hours 21 to 24), less energy is sold to the main grid, and more energy must be obtained from the power grid to meet demand.

The potential for free energy trading between microgrids is efficiently leveraged to meet demand during peak load periods when electricity is costlier. All microgrids in this arrangement make an effort to trade surplus energy with the power system when the price is high and to buy energy from the grid jointly when the price is low. Additionally, the potential of clean energy sources is also utilized, particularly during peak load periods, not only to meet a substantial portion of demand but also to give microgrids an additional option to sell their excess energy in order to lower their energy costs.

It can be observed from Figure 7-8 (b) that in case 2, the local energy market has the highest contribution in meeting electrical loads, followed by SPV, energy purchased from the grid, and wind turbines, respectively. This ensures that the size of SPV and wind turbine installation will also decrease as most of the energy deficit in a microgrid is being met by the resources of the neighboring microgrids.

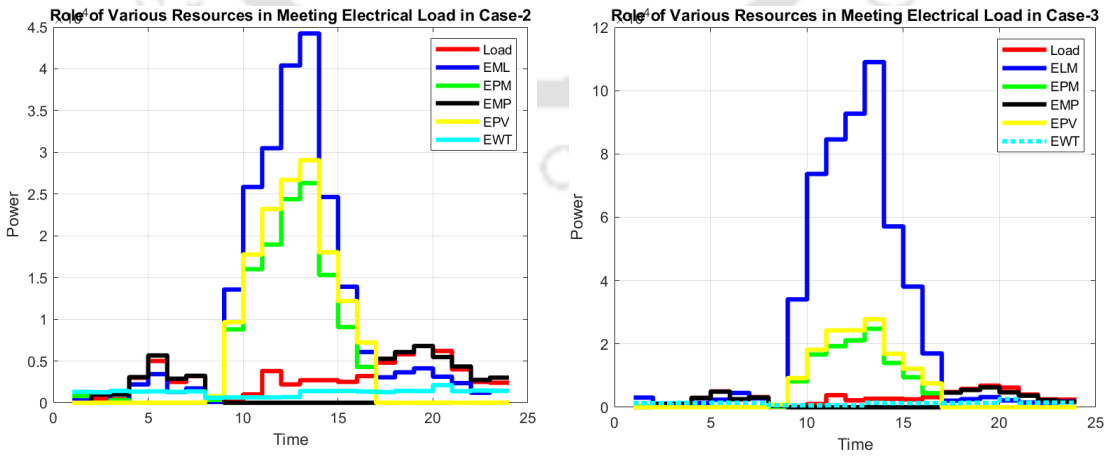

(a) *(b)*

Figure 7-8 Electricity sharing between multiple microgrid components participating in TEM in case 2 and case 3

Table 7-2 Comparision of simulation results in case 1(no TEM) and case 3 (TEM between 10 microgrids)

Microgrid No.	Cost of Energy Exchange in Case 1	Cost of Energy Exchange in Case 2	Amount of cost saving	Percentage of cost saving
1	557.73	411.65	146.08	26.191
2	555.24	489.57	65.678	11.829
3	555.46	403.07	152.4	27.436
4	556.96	453.58	103.38	18.561
5	555.26	390.12	165.14	29.741
6	556.96	453.58	103.38	18.561
7	557.18	382.39	174.79	31.37
8	558.6	437.2	121.4	21.733
9	556.61	374.67	181.95	32.689
10	558.19	410.75	147.44	26.414
Total	Total Energy cost in Case 1	Total Energy cost in Case3	Total amount of cost saving	Total percentage of cost saving
	5568.2	4217.8	1350.4	24.251

On comparing Figure 7-8 (a) and Figure 7-8 (b), it can be seen that the role of local energy market in meeting the local demands of a microgrid participating in the collaborative microgrid network further increases with increase in the number of microgrids participating in the collaborative network. In case 2, only 4 microgrids are contributing to the transactive energy management, hence the peak power contributed by LEM is 4.5kW. Whereas, in case 3, 10 mcrogrids are contributing to the transactive energy management, increasing the peak power contributed by the LEM. In case 3, LEM contributes 11kW peak power. This also shows that the size of SPV, wind turbine, and

battery installations will further decrease with an increase in the number of collaborative microgrids.

7.7 Conclusion

In this study, ten microgrids are taken into account for transactive energy technology analysis in the network, sharing energy with the three suggested operation instances. Since each microgrid exclusively uses RESs to generate electricity, there are no environmental issues with their energy production. The outcomes of the three simulations demonstrate that all microgrids can see cost savings when using the transactive energy architecture. The study proves that transactive energy structure-based energy trading between Microgrids enables them to fulfill their energy needs (especially during peak load hours) by selling energy to the main grid and maximizing their profits. An accurate evaluation of the proposed model in Case 3 highlights its scalability characteristic and shows that it can be successfully deployed in the power grid with many microgrids while taking the profitability of each microgrid into account. As a result, TE technology is advised for microgrids with significant RES penetration in order to manage and control the best possible energy exchange in the power grid. When microgrids join the energy trading market, they save varying amounts of money. The amount of cost savings realized varies for each microgrid, and the participation rate of microgrids is not taken into account while calculating their profit. In light of this, new operational models can be suggested that take into account the degree to which microgrids participate in market interactions, or alternatively, other models can be focused on proposing new mechanisms for delivering the same percentage of cost savings for all of the participating microgrids in the market environment. On the other hand, a number of case studies can be used to evaluate security and dependability issues with the presented models. Additionally, the TE models may thoroughly study the loss allocation problem as one crucial topic to offer better conditions for obtaining cost savings for all microgrids. Future works will examine these subjects.

Chapter 8

Conclusion and Future Work

Sustainable development goals set by the united nations are pushing researchers and economies worldwide toward finding innovative ways to increase renewable penetration in total power production. Oil and gas fields are major contributors to increasing carbon emissions and global warming as they flare off the surplus natural gas generation into the atmosphere. The presented thesis is an attempt to suggest innovative ways to minimize gas flaring and utilize the waste flare gas to produce power.

- The first objective of this thesis was to determine an optimal gas microturbine-based power generation and distribution infrastructure. In this chapter, a newly developed optimization model is implemented successfully to estimate the capacity of the power generator and the best network to distribute power while minimizing transmission losses. The formulated model assures full utilization of available fuel to satisfy power demand and sell remaining power to the grid, if any. Using this formulation, a higher capacity microturbine will be preferred in the design only when demand is higher, and fuel availability exceeds corresponding power capacity. This is important to keep a check on the installation cost of the system as the price of a higher capacity microturbine will also be higher. Therefore the number and capacity of microturbines should be optimized to satisfy local power demands while utilizing all available flare gas, and the power generation – distribution network should be chosen to minimize transmission losses and minimize dependency on the primary grid to meet local demands. The analysis proved that the efficiency and cost of the technology affect the gas microturbine capacity selection. In the future advanced optimization techniques can be used to determine an optimal microturbine-based power generation-distribution architecture.

- To level up the renewable production and utilize all available resource in the area to generate power, solar photovoltaics,battery energy storage, wind turbines were also included along with gas microturbines and their respective controllers in the

next stage to form a Hybrid Renewable Energy System (HRES) or microgrid system. In any oil and gas field, there are hundreds of gas flare locations. Not all of the flaring sites support the installation of any combination of HRES. Therefore the second objective was to develop a novel multi-criteria decision-making algorithm for site selection in oil and gas fields. Normally the oil and gas well-based data is highly ambiguous because of which generic MCDM approaches are not suitable for oil and gas fields. Therefore a combination of the Analytical Hierarchy Process (AHP) for weight determination and TOPSIS for similarity to the ideal solution was proposed for site selection for HRES installation in oil and gas fields. The integrated TOPSIS-AHP approach was found to be a more powerful tool for site-suitability purposes than TOPSIS with equal or random weights. The results suggest that Lakwa GGS 5 is the most appropriate choice for installing all combinations of hybrid energy systems that use waste flare gas to generate power out of the analyzed locations. Whereas Geleky GGS 2 is a superior choice amongst sites having a distance of more than two kilometers from the river.

- In order to include all locally available renewable energy sources in the oil and gas well-based microgrid power management system, it is important to predict the renewable power generation accurately. Therefore the third objective is to come up with a suitable machine learning model for accurate prediction of renewable energy generation, which can help the controllers in strategizing an optimal dispatch of various controllable DERs. In order to achieve this, four distinct machine learning approaches, namely- XGBoost, AdaBoost, Multiple Linear Regression, and gradient boost, were used to predict renewable energy generation. It was observed that gradient boost has a distinct advantage over the regression model with greater accuracy and high robustness when the dataset is huge. It was also observed that XG boost is much better than GBR in terms of computational speed and performance. Also, XG boost gave the best accuracy for solar energy prediction. In the case of wind power prediction, the Ada boost algorithm resulted in maximum accuracy. The linear regression model gave the best performance accuracy when the number of data points was considerably less. In the future, more advanced machine learning models can be developed by more rigorous training using a broader dataset.

- The next objective is to systematize a framework to suggest an optimal size and design of a hybrid energy system. Therefore in the sixth chapter, a novel dispatch algorithm is developed to simulate the real-time operation of the HES to suit the requirements of the oil and gas fields. The techno-commercial and environmental viability of six HESs were analyzed for two different gas flaring sites. The chapter concluded that a system comprising two 30 kW gas microturbines, a 2000 kW solar PV panel set, and a grid connection could save 35.52% net present cost and reduce gas flaring by up to 50%.
- Finally, when there are multiple microgrids in the vicinity of each other, a collaboration between them for sharing power and energy through a transactive approach leads to a reduction in the installation and operational cost of the multi-microgrid network. In the seventh chapter, an algorithm for transactive energy management via the local energy market in a multi-microgrid network was developed. Results indicate cost savings with an increase in the number of microgrids participating in the multi-microgrid network. When there were four microgrids in the collaborative microgrid network, the cost savings were 23.1%, and when there were ten microgrids, the cost savings increased to 30.2%. The dependency on the main grid is also reduced with the multi-microgrid collaboration. In the future, machine learning models can be explored to automate multi-microgrid power and energy trading. Metaheuristic optimization techniques can also be explored for this purpose.

With this research, a one-stop solution to (a) finding suitable location for HRES installation, (b) constituents of the HRES with their capacity ratings, (c) dispatch algorithm to suit oil and gas field-based HRES, and (d) multi-microgrid collaboration has been achieved. The presented research resulted in three journal and three conference publications of high repute. This thesis proposes a complete solution for converting the power-consuming and emission-causing oil and gas fields to power-generating - reduced emission systems. The proposed solution can be a role model for carbon transition and achieving the Intended Nationally Determined Contributions (INDC) set by India to meet the Sustainable Development Goals (SDG). The presented thesis is one of its kind, as similar algorithmic solutions can not be found in the literature. However, due to time and budget constraints, the on-ground implementation of the proposed research could not take place. The practical

implementation of the proposed algorithms might require including more parameters or tweaking the models to suit the project requirements. Microgrid power flow data points can become meaningful for further expansion of the grid by the use of data analytics and artificial intelligence. Microgrids ensure decentralization of the grid. Therefore, MGs serve as the first choice for electrification of the local communities. For remote locations, transmission connections can be very expensive. Though this is a simulative study, the findings of this study can aid the on-ground implementation of the work and contribute in achieving India's goals of electrifying every household and net zero carbon emissions.

References

[1] D. Das, P. Kalita, and O. Roy, “Flat plate hybrid photovoltaic- thermal (PV/T) system: A review on design and development,” *Renew. Sustain. Energy Rev.*, vol. 84, no. February, pp. 111–130, 2018.

[2] “Oghenemavwe, L.E., & Awoyemi, L.O. (2020). Cardiothoracic Ratio of Nigerians in Gas Flaring Communities. American Journal of Medicine and Medical Sciences, 10, 279-283.”

[3] C. D. Elvidge, M. Zhizhin, K. Baugh, F. Hsu, and T. Ghosh, “Methods for Global Survey of Natural Gas Flaring from Visible Infrared Imaging Radiometer Suite Data,” 2015.

[4] U.S. Energy Information Administration (EIA), “Delivery and Storage of Natural Gas,” 2014.

[5] “Gas Collection/ Group Gathering Stations,” 2018. .

[6] R. D. Bott, “Flaring: Questions + Answers.”

[7] C. S. Office, “Central statistics office,” 2017.

[8] O. M. Bamigbola, M. M. Ali, and M. O. Oke, “Mathematical modeling of electric power flow and the minimization of power losses on transmission lines,” *Appl. Math. Comput.*, vol. 241, pp. 214–221, 2014.

[9] K. Sadovskaia, D. Bogdanov, S. Honkapuro, and C. Breyer, “Power transmission and distribution losses – A model based on available empirical data and future trends for all countries globally,” *Int. J. Electr. Power Energy Syst.*, vol. 107, no. November 2018, pp. 98–109, 2019.

[10] M. Badr and S. A. L. I. Ahmed, “24 st International Conference on Electricity Distribution REDUCING HARMONIC DISTORTION AND CORRECTING POWER FACTOR IN DISTRIBUTION SYSTEMS 24 st International Conference on Electricity Distribution Stockholm , 10-13 June 2013,” no. June, pp. 10–13, 2013.

[11] R. R. Borgohain and S. Hazarika, “A Practical Approach for Distribution Loss

Reduction in Assam using Network Re-conductoring Method," vol. 3, no. 9, pp. 392–397, 2014.

[12] M. C. Anumaka, "Analysis of Technical Losses in Electrical Power System (Nigerian 330Kv Network As a Case Study)," *Int. J. Res. Rev. Appl. Sci.*, vol. 12, no. August, pp. 320–327, 2012.

[13] I. Kitta, S. Manjang, I. R. Sahali, and F. Maricar, "Insertion of 275 kV Transmission Line for Improving the Voltage Profile and Efficiency of Electrical Power System," *IOP Conf. Ser. Mater. Sci. Eng.*, vol. 676, no. 1, 2019.

[14] Femi-Jemilohun Oladunni Juliet, "Wireless Power Transmission Approach for Electricity Leakages Minimization in the Nigeria Power Grid," *Int. J. Eng. Res.*, vol. V8, no. 05, pp. 103–108, 2019.

[15] M. D. A. Al-falahi, S. D. G. Jayasinghe, and H. Enshaei, "A review on recent size optimization methodologies for standalone solar and wind hybrid renewable energy system," *Energy Convers. Manag.*, vol. 143, pp. 252–274, 2017.

[16] REN21, *Renewable 2018 global status report*. 2018.

[17] H. Ritchie, "Fossil Fuels," *OurworldInData.org*, 2017. [Online]. Available: https://ourworldindata.org/fossil-fuels. [Accessed: 11-Sep-2020].

[18] A. Kumar, A. R. Singh, Y. Deng, X. He, P. Kumar, and R. C. Bansal, "Multiyear load growth based techno-financial evaluation of a microgrid for an academic institution," *IEEE Access*, vol. 6, pp. 37533–37555, 2018.

[19] H. Ritchie, "Energy production and changing energy sources: Our world in data," 2017. [Online]. Available: ourworldindata.org. [Accessed: 11-Sep-2020].

[20] Allotrope Partners, "Microgrid Market Analysis & Investment Opportunities RURAL ELECTRIFICATION : FROM AID TO MARKET OPPORTUNITY," *Microgrid Invest. Accel.*, vol. 2.1, pp. 1–45, 2017.

[21] A. H. Al-badi, R. Ahshan, N. Hosseinzadeh, and R. Ghorbani, "Survey of Smart Grid Concepts and Technological Demonstrations Worldwide Emphasizing on the Oman Perspective."

[22] D. Bishnoi and H. Chaturvedi, "A Review on Emerging Trends in Smart Grid

Energy Management Systems," *Int. J. Renew. Energy Res.*, vol. 11, no. 3, September 2021, 2021.

[23] copenhaegen accord, "CO2 emission reduction targets for India," 2009. .

[24] "United Nations Framework Convention on Climate Change (UNFCCC). COP21, Paris agreement," 2015. [Online]. Available: http://www.cop21.gouv.fr/en.

[25] Census of India, "India Population Tables," *October*, no. March, 2011.

[26] "IEA (2019), 'World Energy Statistics 2019', IEA, Paris," 2019. [Online]. Available: https://www.iea.org/reports/world-energy-statistics-2019.

[27] world bank, "Global Gas Flaring Tracker Data," *The World Bank group IBRD - IDA*, 2022. [Online]. Available: https://www.ggfrdata.org/.

[28] C. Marnay *et al.*, "Microgrid evolution roadmap," *Proc. - 2015 Int. Symp. Smart Electr. Distrib. Syst. Technol. EDST 2015*, pp. 139–144, 2015.

[29] A. Bidram, F. L. Lewis, and A. Davoudi, "Distributed Control Systems for Small-Scale Power Networks: Using Multiagent Cooperative Control Theory," *IEEE Control Syst. Mag.*, vol. 34, no. 6, pp. 56–77, 2014.

[30] F. Magazine *et al.*, "Fallowfield Gas Processing Plant," 2011.

[31] M. W. Davis, "Mini gas turbines and high speed generators - A preferred choice for serving large commercial customers and microgrids; Part I: Generating system," *Proc. IEEE Power Eng. Soc. Transm. Distrib. Conf.*, vol. 2, no. SUMMER, pp. 669–676, 2002.

[32] A. Kumar, A. R. Singh, Y. Deng, X. He, P. Kumar, and R. C. Bansal, "A Novel Methodological Framework for the Design of Sustainable Rural Microgrid for Developing Nations," *IEEE Access*, vol. 6, pp. 24925–24951, 2018.

[33] M. A. Nazari, A. Aslani, and R. Ghasempour, "Analysis of solar farm site selection based on TOPSIS approach," *Int. J. Soc. Ecol. Sustain. Dev.*, vol. 9, no. 1, pp. 12–25, 2018.

[34] M. Azizkhani, A. Vakili, Y. Noorollahi, and F. Naseri, "Potential survey of photovoltaic power plants using Analytical Hierarchy Process (AHP) method in Iran," *Renew. Sustain. Energy Rev.*, vol. 75, no. May 2016, pp. 1198–1206, 2017.

[35] S. Sindhu, V. Nehra, and S. Luthra, "Investigation of feasibility study of solar farms deployment using hybrid AHP-TOPSIS analysis: Case study of India," *Renew. Sustain. Energy Rev.*, vol. 73, no. January 2017, pp. 496–511, 2017.

[36] W. Yunna and S. Geng, "Multi-criteria decision making on selection of solar-wind hybrid power station location: A case of China," *Energy Convers. Manag.*, vol. 81, pp. 527–533, 2014.

[37] D. Jun, F. Tian-Tian, Y. Yi-Sheng, and M. Yu, "Macro-site selection of wind/solar hybrid power station based on ELECTRE-II," *Renew. Sustain. Energy Rev.*, vol. 35, pp. 194–204, 2014.

[38] I. Siksnelyte-Butkiene, E. K. Zavadskas, and D. Streimikiene, "Multi-criteria decision-making (MCDM) for the assessment of renewable energy technologies in a household: A review," *Energies*, vol. 13, no. 5, 2020.

[39] M. Ramezanzade, J. Saebi, H. Karimi, and A. Mostafaeipour, "A new hybrid decision-making framework to rank power supply systems for government organizations: A real case study," *Sustain. Energy Technol. Assessments*, vol. 41, no. May, p. 100779, 2020.

[40] A. T. D. Perera, R. A. Attalage, K. K. C. K. Perera, and V. P. C. Dassanayake, "A hybrid tool to combine multi-objective optimization and multi-criterion decision making in designing standalone hybrid energy systems," *Appl. Energy*, vol. 107, pp. 412–425, 2013.

[41] J. Sliogeriene, Z. Turskis, and D. Streimikiene, "Analysis and choice of energy generation technologies: The multiple criteria assessment on the case study of Lithuania," *Energy Procedia*, vol. 32, pp. 11–20, 2013.

[42] V. Çoban, "Solar energy plant project selection with AHP decision-making method based on hesitant fuzzy linguistic evaluation," *Complex Intell. Syst.*, vol. 6, no. 3, pp. 507–529, 2020.

[43] O. Taylan, R. Alamoudi, M. Kabli, A. Aljifri, F. Ramzi, and E. Herrera-Viedma, "Assessment of energy systems using extended fuzzy AHP, fuzzy VIKOR, and TOPSIS approaches to manage non-cooperative opinions," *Sustain.*, vol. 12, no. 7, 2020.

[44] J. Zhou, Y. Wu, C. Wu, F. He, B. Zhang, and F. Liu, “A geographical information system based multi-criteria decision-making approach for location analysis and evaluation of urban photovoltaic charging station: A case study in Beijing,” *Energy Convers. Manag.*, vol. 205, no. December 2019, p. 112340, 2020.

[45] M. Tahri, M. Hakdaoui, and M. Maanan, “The evaluation of solar farm locations applying Geographic Information System and Multi-Criteria Decision-Making methods: Case study in southern Morocco,” *Renew. Sustain. Energy Rev.*, vol. 51, pp. 1354–1362, 2015.

[46] A. Alami Merrouni, F. Elwali Elalaoui, A. Mezrhab, A. Mezrhab, and A. Ghennioui, “Large scale PV sites selection by combining GIS and Analytical Hierarchy Process. Case study: Eastern Morocco,” *Renew. Energy*, vol. 119, pp. 863–873, 2018.

[47] M. Mokarram, M. J. Mokarram, M. Gitizadeh, T. Niknam, and J. Aghaei, “A novel optimal placing of solar farms utilizing multi-criteria decision-making (MCDA) and feature selection,” *J. Clean. Prod.*, vol. 261, p. 121098, 2020.

[48] Y. Wu, B. Zhang, C. Xu, and L. Li, “Site selection decision framework using fuzzy ANP-VIKOR for large commercial rooftop PV system based on sustainability perspective,” *Sustain. Cities Soc.*, vol. 40, no. January, pp. 454–470, 2018.

[49] M. Taoufik and A. Fekri, “GIS-based multi-criteria analysis of offshore wind farm development in Morocco,” *Energy Convers. Manag. X*, vol. 11, p. 100103, 2021.

[50] A. U. Rehman, M. H. Abidi, U. Umer, and Y. S. Usmani, “Multi-criteria decision-making approach for selecting wind energy power plant locations,” *Sustain.*, vol. 11, no. 21, 2019.

[51] J. Lai, Y. Chang, C. Chen, and P. Pai, “applied sciences A Survey of Machine Learning Models in Renewable Energy Predictions,” 2020.

[52] K. Ronay, D. Bica, and C. Munteanu, “Micro-grid Development Using Artificial Neural Network for Renewable Energy Forecast and System Control,” *Procedia Eng.*, vol. 181, pp. 818–823, 2017.

[53] D. B. De Alencar, C. De Mattos Affonso, R. C. L. De Oliveira, J. L. M. Rodríguez, J. C. Leite, and J. C. R. Filho, “Different Models for Forecasting Wind Power

Generation: Case Study," *Energies*, vol. 10, no. 12, 2017.

[54] A. M. Foley, P. G. Leahy, A. Marvuglia, and E. J. McKeogh, "Current methods and advances in forecasting of wind power generation," *Renew. Energy*, vol. 37, no. 1, pp. 1–8, 2012.

[55] J. Liu, W. Fang, X. Zhang, and C. Yang, "An Improved Photovoltaic Power Forecasting Model With the Assistance of Aerosol Index Data," *IEEE Trans. Sustain. Energy*, vol. 6, no. 2, pp. 434–442, 2015.

[56] M. Trigo-González *et al.*, "Hourly PV production estimation by means of an exportable multiple linear regression model," *Renew. Energy*, vol. 135, pp. 303–312, May 2019.

[57] E. Nikitidou, A. Zagouras, V. Salamalikis, and A. Kazantzidis, "Short-term cloudiness forecasting for solar energy purposes in Greece, based on satellite-derived information," *Meteorol. Atmos. Phys.*, vol. 131, no. 2, pp. 175–182, 2019.

[58] T. Watanabe, Y. Oishi, and T. Y. Nakajima, "Characterization of surface solar-irradiance variability using cloud properties based on satellite observations," *Sol. Energy*, vol. 140, pp. 83–92, 2016.

[59] L. Feng, A. Lin, L. Wang, W. Qin, and W. Gong, "Evaluation of sunshine-based models for predicting diffuse solar radiation in China," *Renew. Sustain. Energy Rev.*, vol. 94, no. June, pp. 168–182, 2018.

[60] J. Fan, B. Chen, L. Wu, F. Zhang, X. Lu, and Y. Xiang, "Evaluation and development of temperature-based empirical models for estimating daily global solar radiation in humid regions," *Energy*, vol. 144, pp. 903–914, 2018.

[61] M. Blal *et al.*, "A prediction models for estimating global solar radiation and evaluation meteorological effect on solar radiation potential under several weather conditions at the surface of Adrar environment," *Meas. J. Int. Meas. Confed.*, vol. 152, p. 107348, 2020.

[62] J. I. Prieto and D. García, "Global solar radiation models: A critical review from the point of view of homogeneity and case study," *Renew. Sustain. Energy Rev.*, vol. 155, p. 111856, 2022.

[63] M. S. Okundamiya, J. O. Emagbetere, and E. A. Ogujor, "Evaluation of various

global solar radiation models for Nigeria," *Int. J. Green Energy*, vol. 13, no. 5, pp. 505–512, 2016.

[64] Y. Feng, N. Cui, Q. Zhang, L. Zhao, and D. Gong, "Comparison of artificial intelligence and empirical models for estimation of daily diffuse solar radiation in North China Plain," *Int. J. Hydrogen Energy*, vol. 42, no. 21, pp. 14418–14428, 2017.

[65] A. Khosravi, L. Machado, and R. O. Nunes, "Time-series prediction of wind speed using machine learning algorithms: A case study Osorio wind farm, Brazil," *Appl. Energy*, vol. 224, no. April, pp. 550–566, 2018.

[66] P. Kumari and D. Toshniwal, "Extreme gradient boosting and deep neural network based ensemble learning approach to forecast hourly solar irradiance," *J. Clean. Prod.*, vol. 279, p. 123285, Jan. 2021.

[67] S. Aslam, H. Herodotou, N. Ayub, and S. M. Mohsin, "Deep learning based techniques to enhance the performance of microgrids: A review," *Proc. - 2019 Int. Conf. Front. Inf. Technol. FIT 2019*, pp. 116–121, 2019.

[68] J. Fan *et al.*, "Comparison of Support Vector Machine and Extreme Gradient Boosting for predicting daily global solar radiation using temperature and precipitation in humid subtropical climates: A case study in China," *Energy Convers. Manag.*, vol. 164, no. March, pp. 102–111, 2018.

[69] E. Ogliari, A. Dolara, G. Manzolini, and S. Leva, "Physical and hybrid methods comparison for the day ahead PV output power forecast," *Renew. Energy*, vol. 113, pp. 11–21, 2017.

[70] R. Meenal and A. I. Selvakumar, "Assessment of SVM, empirical and ANN based solar radiation prediction models with most influencing input parameters," *Renew. Energy*, vol. 121, pp. 324–343, 2018.

[71] C. Yang and L. Xie, "A novel ARX-based multi-scale spatio-temporal solar power forecast model," *2012 North Am. Power Symp. NAPS 2012*, 2012.

[72] Q. Mo and F. Liu, "Modeling and optimization for distributed microgrid based on Modelica language," *Appl. Energy*, vol. 279, no. May, p. 115766, 2020.

[73] S. Sanajaoba Singh and E. Fernandez, "Modeling, size optimization and sensitivity

analysis of a remote hybrid renewable energy system," *Energy*, vol. 143, pp. 719–731, 2018.

[74] F. Fodhil, A. Hamidat, and O. Nadjemi, "Potential, optimization and sensitivity analysis of photovoltaic-diesel-battery hybrid energy system for rural electrification in Algeria," *Energy*, vol. 169, pp. 613–624, 2019.

[75] A. Yahiaoui, K. Benmansour, and M. Tadjine, "Control, analysis and optimization of hybrid PV-Diesel-Battery systems for isolated rural city in Algeria," *Sol. Energy*, vol. 137, pp. 1–10, 2016.

[76] E. Ayodele, S. Misra, R. Damasevicius, and R. Maskeliunas, "Hybrid microgrid for microfinance institutions in rural areas – A field demonstration in West Africa," *Sustain. Energy Technol. Assessments*, vol. 35, no. June, pp. 89–97, 2019.

[77] R. Sen and S. C. Bhattacharyya, "Off-grid electricity generation with renewable energy technologies inIndia: An application of HOMER," *Renew. Energy*, vol. 62, pp. 388–398, 2014.

[78] W. Astatike and P. Chandrasekar, "Design and performance analysis of hybrid micro-grid power supply system using HOMER software for rural village in adama area, Ethiopia," *Int. J. Sci. Technol. Res.*, vol. 8, no. 6, pp. 267–275, 2019.

[79] S. Srinivasa Murthy, P. Dutta, B. S. Rao, and R. Sharma, "Performance analysis of a stand-alone polygeneration microgrid," *Therm. Sci. Eng. Prog.*, vol. 19, no. January, p. 100623, 2020.

[80] M. K. Shahzad, A. Zahid, T. Rashid, M. A. Rehan, M. Ali, and M. Ahmad, "Techno-economic feasibility analysis of a solar-biomass off grid system for the electrification of remote rural areas in Pakistan using HOMER software," *Renew. Energy*, vol. 106, pp. 264–273, 2017.

[81] H. Rezk and G. M. Dousoky, "Technical and economic analysis of different configurations of stand-alone hybrid renewable power systems – A case study," *Renew. Sustain. Energy Rev.*, vol. 62, pp. 941–953, 2016.

[82] A. López-González, M. Ranaboldo, B. Domenech, and L. Ferrer-Martí, "Evaluation of small wind turbines for rural electrification: Case studies from extreme climatic conditions in Venezuela," *Energy*, vol. 209, 2020.

[83] S. A. Shezan *et al.*, "Performance analysis of an off-grid wind-PV (photovoltaic)-diesel-battery hybrid energy system feasible for remote areas," *J. Clean. Prod.*, vol. 125, pp. 121–132, 2016.

[84] G. Singh, P. Baredar, A. Singh, and D. Kurup, "Optimal sizing and location of PV, wind and battery storage for electrification to an island: A case study of Kavaratti, Lakshadweep," *J. Energy Storage*, vol. 12, pp. 78–86, 2017.

[85] F. Fazelpour, N. Soltani, and M. A. Rosen, "Feasibility of satisfying electrical energy needs with hybrid systems for a medium-size hotel on Kish Island , Iran," *Energy*, vol. 73, pp. 856–865, 2014.

[86] S. Bhakta and V. Mukherjee, "Performance indices evaluation and techno economic analysis of photovoltaic power plant for the application of isolated India's island," *Sustain. Energy Technol. Assessments*, vol. 20, pp. 9–24, 2017.

[87] C. T. Tsai, T. M. Beza, W. Bin Wu, and C. C. Kuo, "Optimal configuration with capacity analysis of a hybrid renewable energy and storage system for an island application," *Energies*, vol. 13, no. 1, 2019.

[88] M. R. Basir Khan, R. Jidin, J. Pasupuleti, and S. A. Shaaya, "Optimal combination of solar, wind, micro-hydro and diesel systems based on actual seasonal load profiles for a resort island in the South China Sea," *Energy*, vol. 82, pp. 80–97, 2015.

[89] C. T. Tsai, T. M. Beza, E. M. Molla, and C. C. Kuo, "Analysis and Sizing of Mini-Grid Hybrid Renewable Energy System for Islands," *IEEE Access*, vol. 8, pp. 70013–70029, 2020.

[90] A. Kumar, A. R. Singh, Y. Deng, X. He, P. Kumar, and R. C. Bansal, "Multiyear load growth based techno-financial evaluation of a microgrid for an academic institution," *IEEE Access*, vol. 6, no. July, pp. 37533–37555, 2018.

[91] T. Sarkar, A. Bhattacharjee, H. Samanta, K. Bhattacharya, and H. Saha, "Optimal design and implementation of solar PV-wind-biogas-VRFB storage integrated smart hybrid microgrid for ensuring zero loss of power supply probability," *Energy Convers. Manag.*, vol. 191, no. April, pp. 102–118, 2019.

[92] S. Bhattacharjee and S. Acharya, "PV-wind hybrid power option for a low wind

topography," *Energy Convers. Manag.*, vol. 89, pp. 942–954, 2015.

[93] N. Saiprasad, A. Kalam, and A. Zayegh, *Optimum sizing and economic analysis of renewable energy system integration into a micro-grid for an academic institution—a case study*, vol. 749. Springer International Publishing, 2019.

[94] C. Ghenai and M. Bettayeb, "Modelling and performance analysis of a stand-alone hybrid solar PV/Fuel Cell/Diesel Generator power system for university building," *Energy*, vol. 171, pp. 180–189, 2019.

[95] J. Liu, M. Wang, J. Peng, X. Chen, S. Cao, and H. Yang, "Techno-economic design optimization of hybrid renewable energy applications for high-rise residential buildings," *Energy Convers. Manag.*, vol. 213, no. March, p. 112868, 2020.

[96] E. A. Al-Ammar *et al.*, "Residential Community Load Management Based on Optimal Design of Standalone HRES with Model Predictive Control," *IEEE Access*, vol. 8, pp. 12542–12572, 2020.

[97] A. Tiwary, S. Spasova, and I. D. Williams, "A community-scale hybrid energy system integrating biomass for localised solid waste and renewable energy solution: Evaluations in UK and Bulgaria," *Renew. Energy*, vol. 139, pp. 960–967, 2019.

[98] M. A. V. Rad, R. Ghasempour, P. Rahdan, S. Mousavi, and M. Arastounia, "Techno-economic analysis of a hybrid power system based on the cost-effective hydrogen production method for rural electrification, a case study in Iran," *Energy*, vol. 190, p. 116421, 2020.

[99] R. Velo, L. Osorio, M. D. Fernández, and M. R. Rodríguez, "An economic analysis of a stand-alone and grid-connected cattle farm," *Renew. Sustain. Energy Rev.*, vol. 39, pp. 883–890, 2014.

[100] H. Maammeur, A. Hamidat, L. Loukarfi, M. Missoum, K. Abdeladim, and T. Nacer, "Performance investigation of grid-connected PV systems for family farms: Case study of North-West of Algeria," *Renew. Sustain. Energy Rev.*, vol. 78, no. March, pp. 1208–1220, 2017.

[101] E. N. Nyeche and E. O. Diemuodeke, "Modelling and optimisation of a hybrid

PV-wind turbine-pumped hydro storage energy system for mini-grid application in coastline communities," *J. Clean. Prod.*, vol. 250, p. 119578, 2020.

[102] S. Sukumar, H. Mokhlis, S. Mekhilef, K. Naidu, and M. Karimi, "Mix-mode energy management strategy and battery sizing for economic operation of grid-tied microgrid," *Energy*, vol. 118, pp. 1322–1333, 2017.

[103] G. Comodi *et al.*, "Multi-apartment residential microgrid with electrical and thermal storage devices: Experimental analysis and simulation of energy management strategies," *Appl. Energy*, vol. 137, pp. 854–866, 2015.

[104] D. Tenfen and E. C. Finardi, "A mixed integer linear programming model for the energy management problem of microgrids," *Electr. Power Syst. Res.*, vol. 122, pp. 19–28, 2015.

[105] B. V. Solanki, K. Bhattacharya, and C. A. Canizares, "A Sustainable Energy Management System for Isolated Microgrids," *IEEE Trans. Sustain. Energy*, vol. 8, no. 4, pp. 1507–1517, 2017.

[106] S. A. Helal, M. O. Hanna, R. J. Najee, M. F. Shaaban, A. H. Osman, and M. S. Hassan, "Energy Management System for Smart Hybrid AC/DC Microgrids in Remote Communities," *Electr. Power Components Syst.*, vol. 47, no. 11–12, pp. 1012–1024, 2019.

[107] M. A. M. Ramli, H. R. E. H. Bouchekara, and A. S. Alghamdi, "Efficient energy management in a microgrid with intermittent renewable energy and storage sources," *Sustain.*, vol. 11, no. 14, 2019.

[108] N. Nikmehr, S. Najafi-Ravadanegh, and A. Khodaei, "Probabilistic optimal scheduling of networked microgrids considering time-based demand response programs under uncertainty," *Appl. Energy*, vol. 198, pp. 267–279, 2017.

[109] D. Bishnoi, O. Prakash, and H. Chaturvedi, "Utilizing Flared Gas for Distributed Generation : An Optimization Based Approach," *AIP Conf. Proc. "Current Trends Renew. Altern. Energy,"* vol. 020007, no. April, 2019.

[110] S. Barakat, H. Ibrahim, and A. A. Elbaset, "Multi-objective optimization of grid-connected PV-wind hybrid system considering reliability, cost, and environmental aspects," *Sustain. Cities Soc.*, vol. 60, no. March, p. 102178, 2020.

[111] R. Janzen, M. Davis, and A. Kumar, “An assessment of opportunities for cogenerating electricity to reduce greenhouse gas emissions in the oil sands,” *Energy Convers. Manag.*, vol. 211, no. March, p. 112755, 2020.

[112] S. Rehman, H. U. R. Habib, S. Wang, M. S. Buker, L. M. Alhems, and H. Z. Al Garni, “Optimal Design and Model Predictive Control of Standalone HRES: A Real Case Study for Residential Demand Side Management,” *IEEE Access*, vol. 8, pp. 29767–29814, 2020.

[113] M. Mohammadjafari, R. Ebrahimi, and V. P. Darabad, “Multi-Objective Dynamic Economic Emission Dispatch of Microgrid Using Novel Efficient Demand Response And Zero Energy Balance Approach State of Charge,” vol. 10, no. 1, 2020.

[114] J. Shen, C. Jiang, Y. Liu, and J. Qian, “A Microgrid Energy Management System with Demand Response for Providing Grid Peak Shaving,” *Electr. Power Components Syst.*, vol. 44, no. 8, pp. 843–852, 2016.

[115] M. H. Amrollahi and S. M. T. Bathaee, “Techno-economic optimization of hybrid photovoltaic/wind generation together with energy storage system in a stand-alone micro-grid subjected to demand response,” *Appl. Energy*, vol. 202, pp. 66–77, 2017.

[116] C. Zhang, J. Wu, Y. Zhou, M. Cheng, and C. Long, “Peer-to-Peer energy trading in a Microgrid,” *Appl. Energy*, vol. 220, no. March, pp. 1–12, 2018.

[117] Z. Zhang and M. Y. Chow, “Convergence analysis of the incremental cost consensus algorithm under different communication network topologies in a smart grid,” *IEEE Trans. Power Syst.*, vol. 27, no. 4, pp. 1761–1768, 2012.

[118] G. Kyriakarakos, A. I. Dounis, K. G. Arvanitis, and G. Papadakis, “A fuzzy logic energy management system for polygeneration microgrids,” *Renew. Energy*, vol. 41, pp. 315–327, 2012.

[119] S. Leonori, M. Paschero, F. M. Frattale Mascioli, and A. Rizzi, “Optimization strategies for Microgrid energy management systems by Genetic Algorithms,” *Appl. Soft Comput. J.*, vol. 86, p. 105903, 2020.

[120] M. S. Mahmoud, N. M. Alyazidi, and M. I. Abouheaf, “Adaptive intelligent

techniques for microgrid control systems: A survey," *Int. J. Electr. Power Energy Syst.*, vol. 90, pp. 292–305, 2017.

[121] I. Zunnurain, M. Nasimul Islam Maruf, M. Moktadir Rahman, and G. M. Shafiullah, "Implementation of advanced demand side management for microgrid incorporating demand response and home energy management system," *Infrastructures*, vol. 3, no. 4, 2018.

[122] Arcos-Aviles, "A Review of Fuzzy-Based Residential Grid-Connected Microgrid Energy Management Strategies for Grid Power Profile Smoothing.," in *Energy Sustainability in Built and Urban Environments. Energy, Environment, and Sustainability.*, B. H. (eds) Motoasca E., Agarwal A., Ed. Singapore: Springer, 2019.

[123] I. Colak, S. Sagiroglu, G. Fulli, M. Yesilbudak, and C. F. Covrig, "A survey on the critical issues in smart grid technologies," *Renew. Sustain. Energy Rev.*, vol. 54, pp. 396–405, 2016.

[124] M. Goyal and A. Ghosh, "Microgrids interconnection to support mutually during any contingency," *Sustain. Energy, Grids Networks*, vol. 6, pp. 100–108, 2016.

[125] F. Luo, Y. Chen, Z. Xu, G. Liang, Y. Zheng, and J. Qiu, "Multiagent-Based Cooperative Control Framework for Microgrids' Energy Imbalance," *IEEE Trans. Ind. Informatics*, vol. 13, no. 3, pp. 1046–1056, 2017.

[126] A. M. Jadhav, Y. Zheng, S. Suryanarayanan, and N. R. Patne, "Energy Management in Multi-Microgrid System with Community Battery Energy Storage," *2018 20th Natl. Power Syst. Conf. NPSC 2018*, 2018.

[127] H. Karimi, R. Bahmani, S. Jadid, and A. Makui, "Dynamic transactive energy in multi-microgrid systems considering independence performance index: A multi-objective optimization framework," *Int. J. Electr. Power Energy Syst.*, vol. 126, no. PA, p. 106563, 2021.

[128] F. H. Aghdam, N. T. Kalantari, and B. Mohammadi-Ivatloo, "A chance-constrained energy management in multi-microgrid systems considering degradation cost of energy storage elements," *J. Energy Storage*, vol. 29, no. November 2019, p. 101416, 2020.

[129] M. Xie, X. Ji, X. Hu, P. Cheng, Y. Du, and M. Liu, “Autonomous optimized economic dispatch of active distribution system with multi-microgrids,” *Energy*, vol. 153, pp. 479–489, 2018.

[130] M. Zadsar, S. S. Sebtahmadi, M. Kazemi, S. M. M. Larimi, and M. R. Haghifam, “Two stage risk based decision making for operation of smart grid by optimal dynamic multi-microgrid,” *Int. J. Electr. Power Energy Syst.*, vol. 118, no. August 2019, p. 105791, 2020.

[131] D. M. L. K. Cheong, T. Fernando, H. C. Iu, M. Reynolds, and J. Fletcher, “Review of clustering algorithms for microgrid formation,” *2017 IEEE Innov. Smart Grid Technol. - Asia Smart Grid Smart Community, ISGT-Asia 2017*, pp. 1–6, 2018.

[132] H. Back Merlin, “Search for a minimal-loss operating spanning tree configuration in an urban power distribution system,” *Proc. 5th Power Syst. Comput. Conf. (PSCC), Cambridge, UK*, pp. 1–18, 1975.

[133] H. Y. Civanlar Sehyan, J.J. Grainger, “Distribution feeder reconfiguration for loss reduction,” *IEEE Trans. Power Del.;(United States)*, no. 3.3, 1988.

[134] W. El-khattam, S. Member, Y. G. Hegazy, and M. M. A. Salama, “An Integrated Distributed Generation Optimization Model for Distribution System Planning,” vol. 20, no. 2, pp. 1158–1165, 2005.

[135] Y. Freund and R. E. Schapire, “Experiments with a New Boosting Algorithm,” *Proc. 13th Int. Conf. Mach. Learn.*, pp. 148–156, 1996.

[136] C. X. Zhang, J. S. Zhang, and G. Y. Zhang, “An efficient modified boosting method for solving classification problems,” *J. Comput. Appl. Math.*, vol. 214, no. 2, pp. 381–392, May 2008.

[137] D. P. Solomatine, “AdaBoost . RT : a Boosting Algorithm for Regression Problems,” pp. 1163–1168.

[138] Á. Alonso, A. Torres, and J. R. Dorronsoro, “Random forests and gradient boosting for wind energy prediction,” in *Lecture Notes in Artificial Intelligence (Subseries of Lecture Notes in Computer Science)*, 2015, vol. 9121, pp. 26–37.

[139] NASA, “NASA Prediction of World wide energy resources,” 2021. .

[140] N. Sharma, P. Sharma, D. Irwin, and P. Shenoy, "Predicting solar generation from weather forecasts using machine learning," in *2011 IEEE International Conference on Smart Grid Communications, SmartGridComm 2011*, 2011, pp. 528–533.

[141] G. Ciulla and A. D'Amico, "Building energy performance forecasting: A multiple linear regression approach," *Appl. Energy*, vol. 253, no. June, p. 113500, 2019.

[142] J. Friedman, T. Hastie, and R. Tibshirani, "Additive logistic regression: a statistical view of boosting (With discussion and a rejoinder by the authors)," *Ann. Stat.*, vol. 28, no. 2, pp. 337–407, 2000.

[143] O. Sagi and L. Rokach, "Ensemble learning: A survey," *Wiley Interdiscip. Rev. Data Min. Knowl. Discov.*, vol. 8, no. 4, pp. 1–18, 2018.

[144] S. Tiwari, R. Sabzchgar, and M. Rasouli, "Short Term Solar Irradiance Forecast Using Numerical Weather Prediction (NWP) with Gradient Boost Regression," in *2018 9th IEEE International Symposium on Power Electronics for Distributed Generation Systems, PEDG 2018*, 2018.

[145] S. Bhavsar and R. Pitchumani, "A novel machine learning based identification of potential adopter of rooftop solar photovoltaics," *Appl. Energy*, vol. 286, p. 116503, Mar. 2021.

[146] C. Persson, P. Bacher, T. Shiga, and H. Madsen, "Multi-site solar power forecasting using gradient boosted regression trees," *Sol. Energy*, vol. 150, pp. 423–436, 2017.

[147] J. H. Friedman, "Greedy function approximation: A gradient boosting machine.," *Ann. Stat.*, vol. 29, no. 5, pp. 1189–1232, Oct. 2001.

[148] T. Chen and C. Guestrin, "XGBoost: A scalable tree boosting system," in *Proceedings of the ACM SIGKDD International Conference on Knowledge Discovery and Data Mining*, 2016, vol. 13-17-Augu, pp. 785–794.

[149] L. G. V. Saaty, L. Thomas, *Models, methods, concepts and applications of the analytic hierarchy process*. .

[150] Z. Pavić and V. Novoselac, "Notes on TOPSIS Method," *Int. J. Res. Eng. Sci.*, vol. 1, no. 2, pp. 5–12, 2013.

[151] K. Sideris, “Decision Networks and Information Theory Application to SWOT analysis,” ARISTOTLE UNIVERSITY of THESSALONIKI, 2021.

[152] Bishnoi Deepika, Chaturvedi Harsh, “Techno-Economic Analysis of Hybrid Energy System for Efficient Utilization of Waste Flare Gas from Oil and Gas Fields,” in *icsmartgrid IEEE conference*, 2021.

[153] P. Mohamed, a Shouman, M. A. El-moaty, and E. Samir, “Decision Making Assessment for Site Selection Using the,” no. Mcdm, 2015.

[154] Department of Economic and Social Affairs, “United Nations Sustainable Development Goals,” 2021. [Online]. Available: https://sdgs.un.org/goals.

[155] A. C. Duman and Ö. Güler, “Techno-economic analysis of off-grid PV/wind/fuel cell hybrid system combinations with a comparison of regularly and seasonally occupied households,” *Sustain. Cities Soc.*, vol. 42, no. June, pp. 107–126, 2018.

[156] P. Gilman and P. Lilienthal, “MICROPOWER SYSTEM MODELING,” pp. 379–418.

[157] A. Demiroren and U. Yilmaz, “Analysis of change in electric energy cost with using renewable energy sources in Gökceada, Turkey: An island example,” *Renew. Sustain. Energy Rev.*, vol. 14, no. 1, pp. 323–333, 2010.

[158] Z. Xu, M. Nthontho, and S. Chowdhury, “Rural electrification implementation strategies through microgrid approach in South African context,” *Int. J. Electr. Power Energy Syst.*, vol. 82, pp. 452–465, 2016.

[159] H. Z. Al, A. Awasthi, and M. A. M. Ramli, “Optimal design and analysis of grid-connected photovoltaic under di ff erent tracking systems using HOMER,” *Energy Convers. Manag.*, vol. 155, no. October 2017, pp. 42–57, 2018.

[160] A. Kumar, A. R. Singh, Y. Deng, X. He, P. Kumar, and R. C. Bansal, “Integrated assessment of a sustainable microgrid for a remote village in hilly region,” *Energy Convers. Manag.*, vol. 180, no. May 2018, pp. 442–472, 2019.

[161] Shodhganga, “CHAPTER 4 River Brahmaputra,” 2014.

[162] B. Kirke, “Hydrokinetic Turbines for Moderate sized rivers,” no. January, 2020.

[163] C. P. F. Currents, “Schottel tidal generator,” p. 2014, 2014.

[164] A. Kumar, A. R. Singh, Y. Deng, X. He, P. Kumar, and R. C. Bansal, "Integrated assessment of a sustainable microgrid for a remote village in hilly region," *Energy Convers. Manag.*, vol. 180, no. October 2018, pp. 442–472, 2019.

[165] T. Givler and P. Lilienthal, "Using HOMER Software, NREL's Micropower Optimization Model, to Explore the Role of Gen-sets in Small Solar Power Systems; Case Study: Sri Lanka," no. May, 2005.

[166] D. Bishnoi and H. Chaturvedi, "Techno-economic analysis of hybrid energy system for efficient utilization of waste flare gas from oil and gas fields," *9th Int. Conf. Smart Grid, icSmartGrid 2021*, pp. 201–206, 2021.

[167] E. N. Ojijiagwo, C. F. Oduoza, and N. Emekwuru, "Technological and economic evaluation of conversion of potential flare gas to electricity in Nigeria," *Procedia Manuf.*, vol. 17, pp. 444–451, 2018.

[168] Assam Power Distribution Company Limited, "Power Tariff in Assam," Guwahati, 2021.

[169] O. Nadjemi, T. Nacer, A. Hamidat, and H. Salhi, "Optimal hybrid PV/wind energy system sizing: Application of cuckoo search algorithm for Algerian dairy farms," *Renew. Sustain. Energy Rev.*, vol. 70, no. November 2015, pp. 1352–1365, 2017.

[170] M. R. Elkadeem, S. Wang, S. W. Sharshir, and E. G. Atia, "Feasibility analysis and techno-economic design of grid-isolated hybrid renewable energy system for electrification of agriculture and irrigation area: A case study in Dongola, Sudan," *Energy Convers. Manag.*, vol. 196, no. February, pp. 1453–1478, 2019.

[171] K. Elmaadawy *et al.*, "Optimal sizing and techno-enviro-economic feasibility assessment of large-scale reverse osmosis desalination powered with hybrid renewable energy sources," *Energy Convers. Manag.*, vol. 224, no. August, 2020.

[172] A. S. Aziz, M. F. N. Tajuddin, M. R. Adzman, M. A. M. Ramli, and S. Mekhilef, "Energy management and optimization of a PV/diesel/battery hybrid energy system using a combined dispatch strategy," *Sustain.*, vol. 11, no. 3, 2019.

[173] T. S. Costa and M. G. Villalva, "Technical evaluation of a PV-diesel hybrid system with energy storage: Case study in the Tapajós-Arapiuns Extractive Reserve, Amazon, Brazil," *Energies*, vol. 13, no. 11, 2020.

[174] ONGC, “ONGC Annual Report,” 2020.

[175] N. ONGC Assam asset, “Additional flare and Technical flare data for the month of January 2018,” 2018.

[176] A. T. Dahiru and C. W. Tan, “Optimal sizing and techno-economic analysis of grid-connected nanogrid for tropical climates of the Savannah,” *Sustain. Cities Soc.*, vol. 52, no. January 2019, p. 101824, 2020.

[177] D. Bishnoi, O. Prakash, and H. Chaturvedi, “Utilizing flared gas for distributed generation: An optimization based approach,” in *AIP Conference Proceedings*, 2019, vol. 2091.

[178] B. R. Ambrosio, “Transactive Energy Systems,” no. December, pp. 4–7, 2016.

[179] M. I. Pathan, M. AlOwaifeer, M. AlMuhaini, and S. Z. Djokic, “A Transactive Energy Framework for Coordinated Energy Management of Networked Microgrids with Distributionally Robust Optimization,” *Arab. J. Sci. Eng.*, vol. 45, no. 8, pp. 6347–6360, 2020.

[180] M. Daneshvar, B. Mohammadi-Ivatloo, M. Abapour, and S. Asadi, “Energy Exchange Control in Multiple Microgrids with Transactive Energy Management,” *J. Mod. Power Syst. Clean Energy*, vol. 8, no. 4, pp. 719–726, 2020.

[181] T. Khatib and W. Elmenreich, “A Model for Hourly Solar Radiation Data Generation from Daily Solar Radiation Data Using a Generalized Regression Artificial Neural Network,” vol. 2015, 2015.

[182] D. R. Myers, “Solar Radiation Modeling and Measurements for Renewable Energy Applications : Data and Model Quality Preprint,” no. March, 2003.

[183] T. R. Ayodele, “Determination of Probability Distribution Function for Modelling Global Solar Radiation : Case Study of Ibadan , Nigeria,” no. June, pp. 233–245, 2015.

[184] P. Kayal and C. K. Chanda, “Optimal mix of solar and wind distributed generations considering performance improvement of electrical distribution network,” *Renew. Energy*, vol. 75, pp. 173–186, 2015.

[185] G. Koudouris, P. Dimitriadis, T. Iliopoulou, N. Mamassis, and D. Koutsoyiannis,

"A stochastic model for the hourly solar radiation process for application in renewable resources management," pp. 139–145, 2018.

[186] J. F. Escobedo and A. P. Oliveira, "Modelling frequency distributions of 5 minute-averaged solar radiation indexes using Beta probability functions," vol. 224, pp. 213–224, 2003.

[187] Y. M. Atwa, S. Member, S. Member, M. M. A. Salama, and R. Seethapathy, "Optimal Renewable Resources Mix for Distribution System Energy Loss Minimization," vol. 25, no. 1, pp. 360–370, 2010.

[188] L. Resources and E. Sciences, "A Beta Regression Model for Improved Solar Radiation Predictions," no. 2011, pp. 1923–1938, 2013.

[189] S. H. Karaki and I. R. B. Chedid, "Probabilistic Performance Assessment of Autonomous Solar-Wind Energy Conversion Systems," vol. 14, no. 3, 1999.

[190] A. P. Oliveira, "Modelling frequency distribution of 5-minute-averaged solar radiation indexes using Beta probability functions Modelling frequency distributions of 5 minute-averaged solar radiation indexes using Beta probability functions," no. September, 2003.

[191] T. C. Silva *et al.*, "Technical and economical evaluation of the photovoltaic system in Brazilian public buildings: A case study for peak and off-peak hours," *Energy*, vol. 190, no. 482, 2020.

[192] Z. Huang, Y. Lu, M. Wei, and J. Liu, "Performance analysis of optimal designed hybrid energy systems for grid-connected nearly/net zero energy buildings," *Energy*, vol. 141, pp. 1795–1809, 2017.

[193] A. Kamjoo, A. Maheri, A. M. Dizqah, and G. A. Putrus, "Multi-objective design under uncertainties of hybrid renewable energy system using NSGA-II and chance constrained programming," *Int. J. Electr. Power Energy Syst.*, vol. 74, pp. 187–194, 2016.

[194] S. Zeinal-Kheiri, A. Mohammadpour Shotorbani, and B. Mohammadi-Ivatloo, "Robust Energy Management of a Microgrid with Uncertain Price, Renewable Generation, and Load using Taguchi's Orthogonal Array Method," *J. Energy Manag. Technol.*, vol. 3, no. 3, pp. 1–13, 2019.

[195] Y. Zheng, B. M. Jenkins, K. Kornbluth, A. Kendall, and C. Træholt, "Optimization of a biomass-integrated renewable energy microgrid with demand side management under uncertainty," *Appl. Energy*, vol. 230, no. September, pp. 836–844, 2018.

[196] R. Dufo-López, I. R. Cristóbal-Monreal, and J. M. Yusta, "Stochastic-heuristic methodology for the optimisation of components and control variables of PV-wind-diesel-battery stand-alone systems," *Renew. Energy*, vol. 99, pp. 919–935, 2016.

[197] Y. Li, C. Wang, G. Li, J. Wang, D. Zhao, and C. Chen, "Improving operational flexibility of integrated energy system with uncertain renewable generations considering thermal inertia of buildings," *Energy Convers. Manag.*, vol. 207, pp. 1–21, 2020.